The Origin of Galactic Cosmic Rays: Supernova Remnants

Siming Liu

Purple Mountain Observatory
liusm@pmo.ac.cn

Yuliang Xin, Houdun Zeng, Xiao Zhang, Qiang Yuan, Xiaoyuan Huang, Chuyuan Yang, Yang Chen

Outline

1: General Properties of Cosmic Rays

2: The Origin of Galactic Cosmic Rays:

Gamma-ray Observations of Supernova Remnants

3: Modeling of Individual SNRs with Multi-Wavelength Observations

4: Conclusion

1: Cosmic Rays

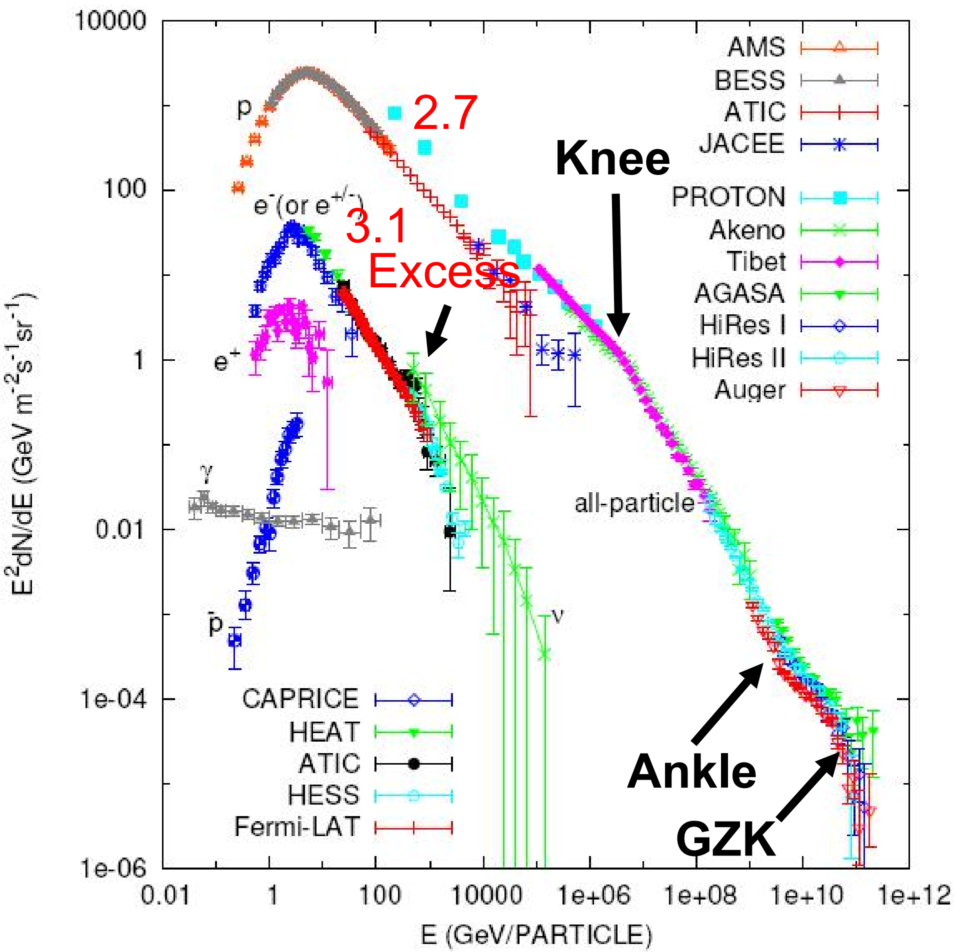

Dominated by Nuclei, there are also electrons, positrons and antiprotons

Age: ~ 10^7 Year

Energy density: ~ 1eV/cm^3

Power: ~ 10^{41} erg/s

~ 3e48 erg/year

e/p ~ 1% at 1GeV

Leptonic Excess at ~ 500GeV

Spectral Knee at ~ 1e15eV

and Ankle at ~ 1e18eV

Maximum Energy: 3×10^{20}eV

~ 50 Joule

GZK Cutoff at ~ 1e20 eV

1: Modeling of Cosmic Ray Spectra

GALPROP
$$\frac{\partial \psi(\vec{r},p,t)}{\partial t} = q(\vec{r},p,t) + \vec{\nabla}\cdot(D_{xx}\vec{\nabla}\psi - \vec{V}\psi) + \frac{\partial}{\partial p}p^2 D_{pp}\frac{\partial}{\partial p}\frac{1}{p^2}\psi - \frac{\partial}{\partial p}\left[\dot{p}\psi - \frac{p}{3}(\vec{\nabla}\cdot\vec{V})\psi\right] - \frac{1}{\tau_f}\psi - \frac{1}{\tau_r}\psi$$

Injection Power:
Proton ~ 3e48 erg/year
Electron ~ 4e46 erg/year

α=1.25 β=3.56 $R_\odot = 8.5\,\mathrm{kpc}$ $z_s \approx 0.2\,\mathrm{kpc}$

$$q_{f}(R,z) \propto \left(\frac{R}{R_\odot}\right)^{\alpha} \exp\left[-\frac{\beta(R-R_\odot)}{R_\odot}\right] \exp\left(-\frac{|z|}{z_s}\right),$$

3 SNRs/100 yrs with
1e50 erg protons and
1e48 erg electrons
For each SNR.

$$q(p) \propto \begin{cases} p^{-\alpha_1}, & p < p_{\rm br}, \\ p^{-\alpha_2}, & p \geq p_{\rm br}, \end{cases}$$

$p_{\rm br}c = 6$ GeV

$\alpha_1 = 1.80, \ \alpha_2 = 2.52$

10% efficiency for type
Ia SNRs with a kinetic
energy of 1e51ergs

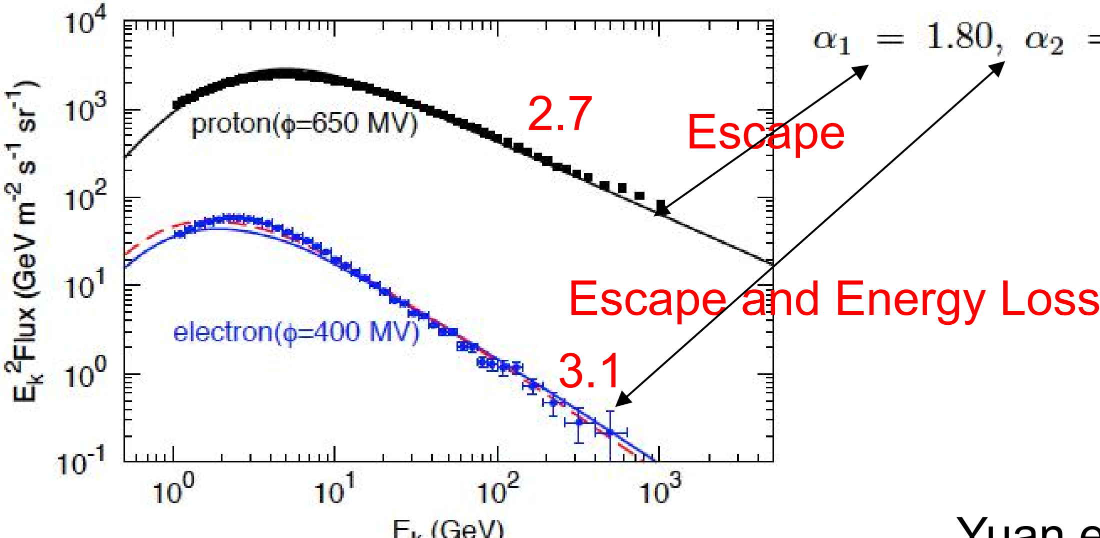

Yuan et al. 2012

2: Radio Supernova Remnants and Galactic Cosmic rays

COSMIC RAYS FROM SUPER-NOVAE

By W. Baade and F. Zwicky

Mount Wilson Observatory, Carnegie Institution of Washington and California Institute of Technology, Pasadena

Communicated March 19, 1934

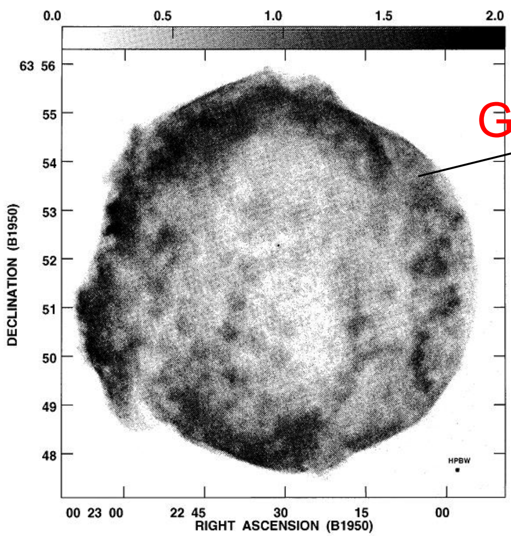

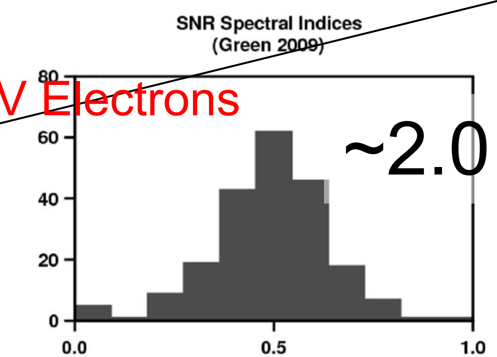

Fig. 1 Histogram of shell SNRs with fairly well-measured radio spectral indices, from Green 2009. PWNe are excluded.

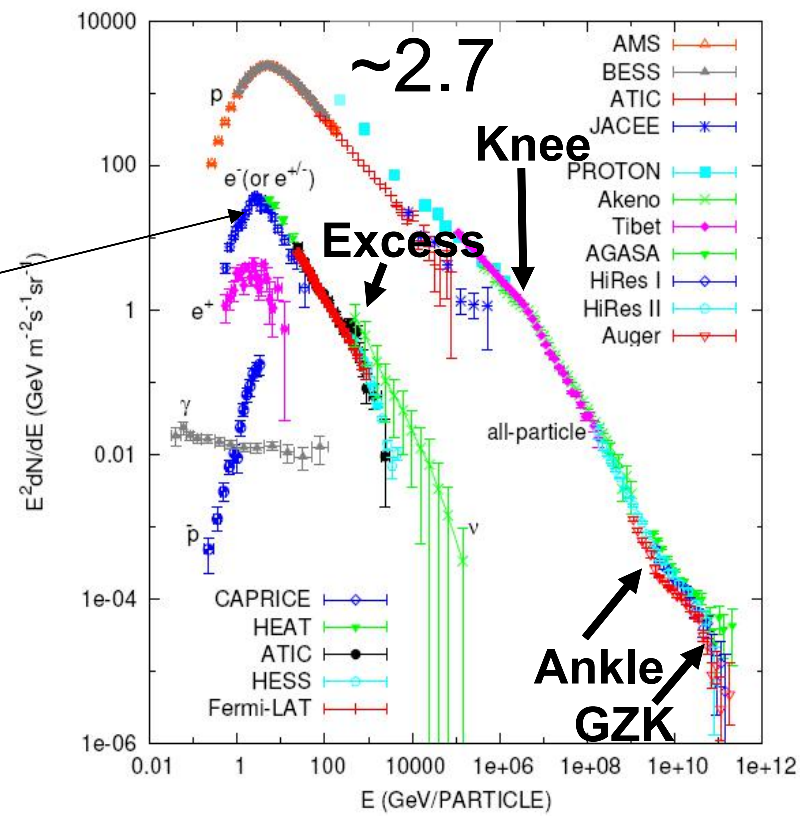

Magnetic fields in supernova remnants and pulsar-wind nebulae

Stephen P. Reynolds · B. M. Gaensler · Fabrizio Bocchino

1912

2: Synchrotron X-rays

TYCHO'S SUPERNOVA REMNANT

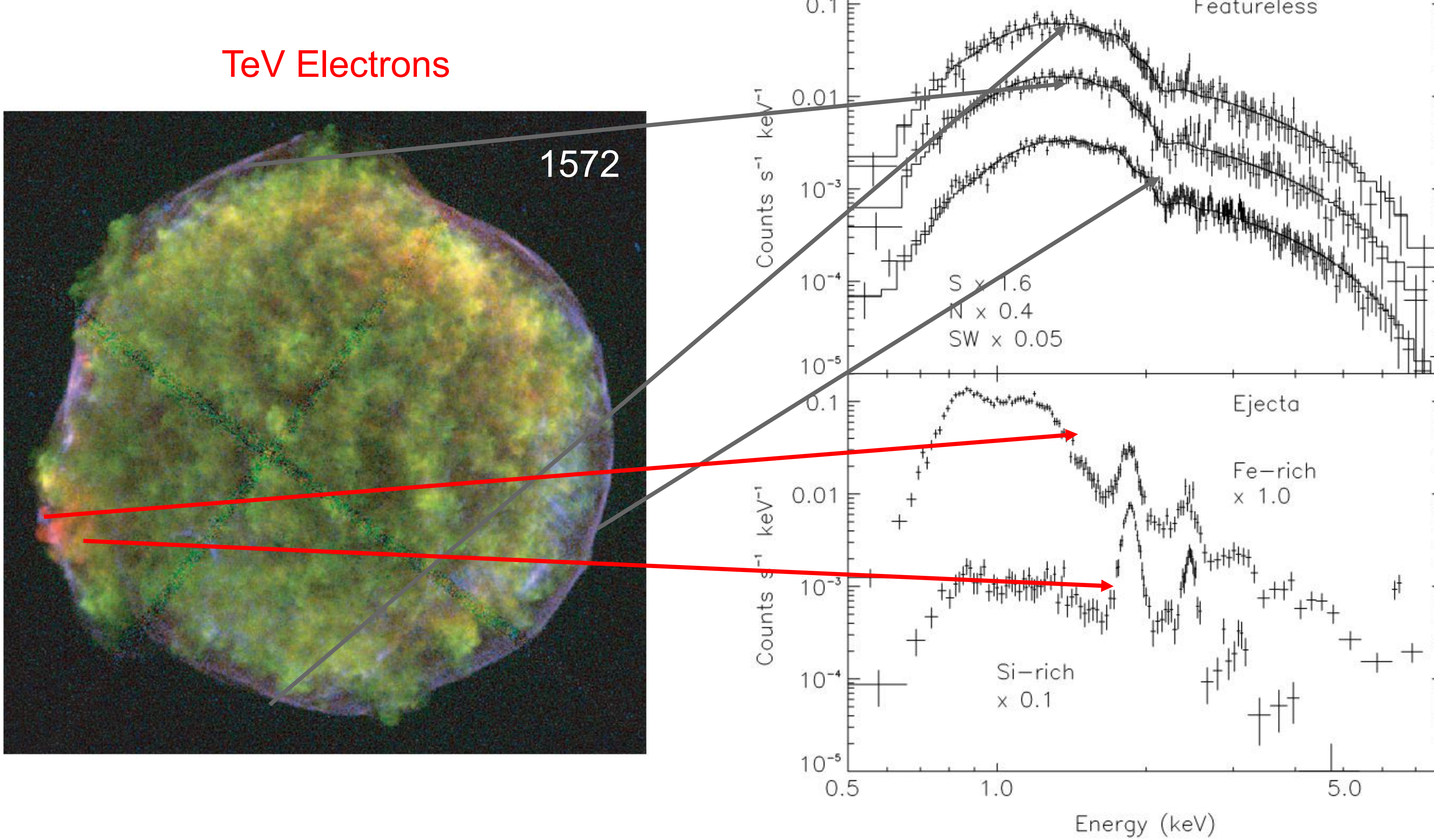

2: Shell Type TeV SNRs

A joint spectro-imaging analysis of the *XMM-Newton* and HESS observations of the supernova remnant RX J1713.7-3946

F. Acero[1], J. Ballet[1], A. Decourchelle[1], M. Lemoine-Goumard[2,3], M. Ortega[4], E. Giacani[4], G. Dubner[4], and G. Cassam-Chenaï[5]

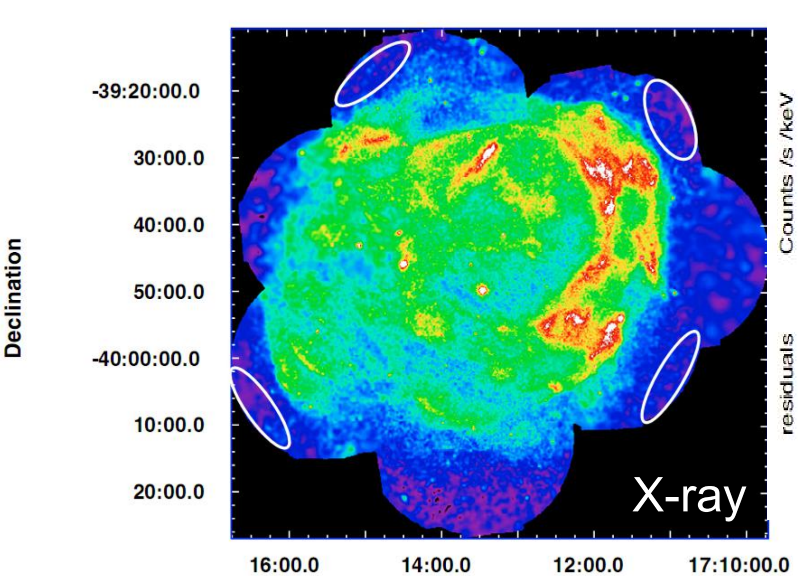

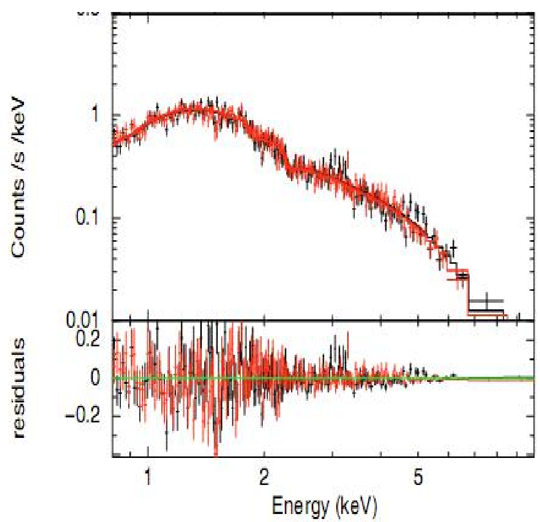

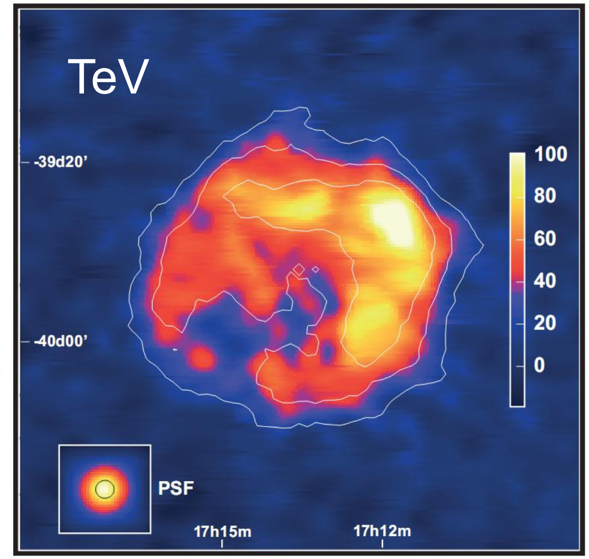

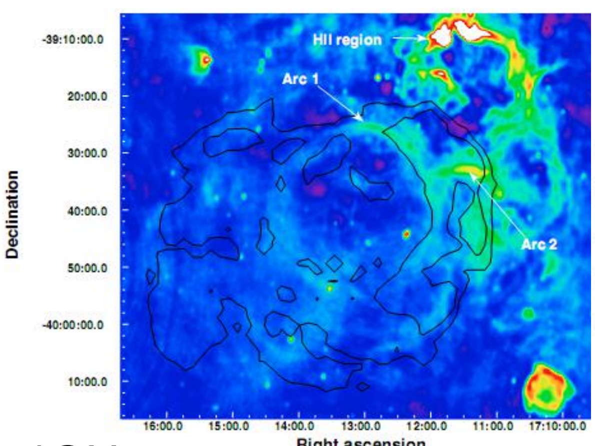

1.4GHz

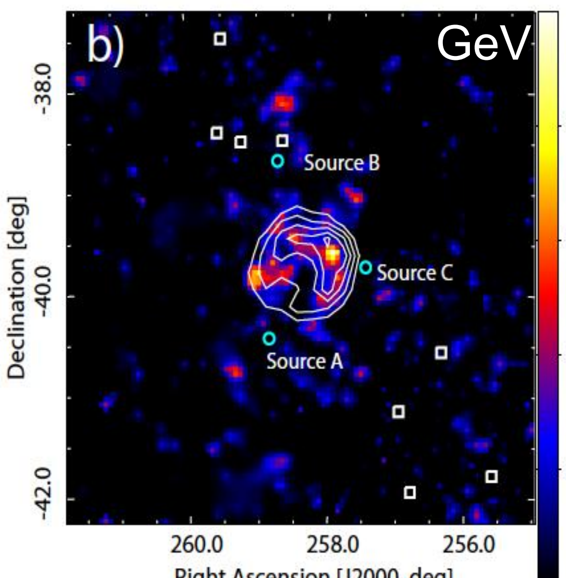

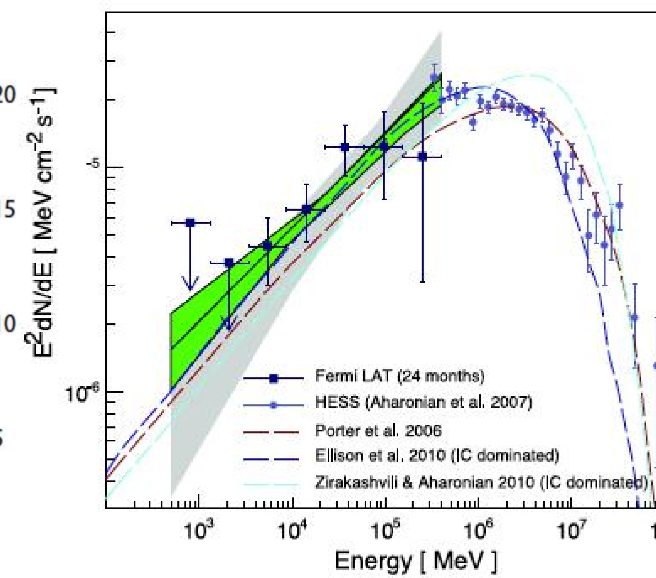

Observations of the young Supernova remnant RX J1713.7−3946 with the *Fermi* Large Area Telescope

A. A. Abdo[2], M. Ackermann[3,1], M. Ajello[3], A. Allafort[3], L. Baldini[4], J. Ballet[5],

The X-ray emission of the supernova remnant W49B observed with *XMM-Newton*

M. Miceli[1,2,3], A. Decourchelle[1], J. Ballet[1], F. Bocchino[3], J. P. Hughes[4], U. Hwang[5,6], and R. Petre[6]

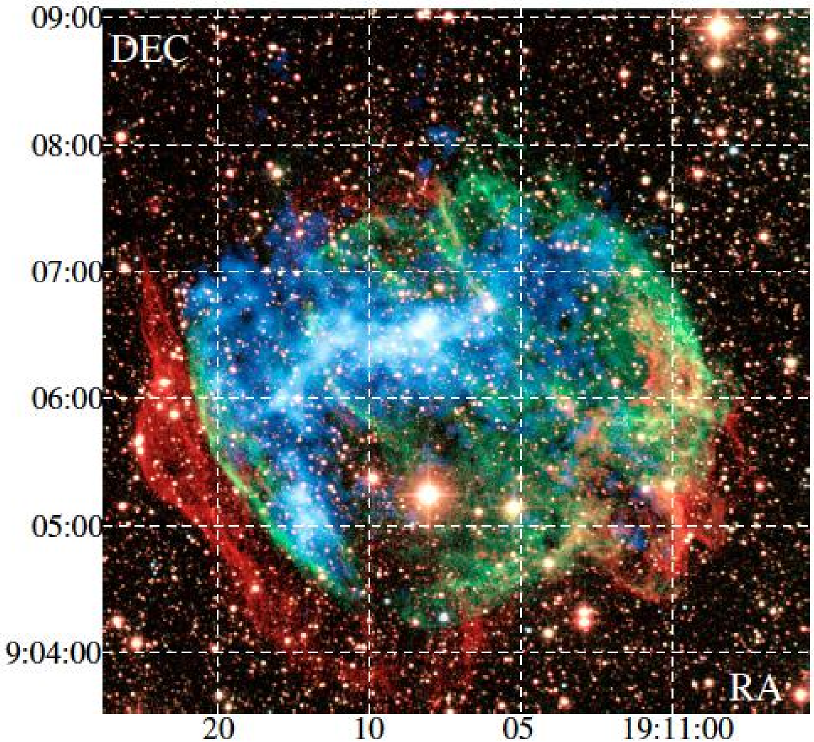

Fig. 2. Color composite *Chandra* X-ray image (in blue), infrared 2.12 μm molecular hydrogen (in red), and 1.64 μm [Fe II] (in green) images of W49B (from `http://chandra.harvard.edu/press/04_releases/press_060204.html`).

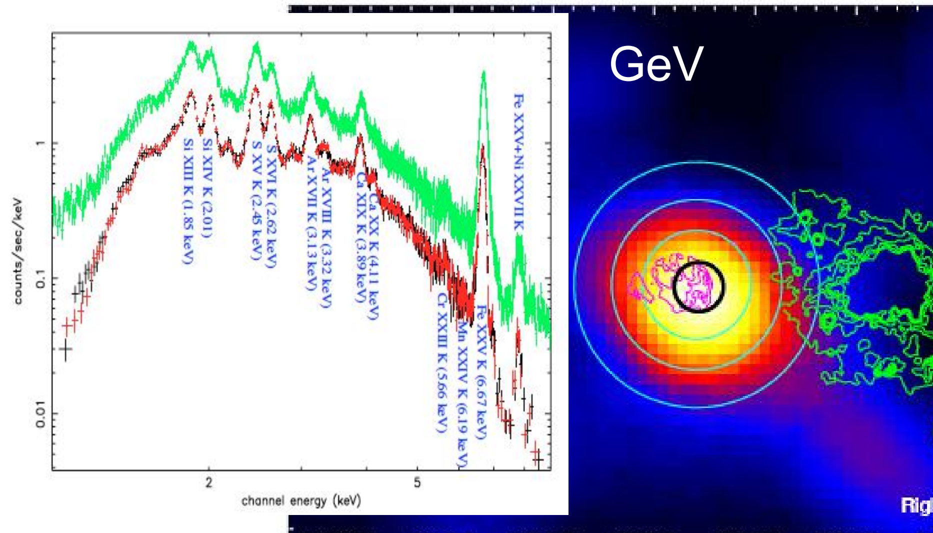

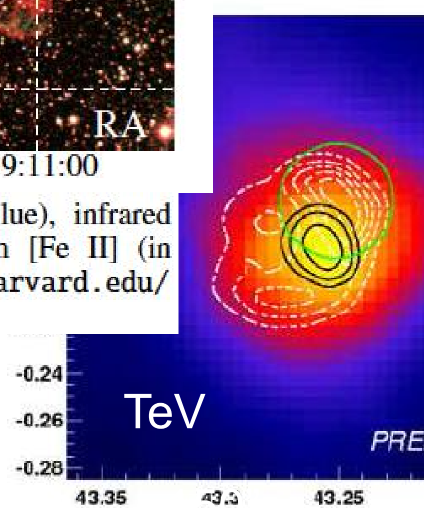

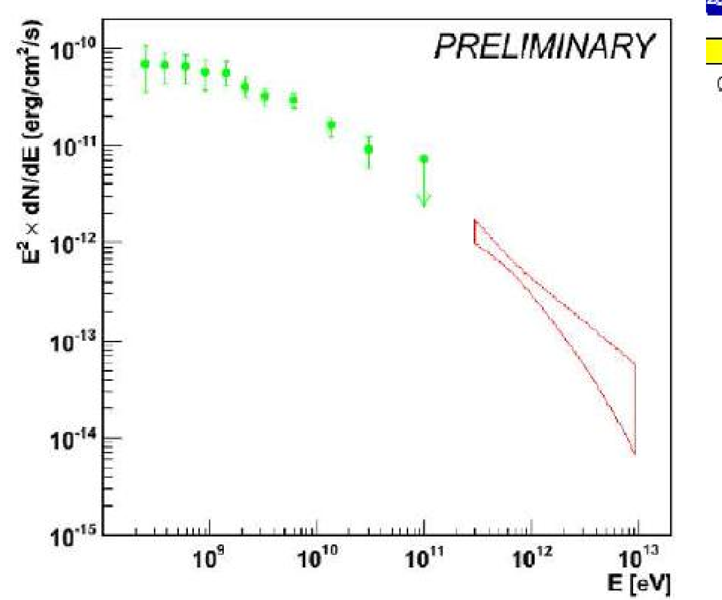

2: Hadronic Gamma-ray Emission

Detection of the Characteristic Pion-Decay Signature in Supernova Remnants
M. Ackermann *et al.*
Science **339**, 807 (2013);
DOI: 10.1126/science.1231160

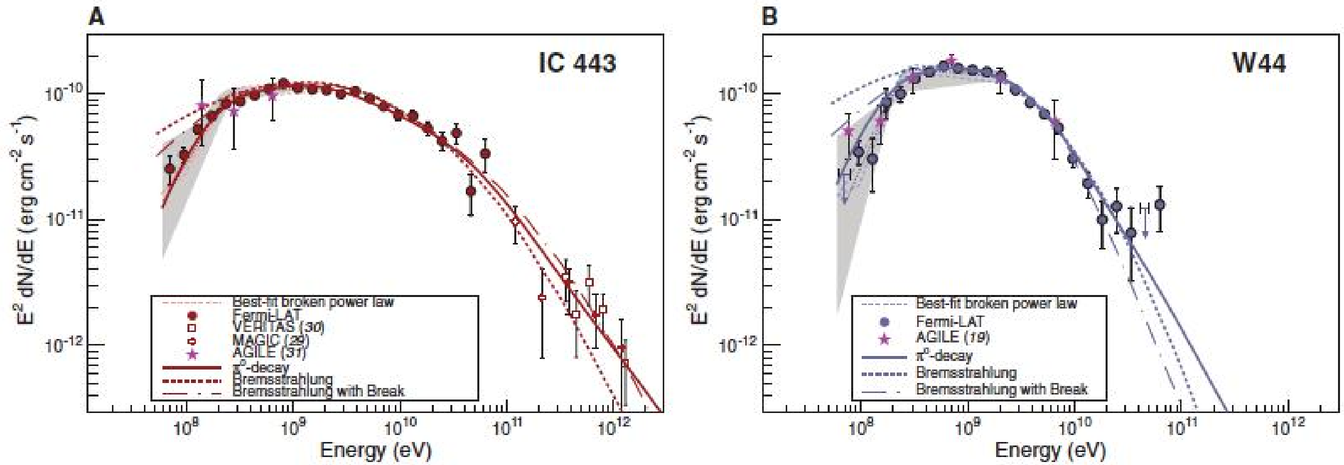

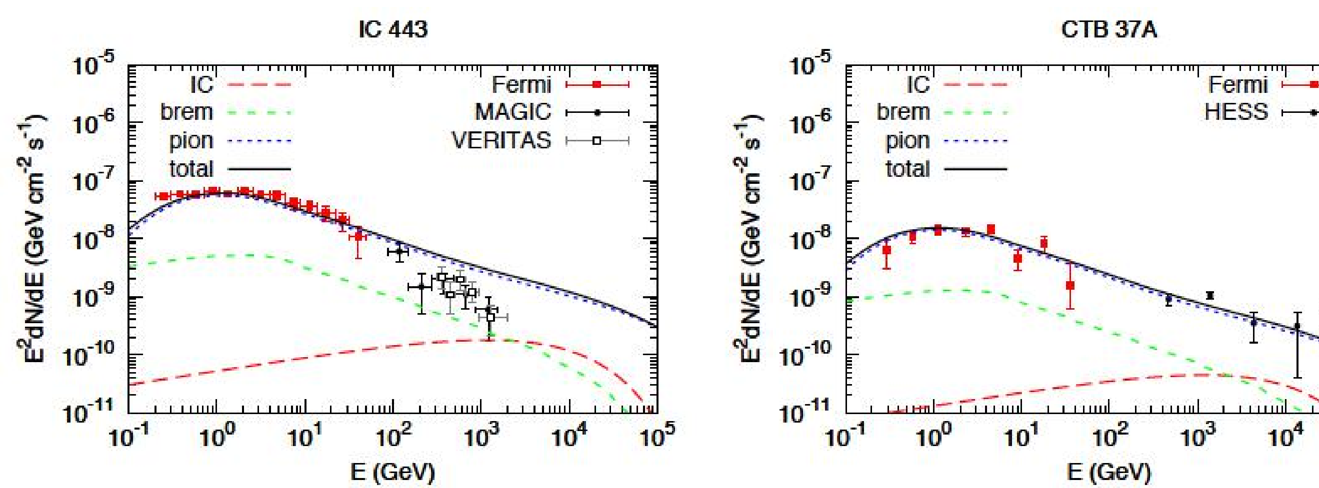

2: Observations of SNRs

Radio SNRs: 279 among them

Synchrotron X-Ray: >14

GeV SNRs: >30 among them

TeV SNRs: >10

3/100*1e5 = 3000

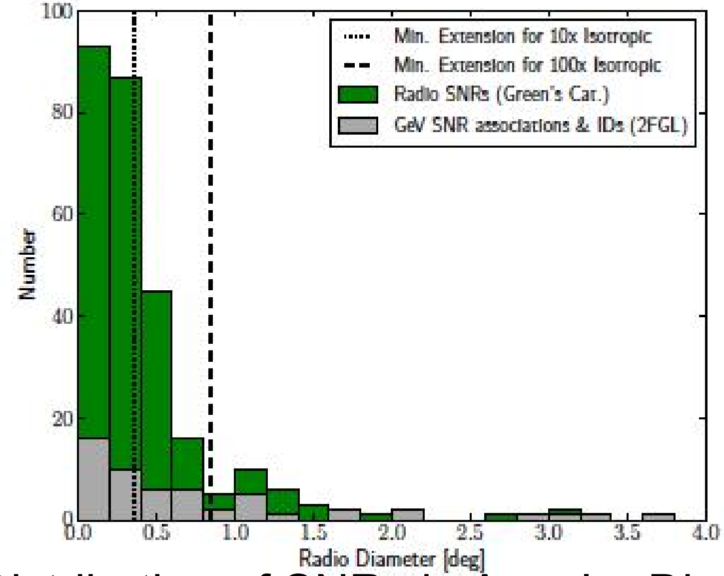

Distribution of SNRs in Angular Diameter

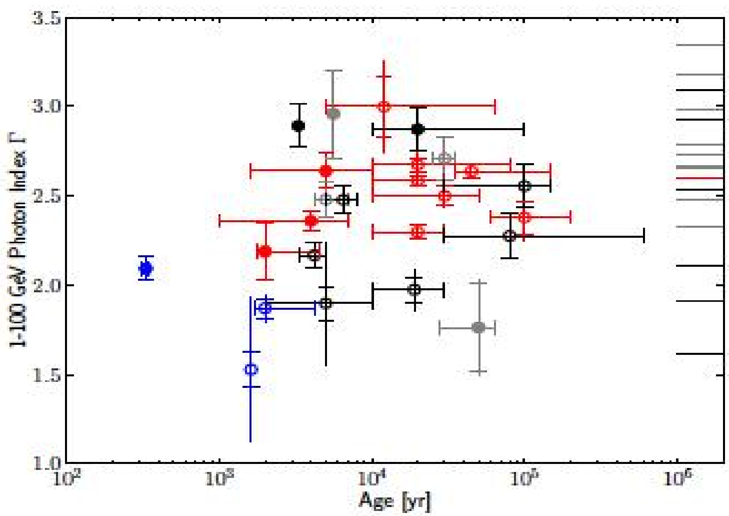

AGE

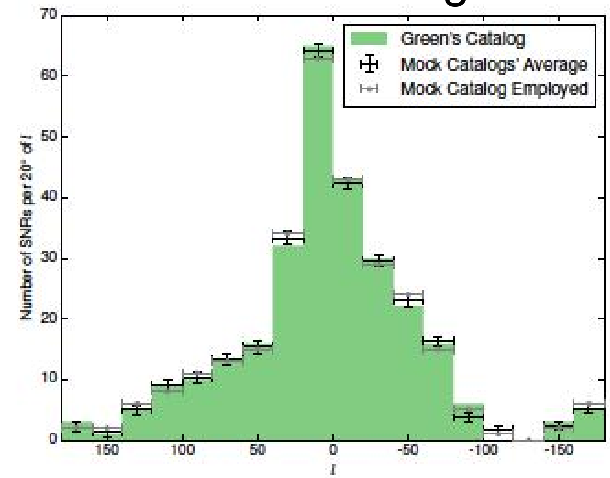

Distribution of SNRs in Galactic Longitude

2: Observations of SNRs

Radio vs GeV fluxes

Radio SNRs: 279 among them

Synchrotron X-Ray: 14

GeV SNRs: 30 among them

TeV SNRs: 10

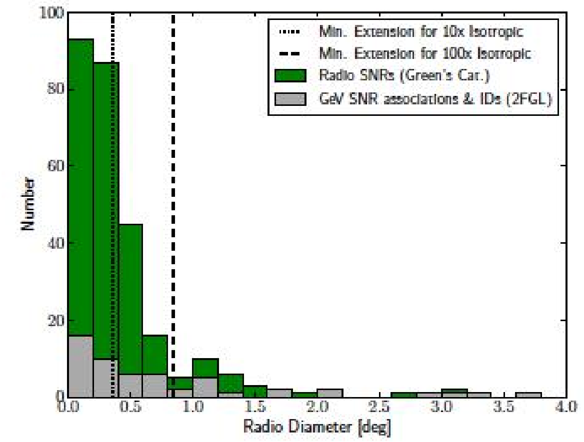

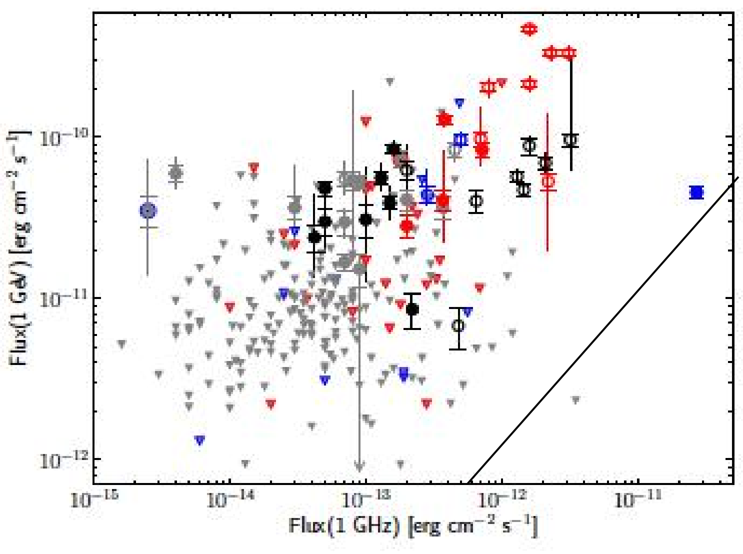

Radio Flux

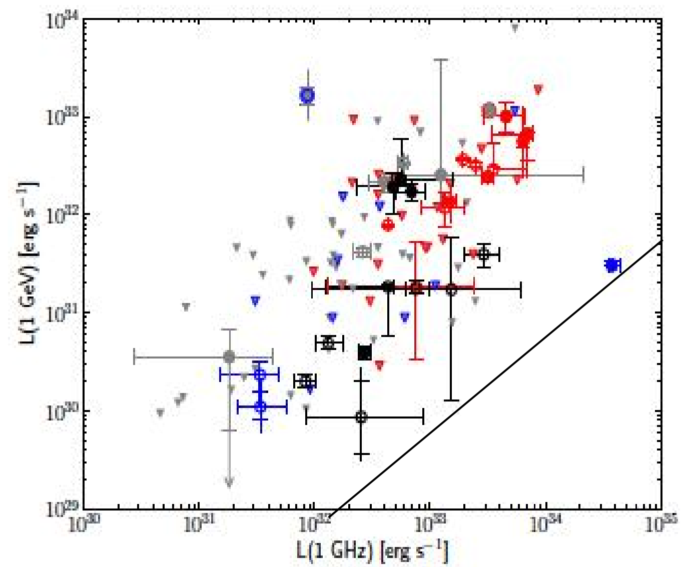

Radio Luminosity

2: Observations of SNRs:

Spectral indexes

Radio SNRs: 279 among them

Synchrotron X-Ray: 14

GeV SNRs: 30 among them

TeV SNRs: 10

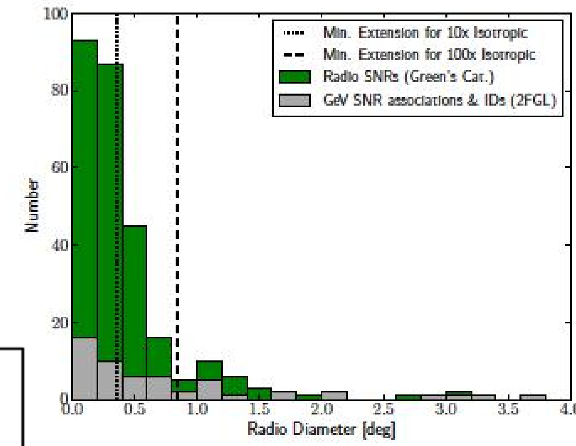

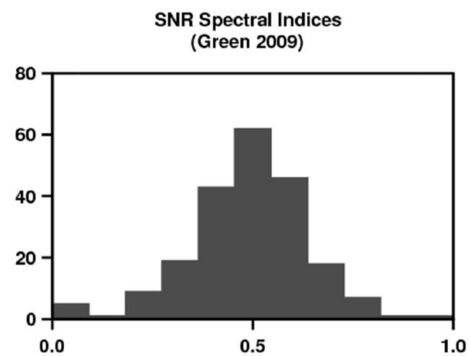

Fig. 1 Histogram of shell SNRs with fairly well-measured radio spectral indices, from Green 2009. PWNe are excluded.

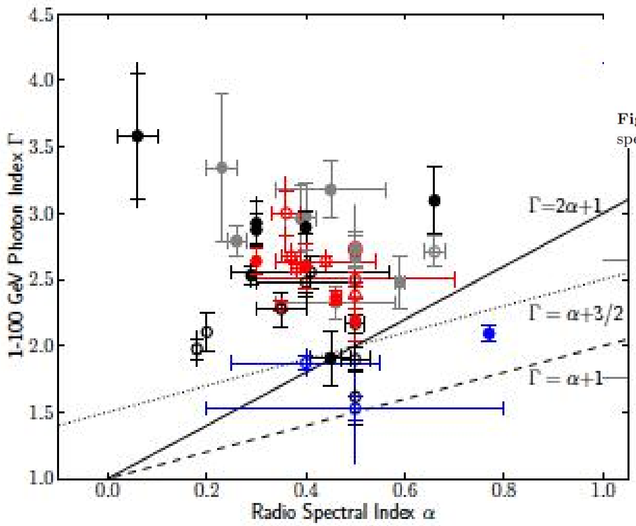

IC

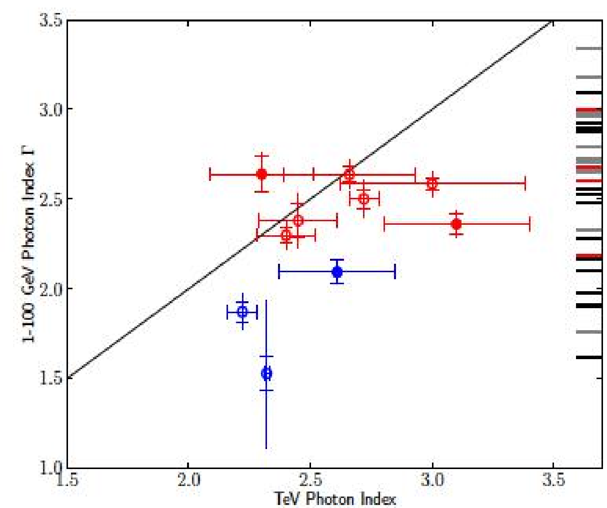

2: Modeling of Cosmic Ray Spectra

$$q_f(R,z) \propto \left(\frac{R}{R_\odot}\right)^{\alpha} \exp\left[-\frac{\beta(R-R_\odot)}{R_\odot}\right] \exp\left(-\frac{|z|}{z_s}\right),$$

$$q(p) \propto \begin{cases} p^{-\alpha_1}, & p < p_{\rm br}, \\ p^{-\alpha_2}, & p \geq p_{\rm br}, \end{cases}$$

$$p_{\rm br}c = 6 \text{ GeV}$$

$$\alpha_1 = 1.80, \ \alpha_2 = 2.52$$

Injection Power:
Proton ~ 3e48 erg/year
Electron ~ 4e46 erg/year

3 SNRs/100 yrs with
1e50 erg protons and
1e48 erg electrons
For each SNR.

10% efficiency for type
Ia SNRs with a kinetic
energy of 1e51ergs

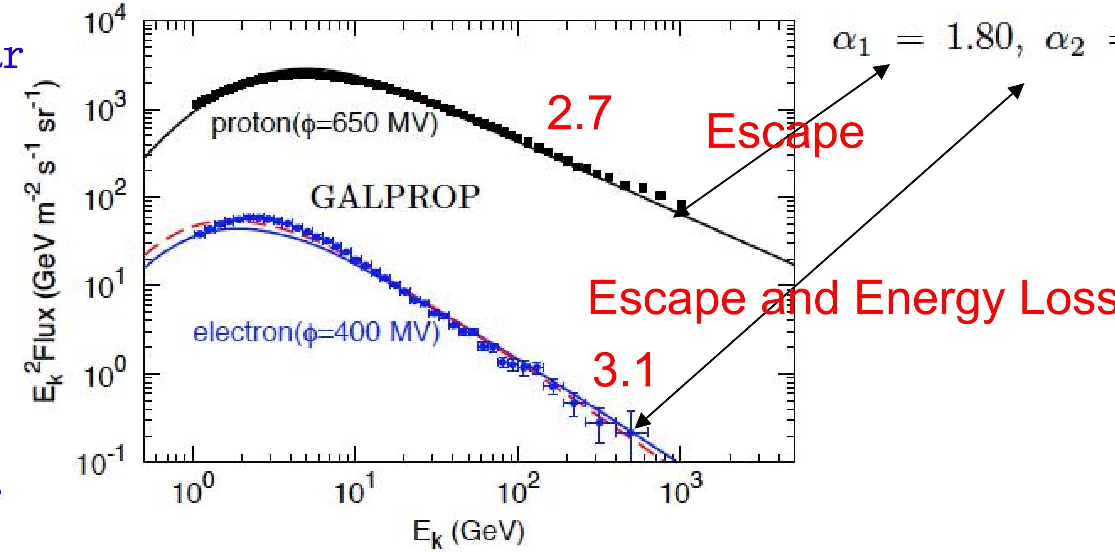

FIG. 1.— The expected fluxes of CR protons and electrons at the Earth, for the same spectral shape of the injected particles, compared with the PAMELA observational data (Adriani et al. 2011a,b). We adopt two parameter settings to calculate the electron spectrum: for solid line the magnetic field is the canonical one adopted in GALPROP and $K_{ep} \approx 1.3\%$; for dashed line the magnetic field is two times larger and $K_{ep} \approx 1.9\%$.

Yuan et al. 2012

2: Emission Processes of Gamma-rays

$n = 0.01\ \mathrm{cm}^{-3}$

$n = 1\ \mathrm{cm}^{-3}$

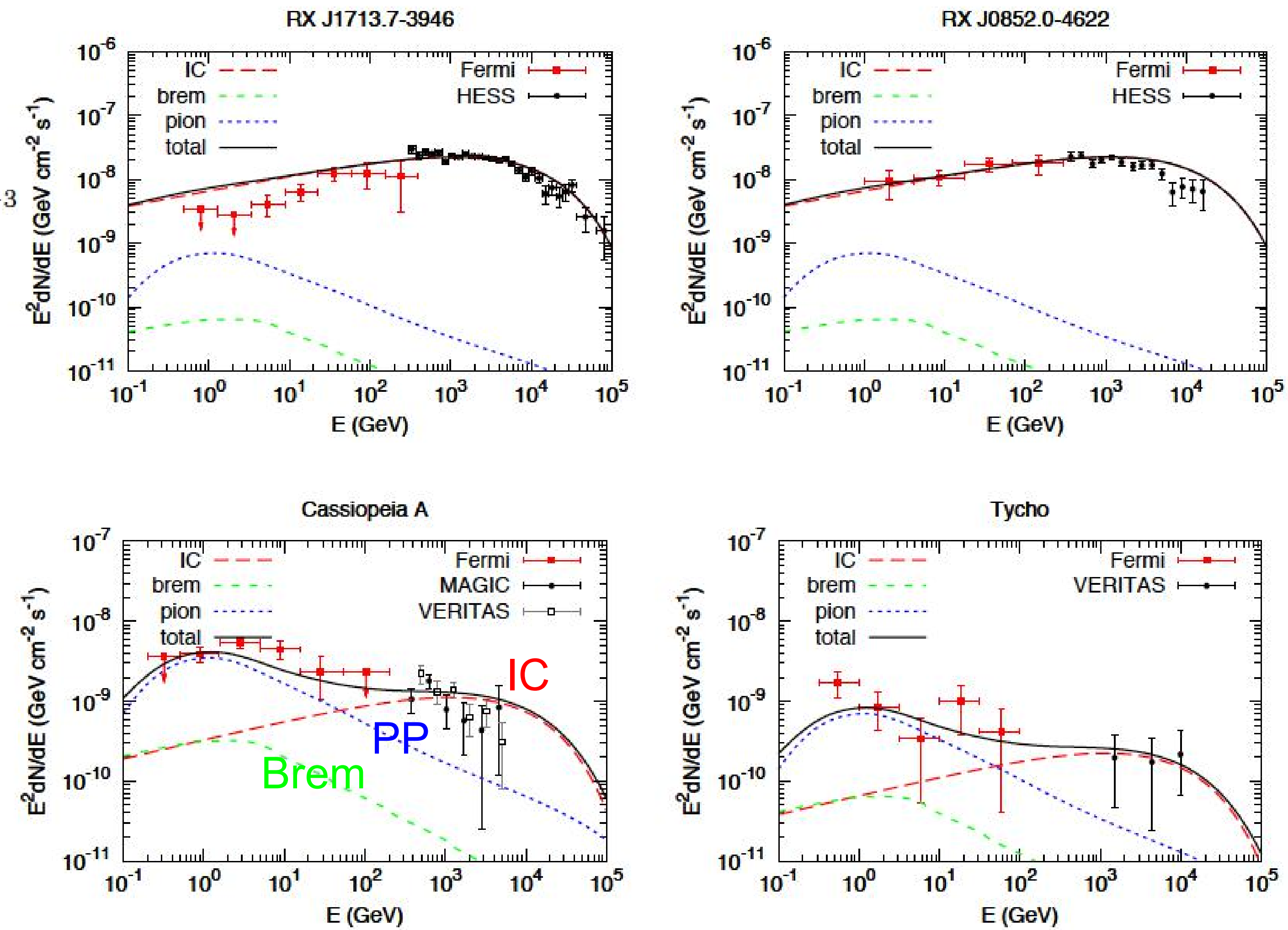

2: Modeling of Gamma-ray Spectra

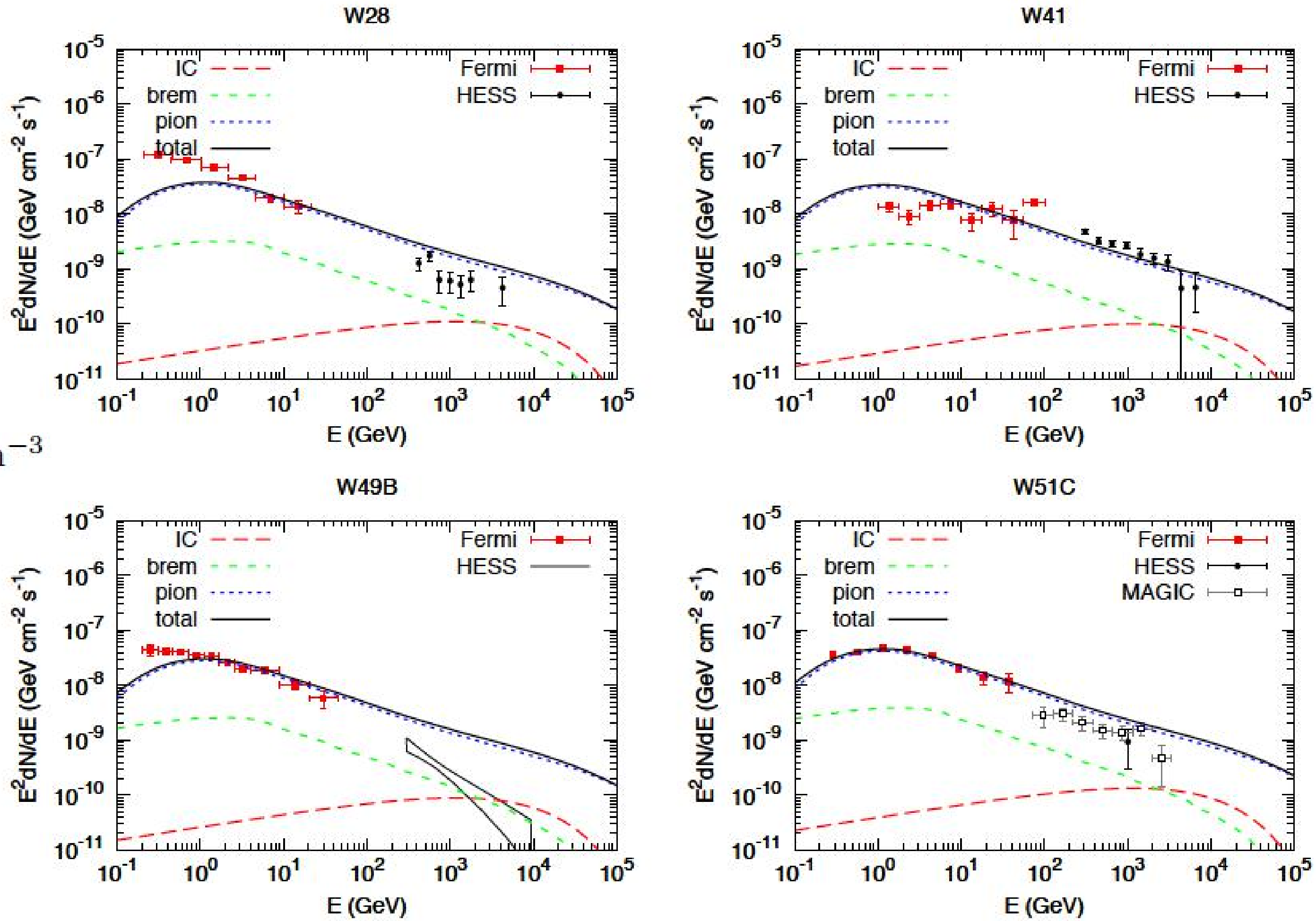

$$n = 100 \ \mathrm{cm}^{-3}$$

2: Summary

The spectra of SNRs show significant variations from source to source, which may be attributed to the evolution of the shocks of SNRs and/or complexity of the environment.

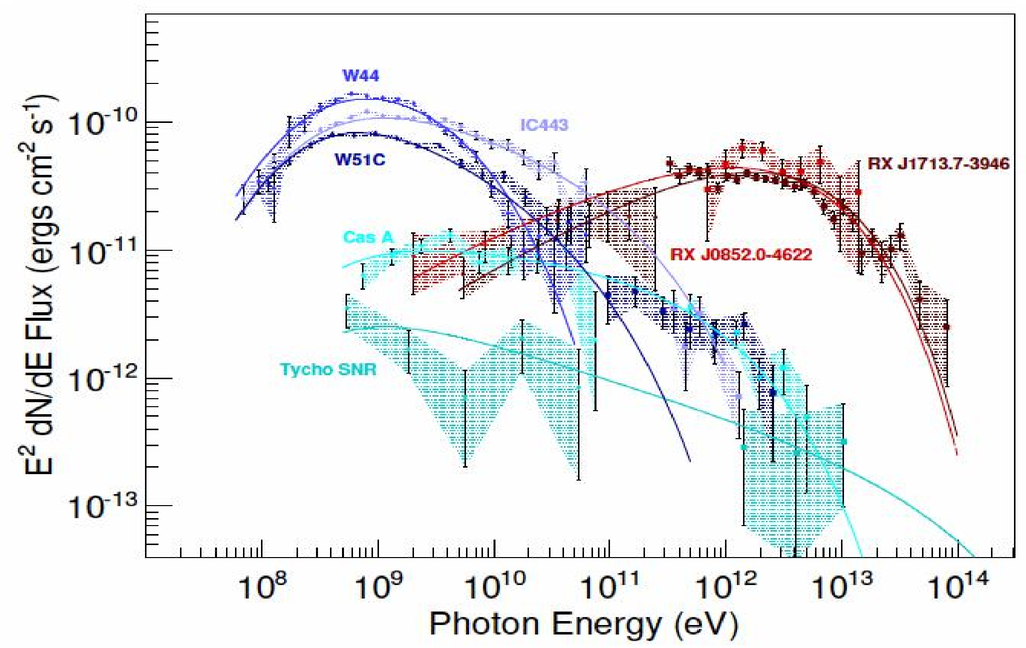

3: Multi-wavelength Observations of Supernova Remnants

Pulsars are not energetically as important as shocks and may dominate the position excess at ~500GeV

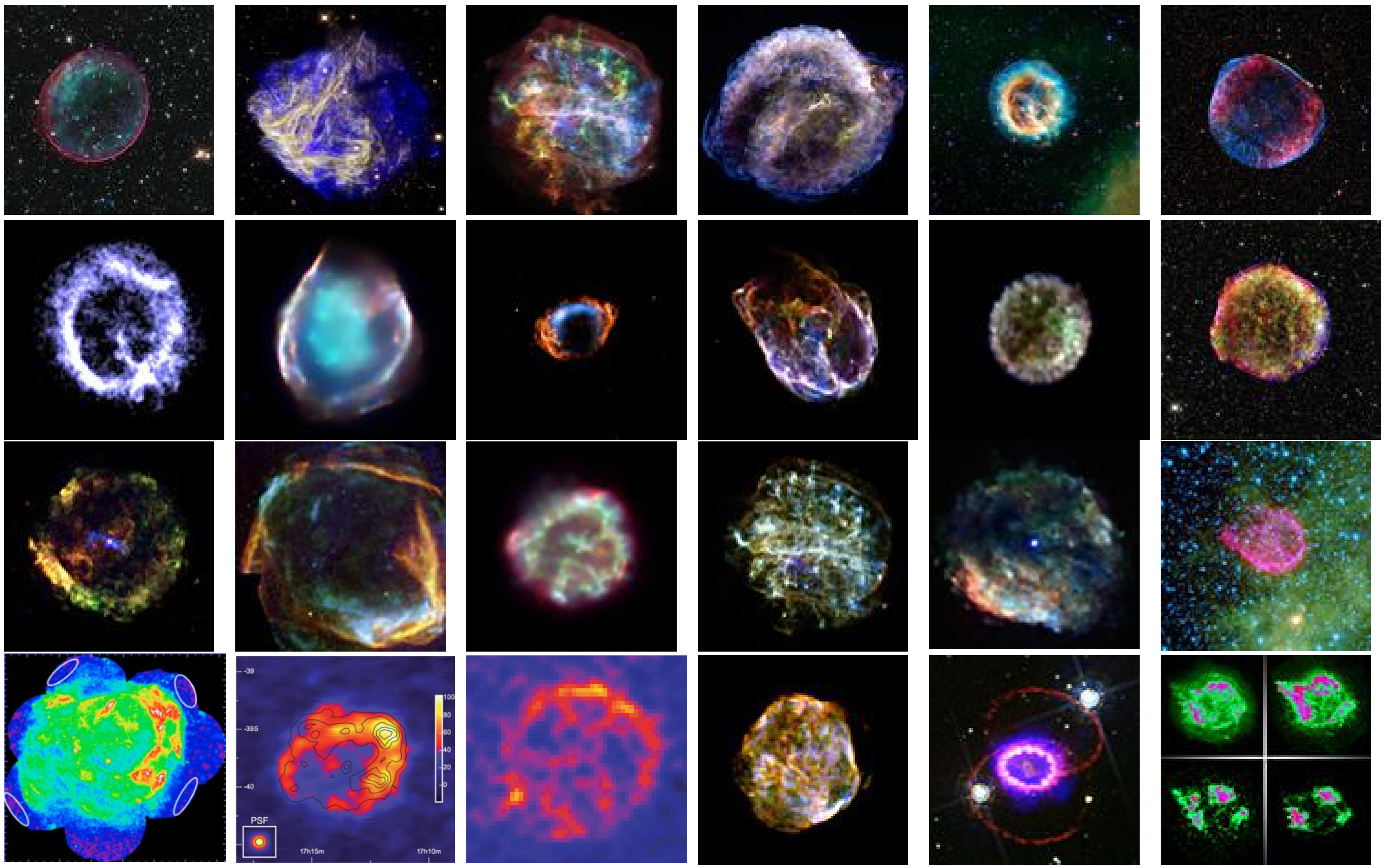

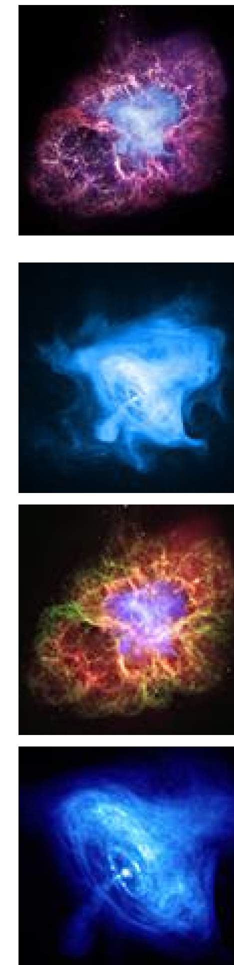

3: Supernova Remnants with Synchrotron X-ray and TeV

With a compact object at the center: Core Collapse SN

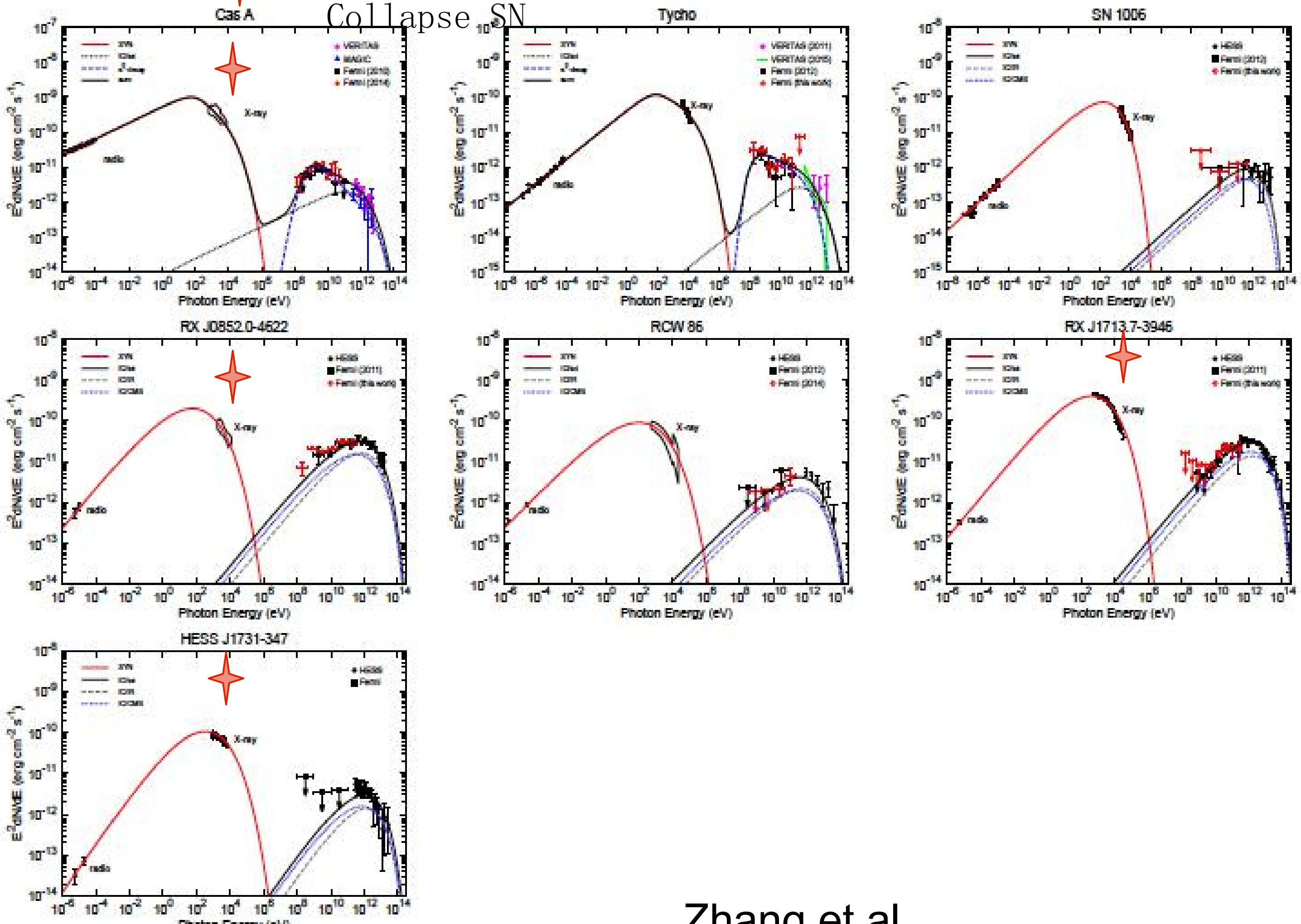

Zhang et al.

3: Evolution of Model Parameters

- With a compact object at the center: Core Collapse SN

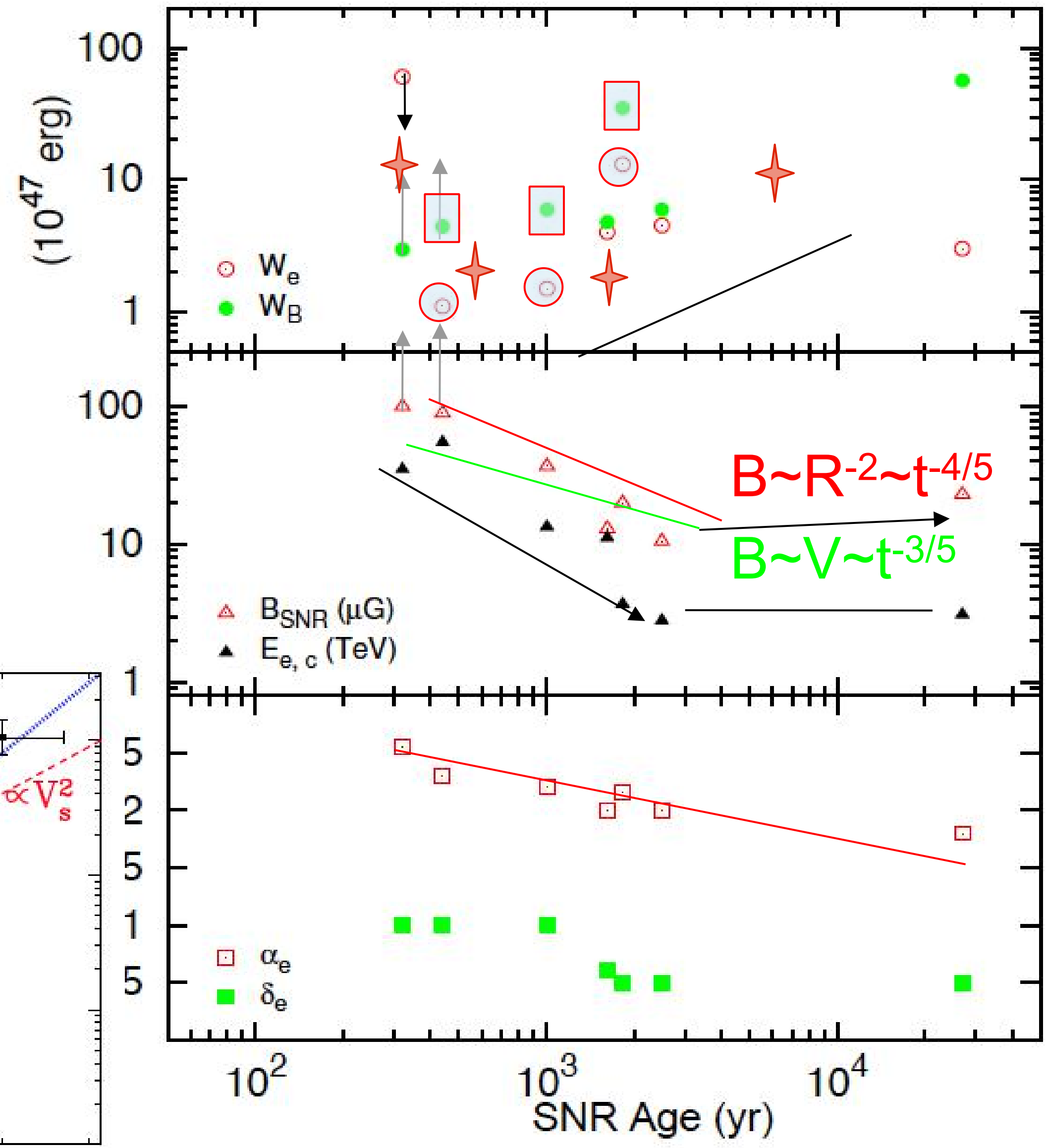

Astron Astrophys Rev (2012) 20:49
DOI 10.1007/s00159-011-0049-1

Supernova remnants: the X-ray perspective

Jacco Vink

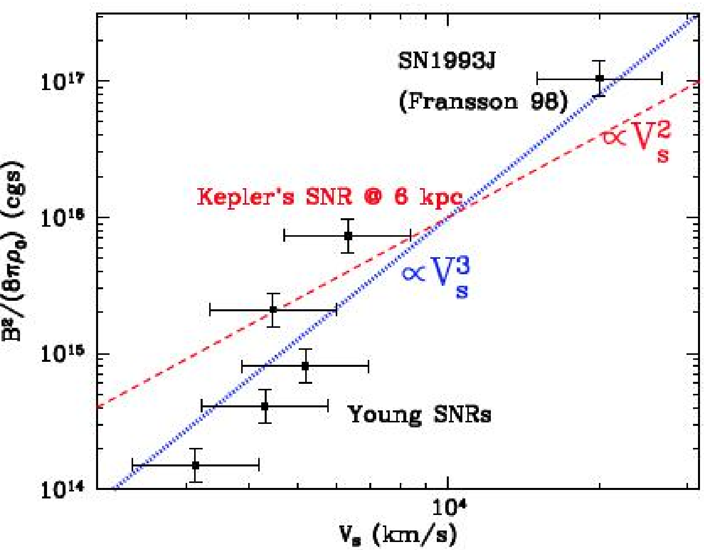

3: Three Supernova Remnants with compact central sources

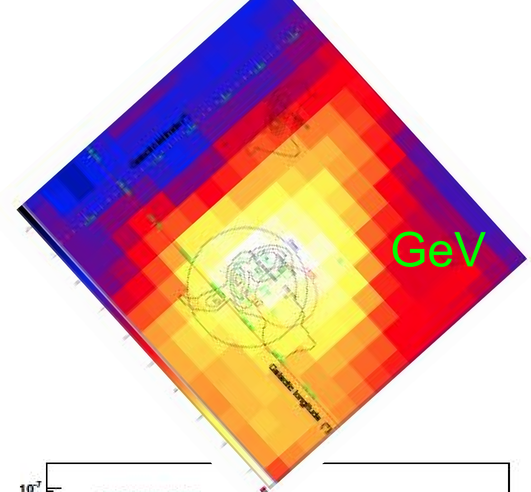

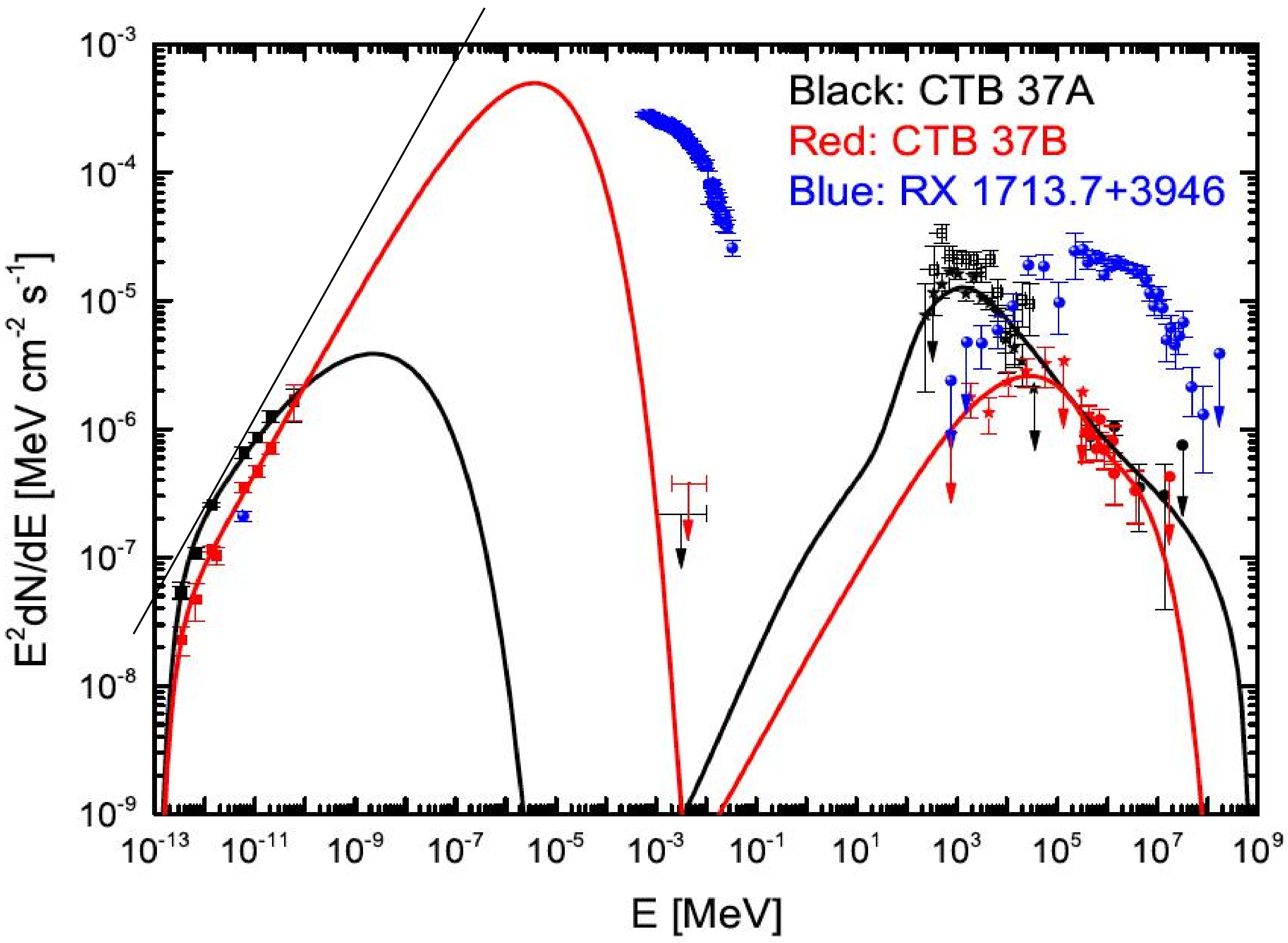

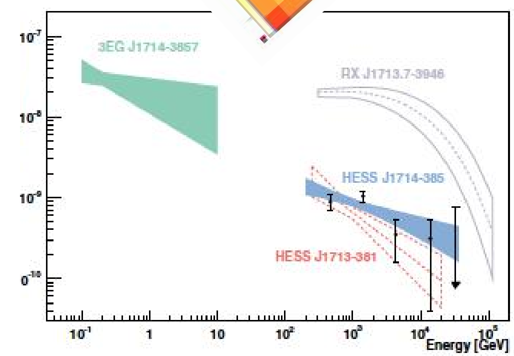

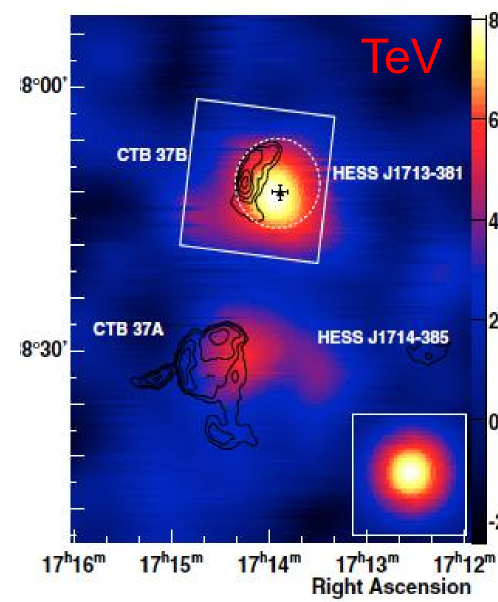

3: Spectral Evolution

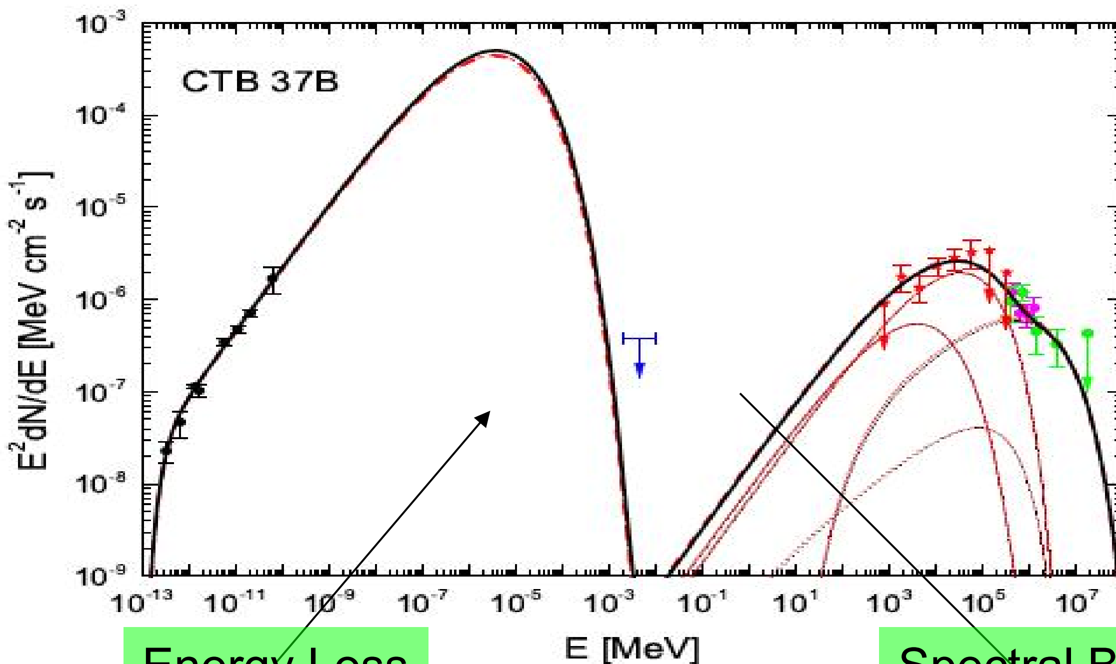

Energy Loss

Spectral Break

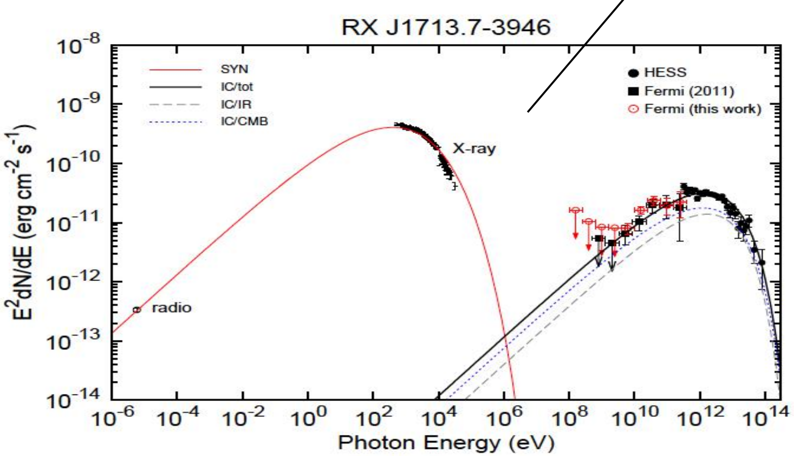

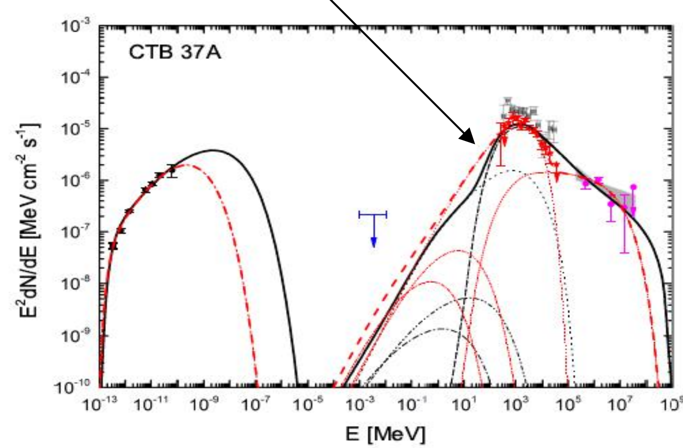

3: Model Parameters

Sources	$\log_{10} K_{ep}$	n_{ISM} cm^{-3}	α	$\log_{10} E_{br}$	$\log_{10} E_{e,cut}$ GeV	$\log_{10} E_{p,cut}$ GeV	$\log_{10} W_p$ erg	B μG
CTB 37A	-2.0	100.0	$2.38^{+0.02}_{-0.02}$		$2.49^{+0.41}_{-0.41}$	$5.20^{+0.52}_{-0.50}$	$49.77^{+0.02}_{-0.02}$	$125.153^{+5.88}_{-6.12}$
(case 1)	$0.13^{+0.08}_{-0.08}$	100.0	$1.43^{+0.13}_{-0.13}$		$0.87^{+0.09}_{-0.09}$	$4.32^{+0.20}_{-0.20}$	$48.57^{+0.08}_{-0.08}$	$42.56^{+2.31}_{-2.31}$
CTB 37A	-2.0	100.0	$1.49^{+0.03}_{-0.03}$	$0.34^{+0.15}_{-0.16}$	$1.81^{+0.69}_{-0.61}$	$6.51^{+0.98}_{-0.69}$	$49.74^{+0.02}_{-0.02}$	$185.80^{+22.52}_{-22.33}$
(case 2)	$-0.25^{+0.28}_{-0.28}$	100.0	$0.96^{+0.25}_{-0.27}$	$0.21^{+0.46}_{-0.49}$	$0.94^{+0.10}_{-0.10}$	$4.97^{+0.54}_{-0.56}$	$48.91^{+0.24}_{-0.24}$	$44.52^{+3.0}_{-3.0}$
CTB 37B	-2.0	0.5	$1.63^{+0.07}_{-0.07}$		$2.70^{+0.13}_{-0.13}$	$4.50^{+0.23}_{-0.31}$	$51.20^{+0.07}_{-0.07}$	$79.51^{+17.94}_{-18.68}$
	$-2.28^{+0.31}_{-0.34}$	0.5	$1.64^{+0.08}_{-0.08}$		$2.62^{+0.22}_{-0.17}$	$4.39^{+0.42}_{-0.70}$	$51.36^{+0.24}_{-0.20}$	$93.81^{+30.06}_{-30.06}$

3: Evolution of Model Parameters

- With a compact object at the center: Core Collapse SN

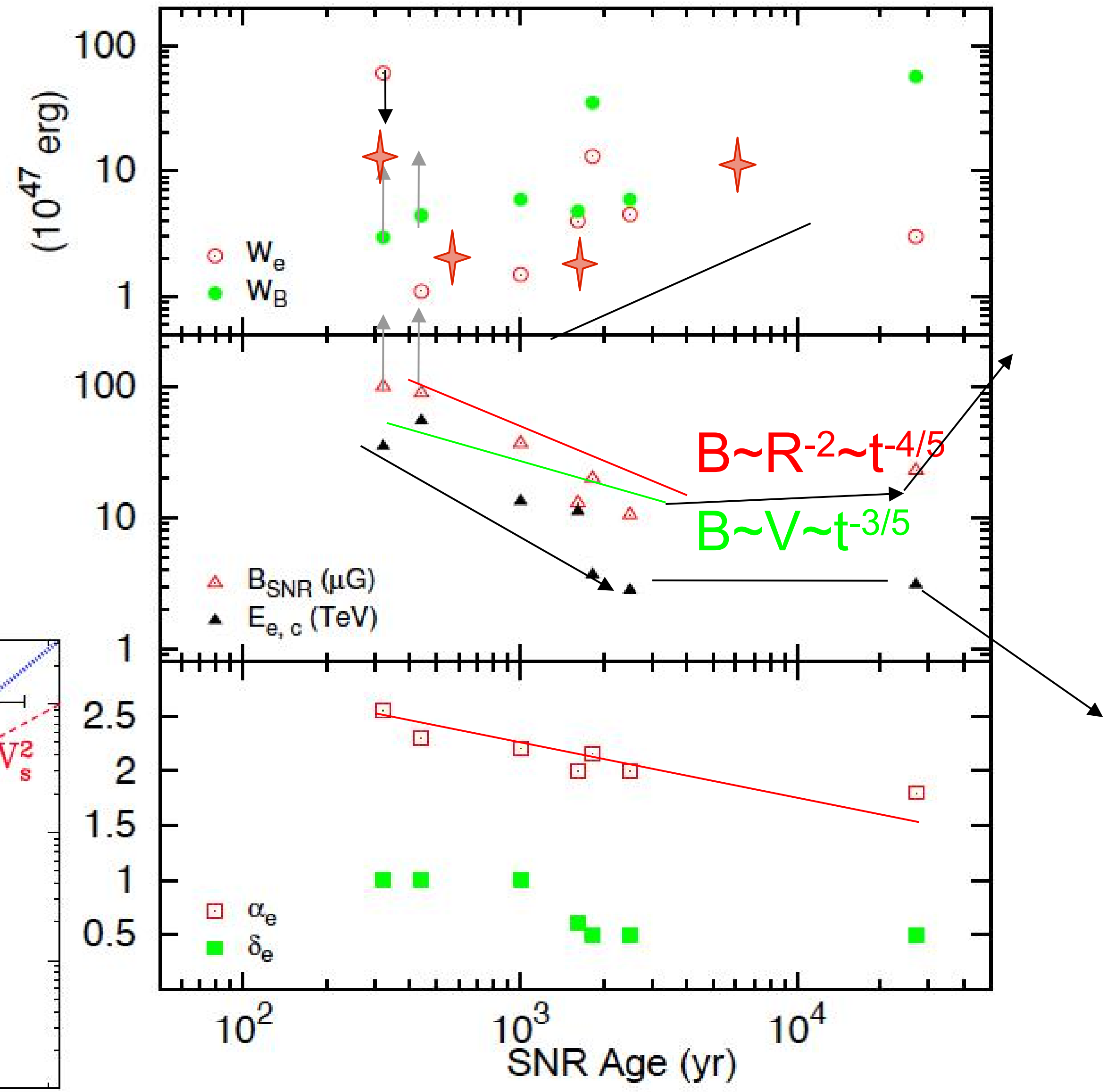

Astron Astrophys Rev (2012) 20:49
DOI 10.1007/s00159-011-0049-1

Supernova remnants: the X-ray perspective

Jacco Vink

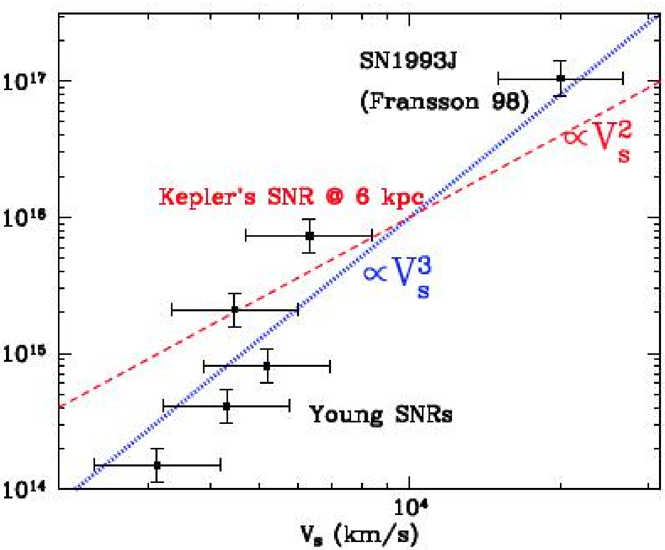

4: Conclusion

A century after the discovery of cosmic rays (1912), recent achievements in Gamma-ray astronomy strengthen the scenario that

SNRs are important sources of Galactic cosmic rays and

The radio to gamma-ray spectra vary significantly from source to source

Environment plays an important role in determining the emission characteristics of SNRs.

4: Conclusion

By carrying out detailed modeling of multi-wavelength observations, we can study the details of the physics relevant to shocks of SNRs:

1) Radio spectrum hardens with time

2) B field decreases with time in the Sedov Phase(<2K year), *then starts to increase gradually*

3) When interacting with molecular clouds, B field increases dramatically and a spectral break appears.

4) Type Ia remnant shows continuous increase in the energy contents of electrons and magnetic field with time

2: Gamma-ray Observations of SNRs

The 1[st] *Fermi* LAT Supernova Remnant Catalog

F. Acero[2], M. Ackermann[3], M. Ajello[4], L. Baldini[5,6], J. Ballet[2], G. Barbiellini[7,8], D. Bastieri[9,10], R. Bellazzini[11], E. Bissaldi[12], R. D. Blandford[6], E. D. Bloom[6],

Radio SNRs:

279

Total Energy:
<300*1e51ergs
=3e53 ergs
=1% 3e55 ergs

Age <1e5 years
=1% 1e7 Years

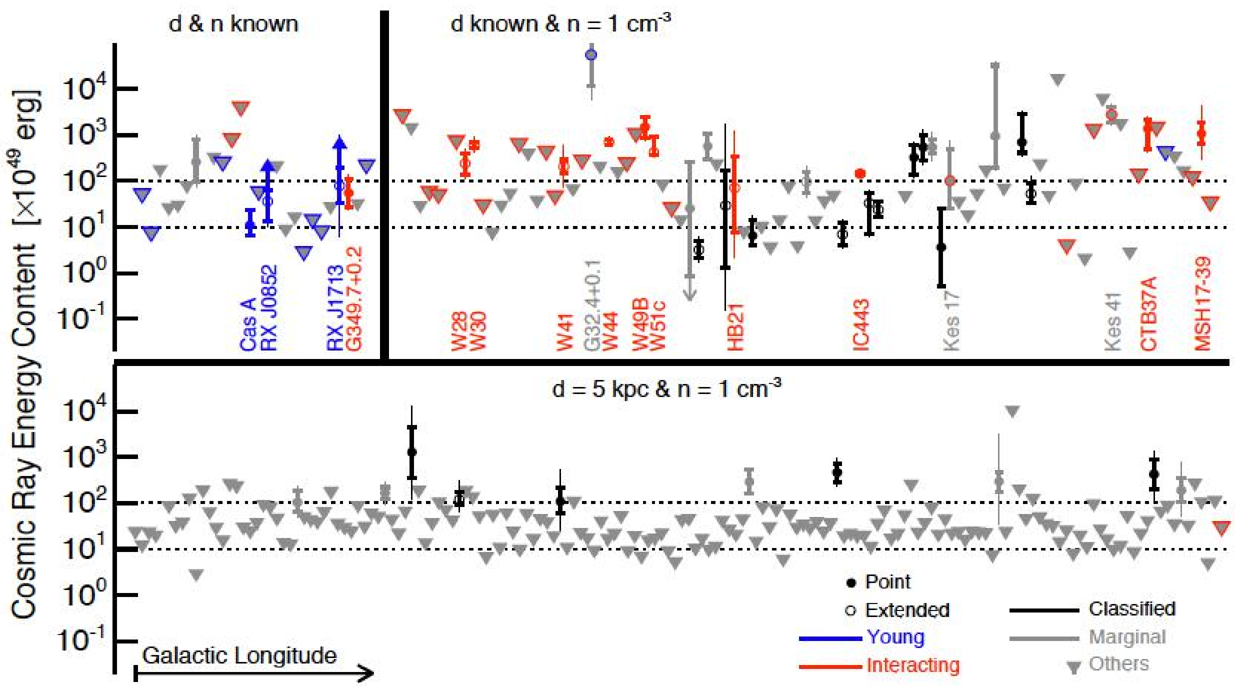

2: Cosmic Rays

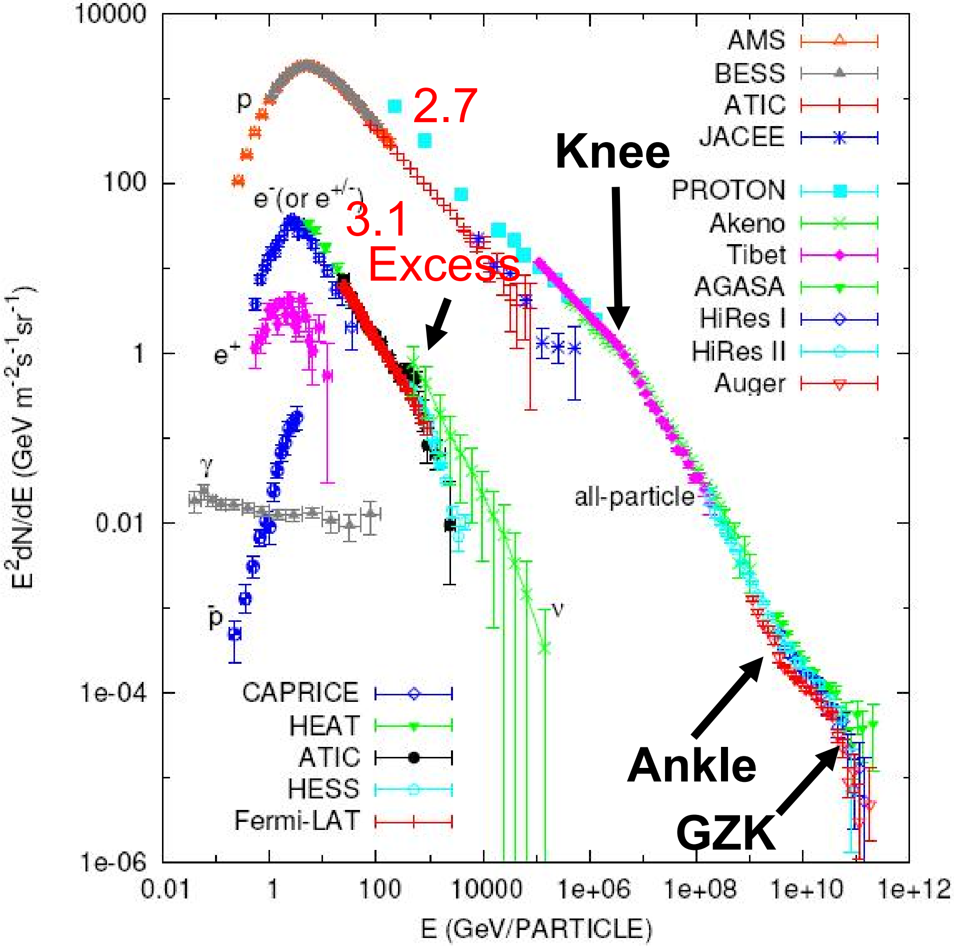

Dominated by Nuclei, there are also electrons, positrons and antiprotons

Age: ~ 10^7 Year

Energy density: ~ $1 eV/cm^3$

Power: ~ 10^{41} erg/s

~ 3e48 erg/year

e/p ~ 1% at 1GeV

Leptonic Excess at ~ 500GeV

Spectral Knee at ~ 1e15eV

and Ankle at ~ 1e18eV

Maximum Energy: 3×10^{20}eV

~ 50 Joule

GZK Cutoff at ~ 1e20 eV

3:RCW 86

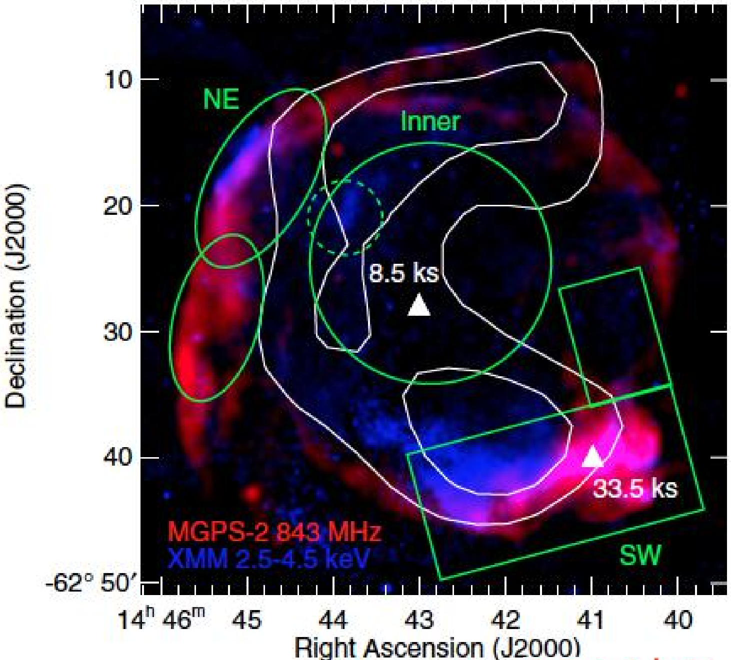

0.5-1.0 keV
1.0-2.0 keV
2.0-6.6 keV

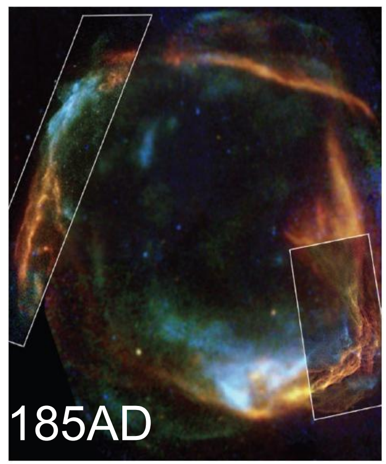

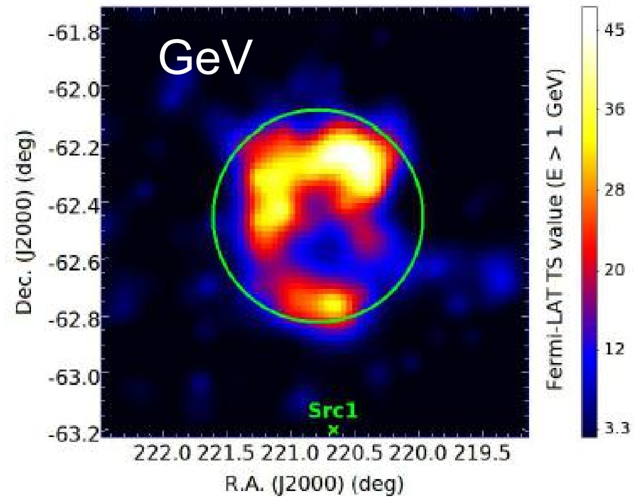

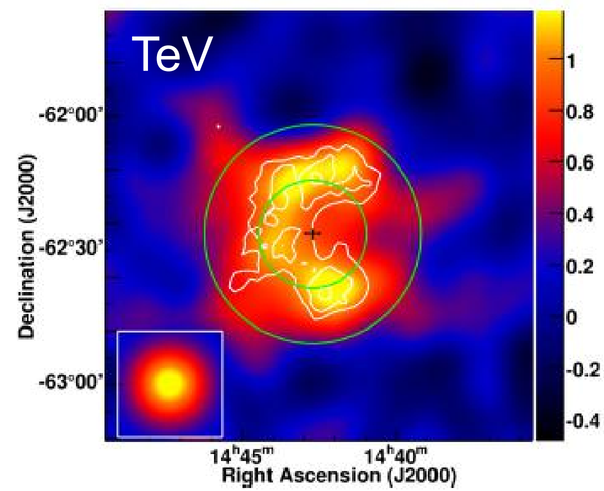

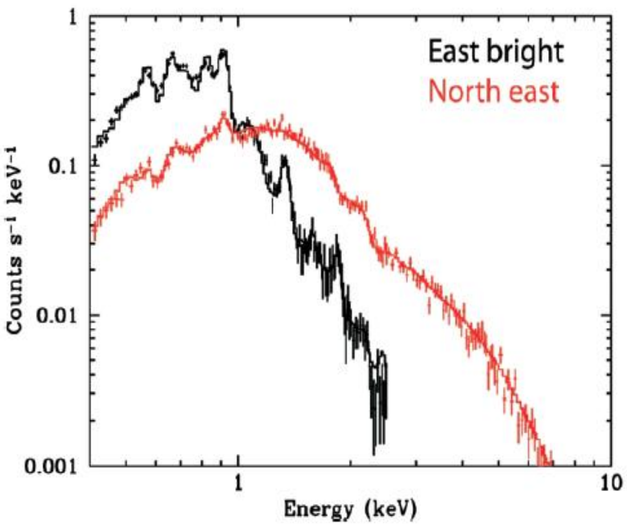

DEEP MORPHOLOGICAL AND SPECTRAL STUDY OF THE SNR RCW 86 WITH *FERMI*-LAT

M. Ajello[2], L. Baldini[3,4], G. Barbiellini[5,6], D. Bastieri[7,8], R. Bellazzini[9], E. Bissaldi[10], E. D. Bloom[4],

For region 1 (NW quadrant) $n_H \sim 1.5$ cm^{-3}; for region 2 (NE quadrant) $n_H \sim 1$ cm^{-3}; for region 3 (SE quadrant) $n_H \sim 1$ cm^{-3} and for region 4 (SW quadrant) $n_H \sim 1.2$ cm^{-3}. In all cases the intrinsic error of the quoted numbers is of about 20% taking into account the

3:RCW 86

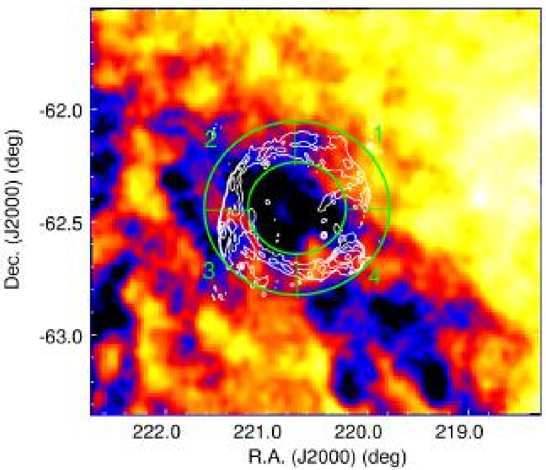

FIG. 8.— Neutral hydrogen distribution around RCW 86 at LSR radial velocity of -34 km s^{-1}. The green annulus delimits regions where the atomic density was estimated.

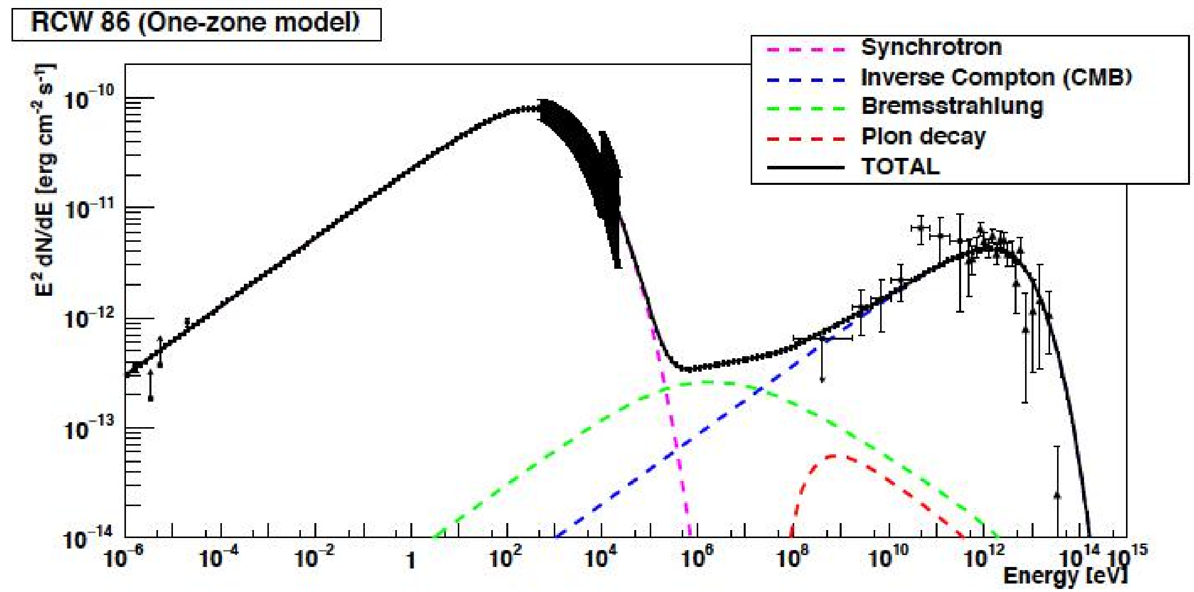

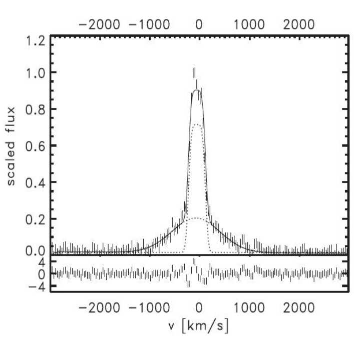

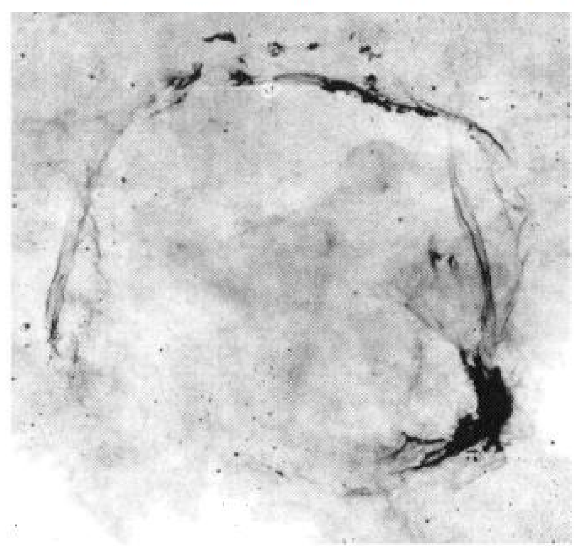

Parameters	One-zone
Density (cm^{-3})	0.1
B (μG)	10.2 ± 0.5
$\Gamma_{e,p}$	2.37 ± 0.03
E_{max} (TeV)	75 ± 5
η_e (% of E_{SN})	3.84 ± 0.5
η_p (% of E_{SN})	2
K_{ep} ($\times 10^{-2}$)	11.1 ± 1.5

2: Observations of SNRs:

Size vs Flux

Radio SNRs: 279 among them

Synchrotron X-Ray: 14

GeV SNRs: 30 among them

TeV SNRs: 10

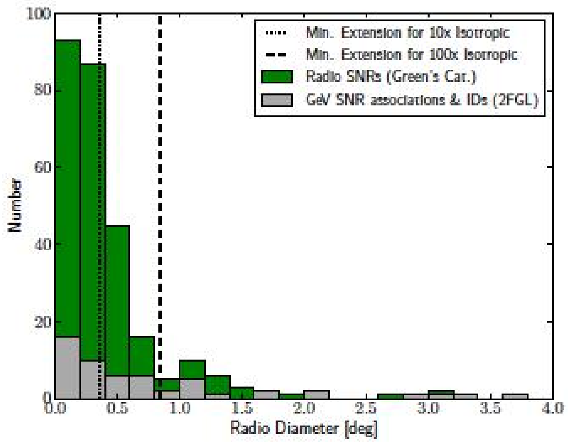

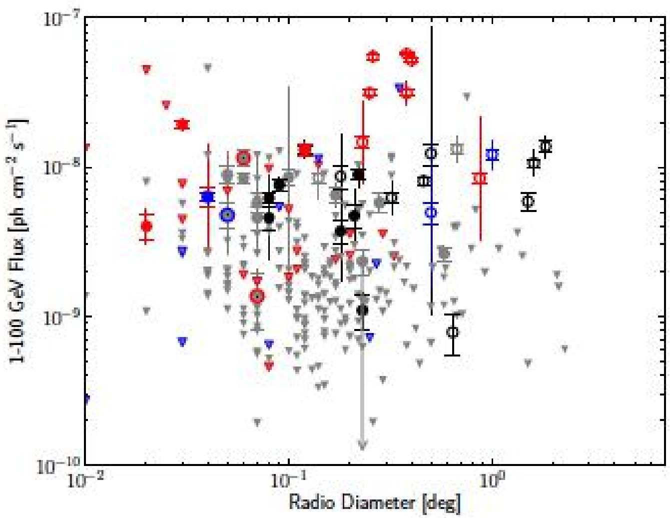

Radio Angular Diameter

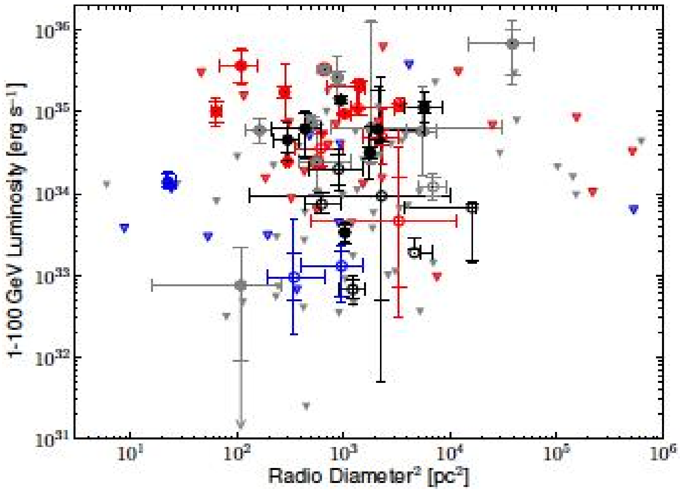

Radio Area

2: Observations of SNRs:

Spectral Index vs Flux

Radio SNRs: 279 among them

Synchrotron X-Ray: 14

GeV SNRs: 30 among them

TeV SNRs: 10

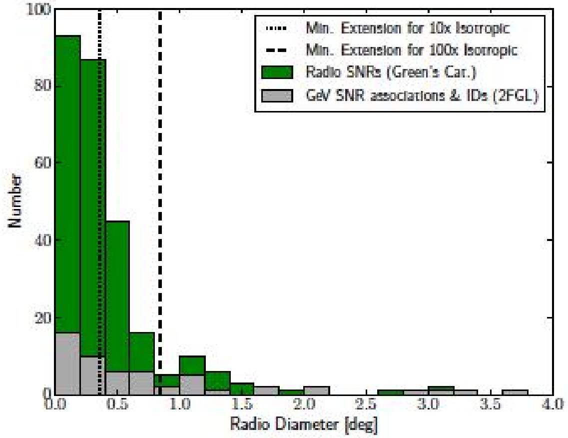

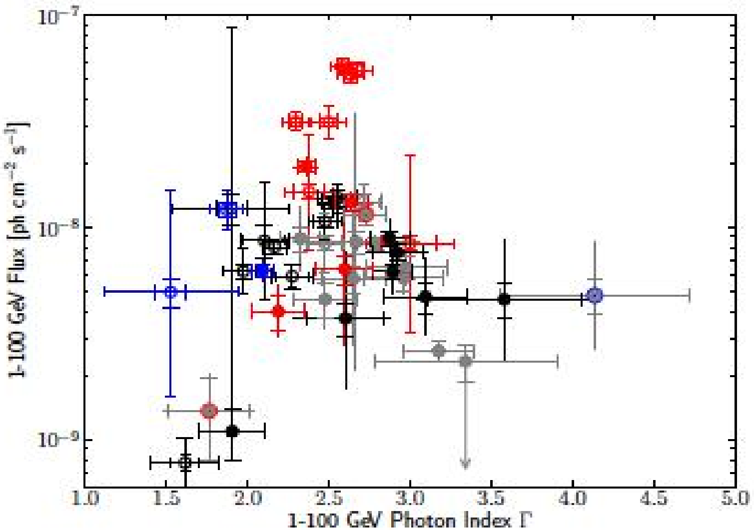

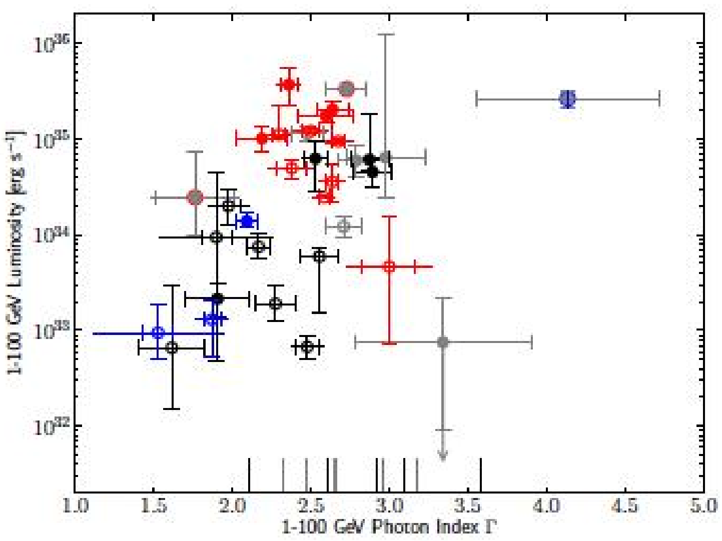

GeV Spectral Index

3: Shock interaction with partially ionised gas: the origin of broken power-laws

$$kp_{\parallel}/m = \pm\omega_c$$

$$p_{\rm br}/mc \simeq 10 B_{\mu}^{2} T_4^{-0.4} n_0^{-1} n_{\rm i}^{-1/2}$$

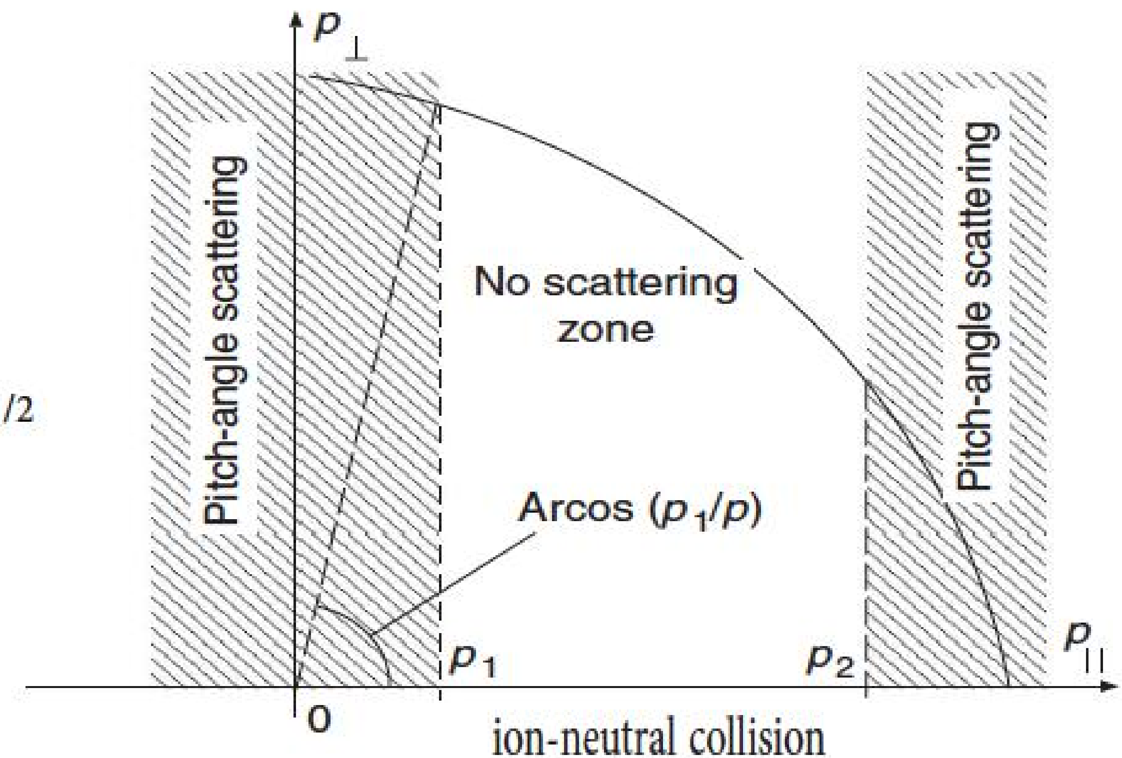

Mechanism for spectral break in cosmic ray proton spectrum of supernova remnant W44

M. A. Malkov[1], P. H. Diamond[1] & R. Z. Sagdeev[2]

2: Modeling of Gamma-ray Spectra

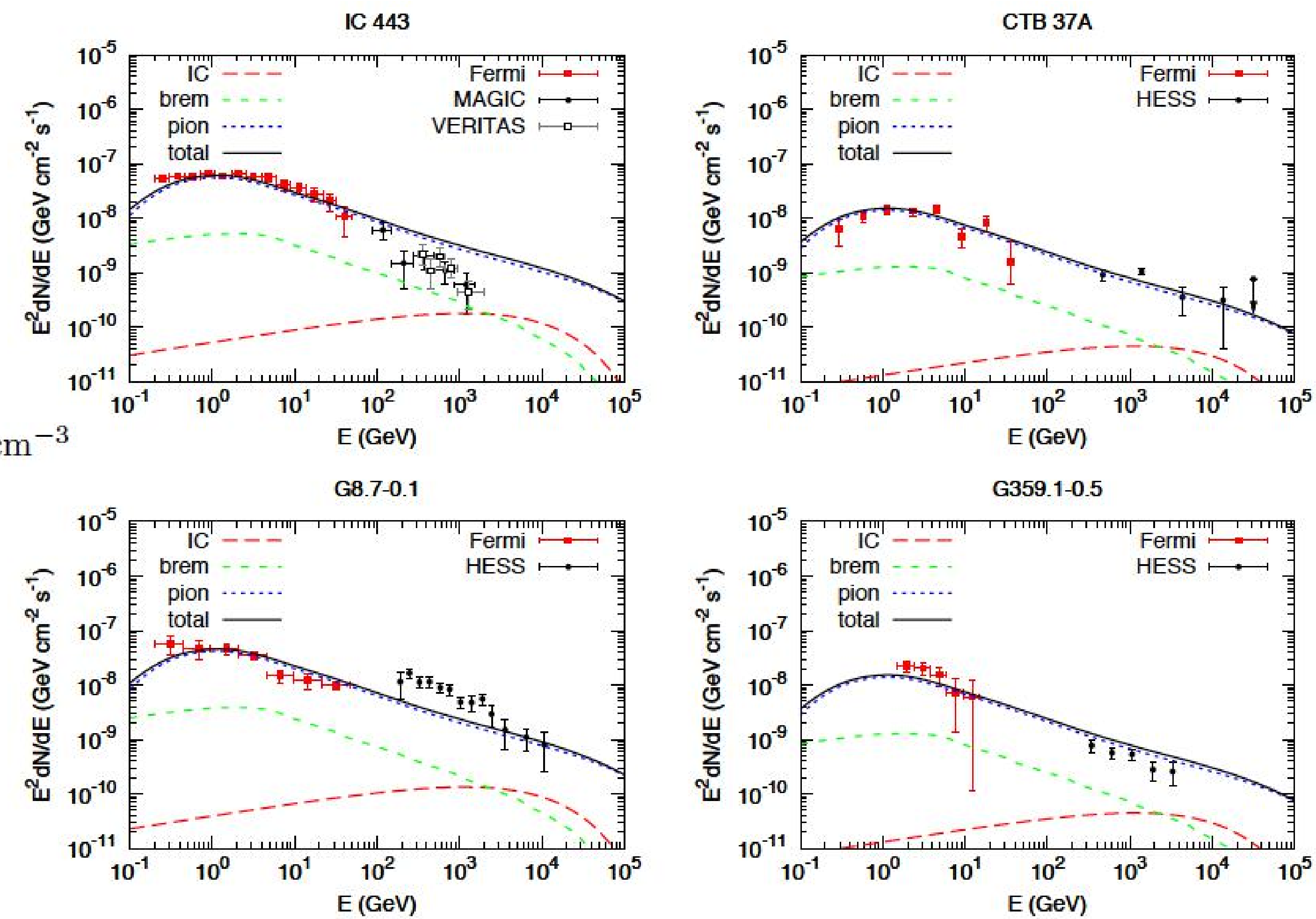

$n = 100 \text{ cm}^{-3}$

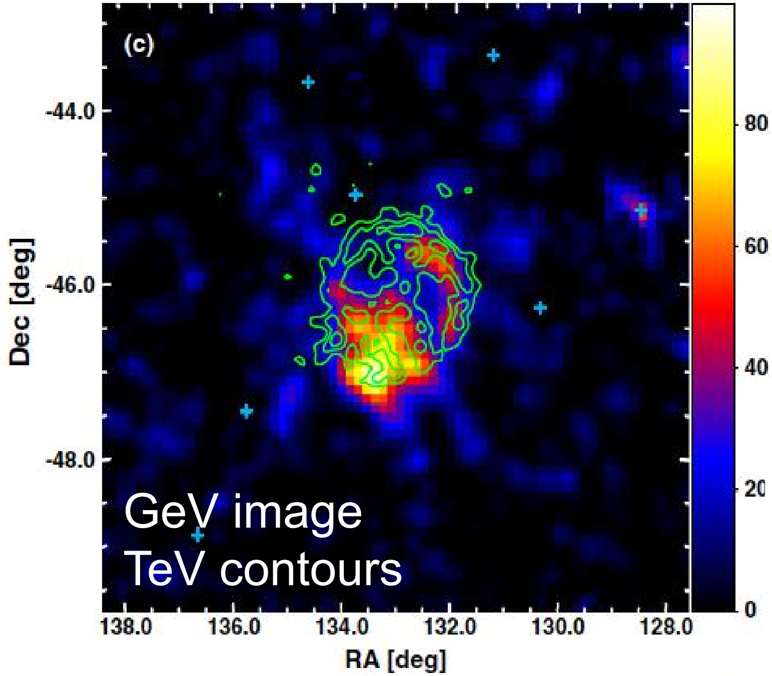

The Astrophysical Journal Letters, 740:L51 (5pp), 2011 October 20
doi:10.1088/2041-8205/74

GAMMA-RAY OBSERVATIONS OF THE SUPERNOVA REMNANT RX J0852.0−4622 WITH THE *FERMI* LARGE AREA TELESCOPE

T. Tanaka[1], A. Allafort[1], J. Ballet[2], S. Funk[1], F. Giordano[3,4], J. Hewitt[5], M. Lemoine-Goumard[6,9], H. Tajima[1,7], O. Tibolla[8], and Y. Uchiyama[1]

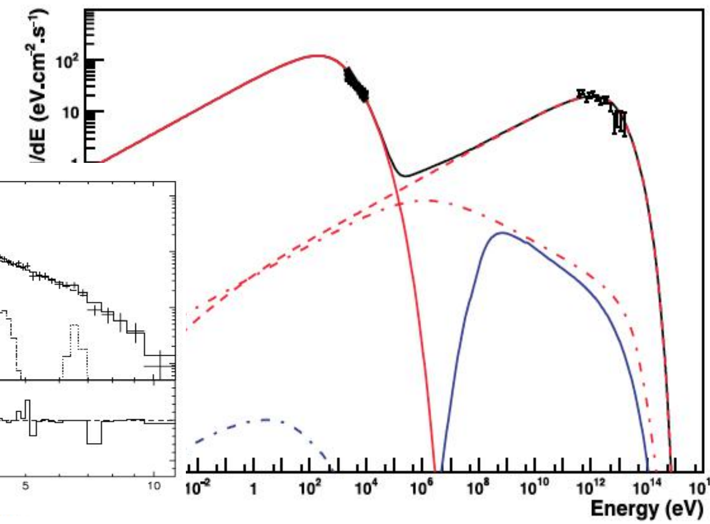

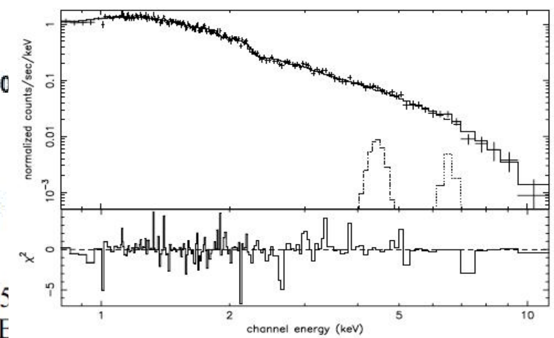

H.E.S.S. OBSERVATIONS OF THE SUPERNOVA REMNANT RX J085
AND SPECTRUM OF A WIDELY EXTENDED VERY HIGH E

F. Aharonian,[1] A. G. Akhperjanian,[2] A. R. Bazer-Bachi,[3] M. Beilicke,[4] W. Benbow,[1] D. Berge,[1,5]

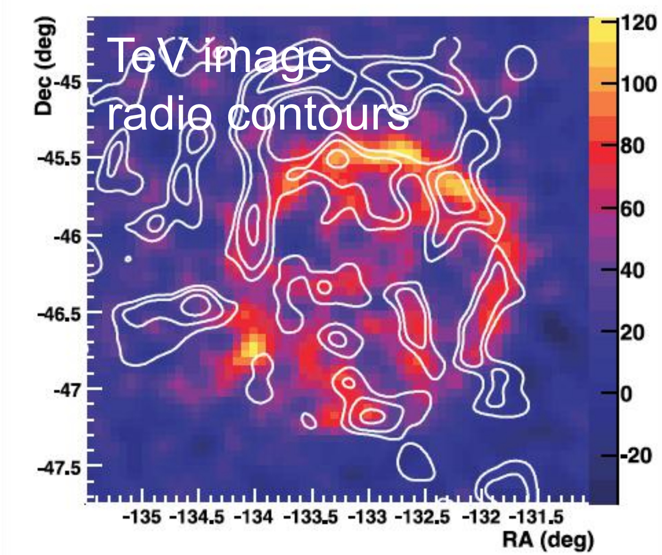

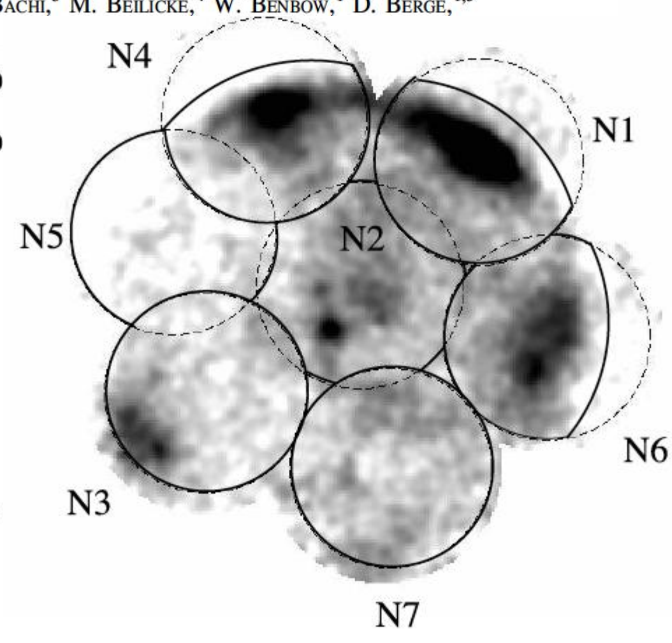

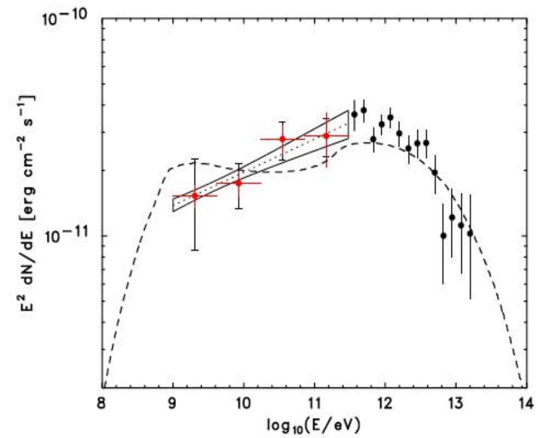

A new SNR with TeV shell-type morphology: HESS J1731-347

HESS Collaboration, A. Abramowski[1], F. Acero[2], F. Aharonian[3,4,5], A. G. Akhperjanian[6,5], G. Anton[7], A. Balzer[7],

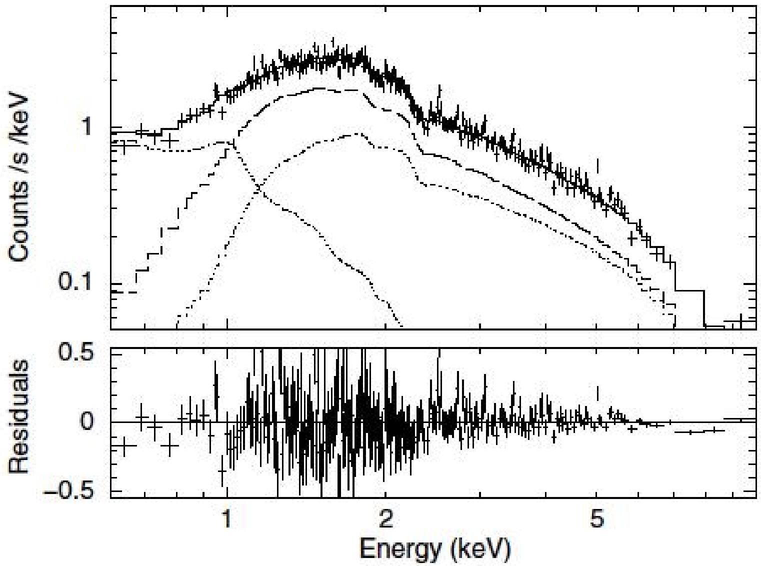

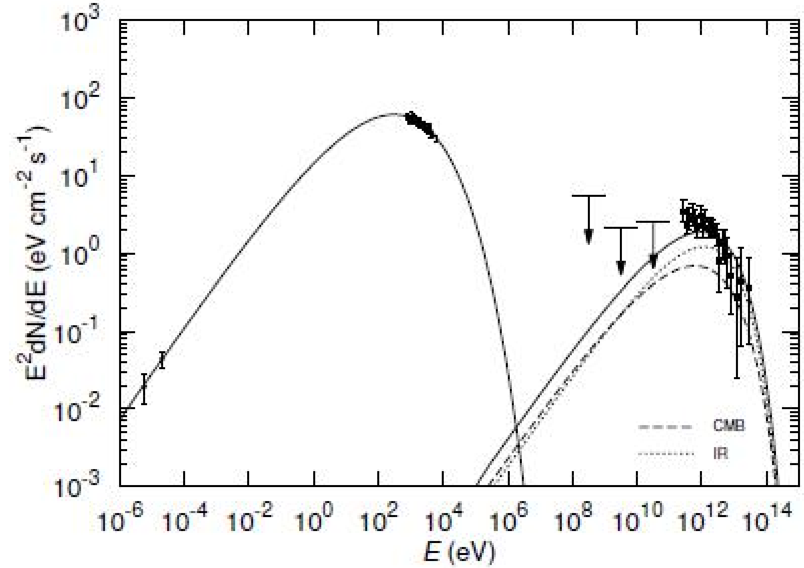

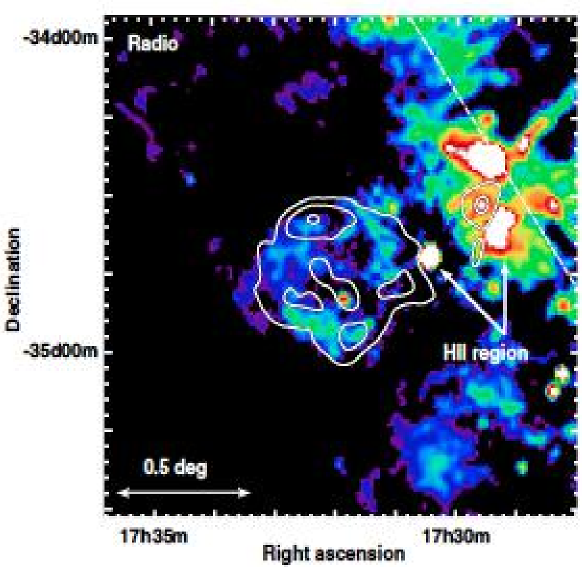

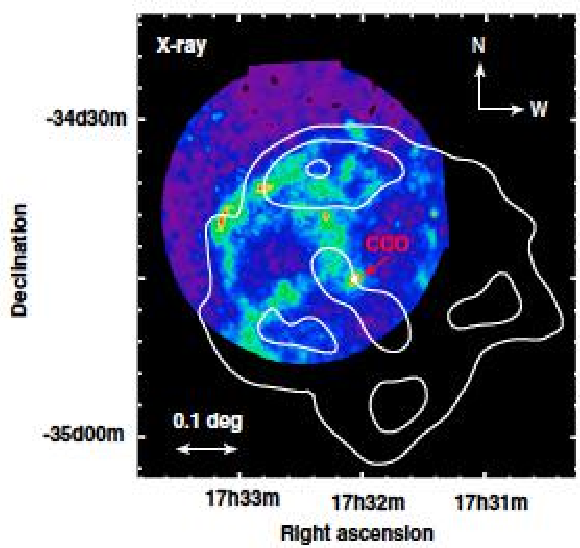

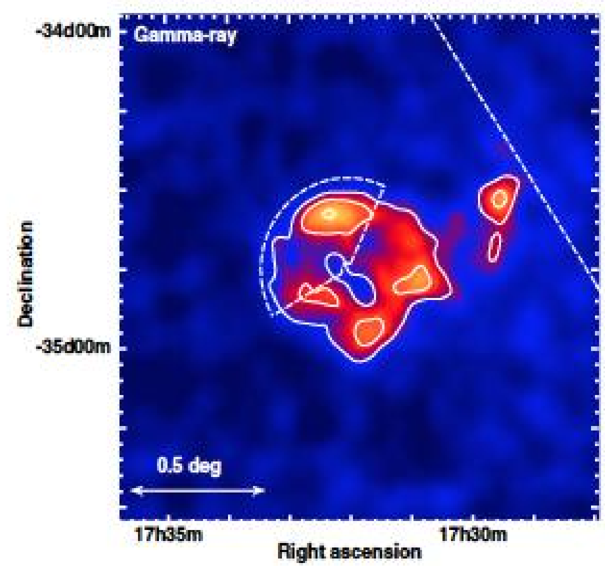

DISCOVERY OF TEV GAMMA RAY EMISSION FROM TYCHO'S SUPERNOVA REMNANT

V. A. Acciari[1], E. Aliu[2], T. Arlen[3], T. Aune[4], M. Beilicke[5], W. Benbow[1], S. M. Bradbury[6], J. H. Buckley[5],

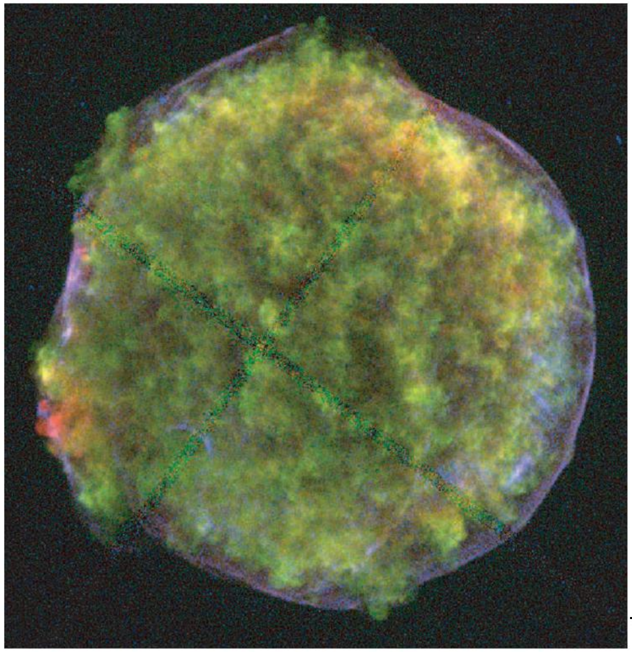

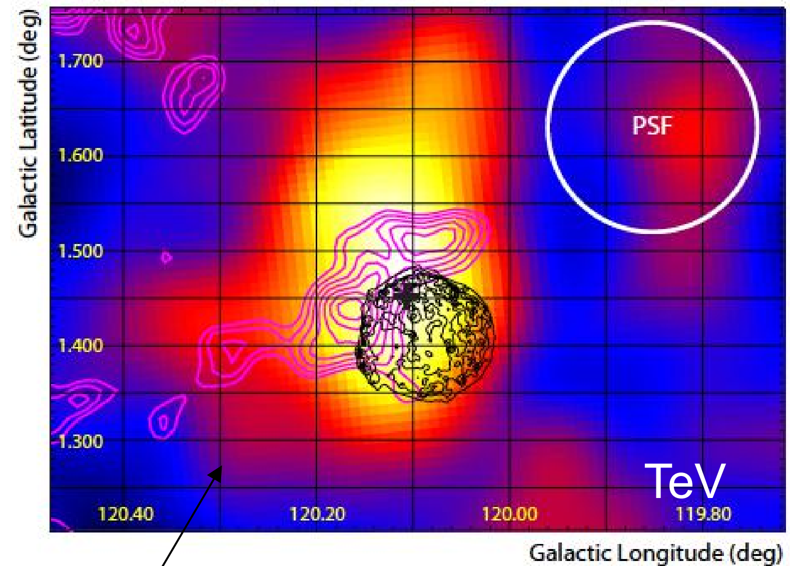

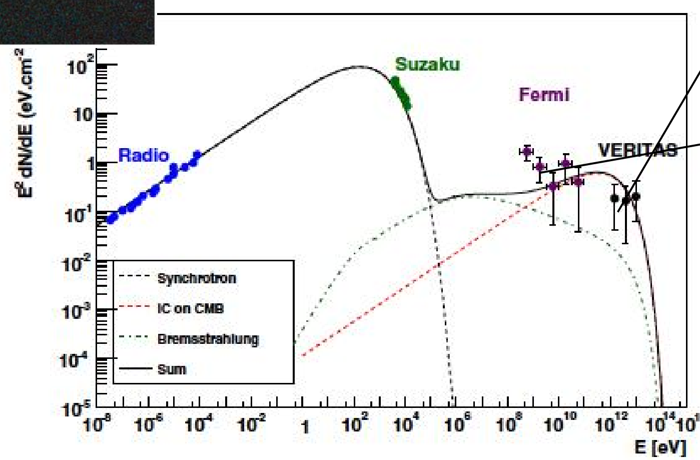

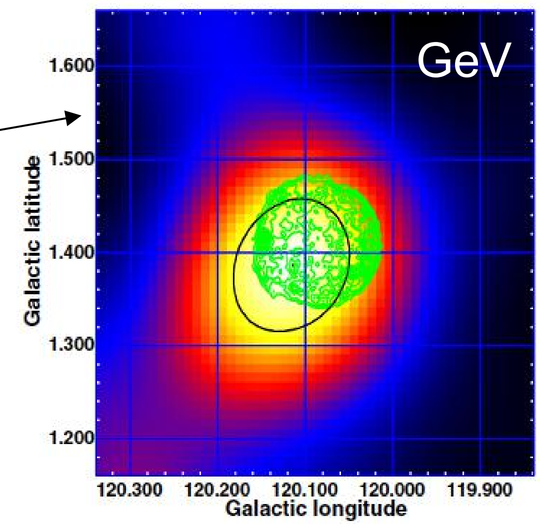

FERMI LARGE AREA TELESCOPE DETECTION OF THE YOUNG SUPERNOVA REMNANT TYCHO

F. Giordano[1,2], M. Naumann-Godo[3], J. Ballet[3], K. Bechtol[4], S. Funk[4], J. Lande[4], M. N. Mazziotta[2], S. Rainò[2],

FERMI-LAT DISCOVERY OF GeV GAMMA-RAY EMISSION FROM THE YOUNG SUPERNOVA REMNANT CASSIOPEIA A

A. A. Abdo[1,2], M. Ackermann[3], M. Ajello[3], A. Allafort[3], L. Baldini[4], J. Ballet[5], G. Barbiellini[6,7], M. G. Baring[8],

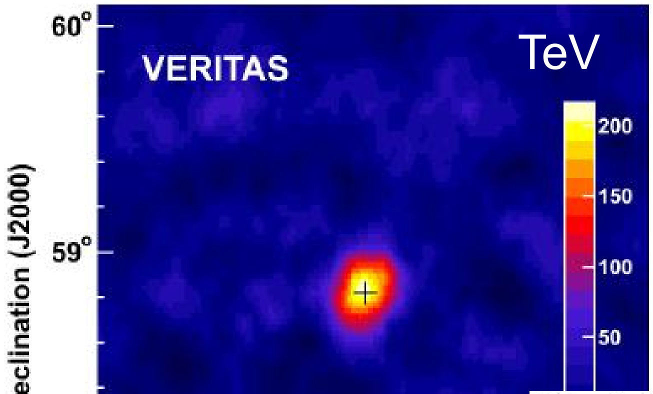

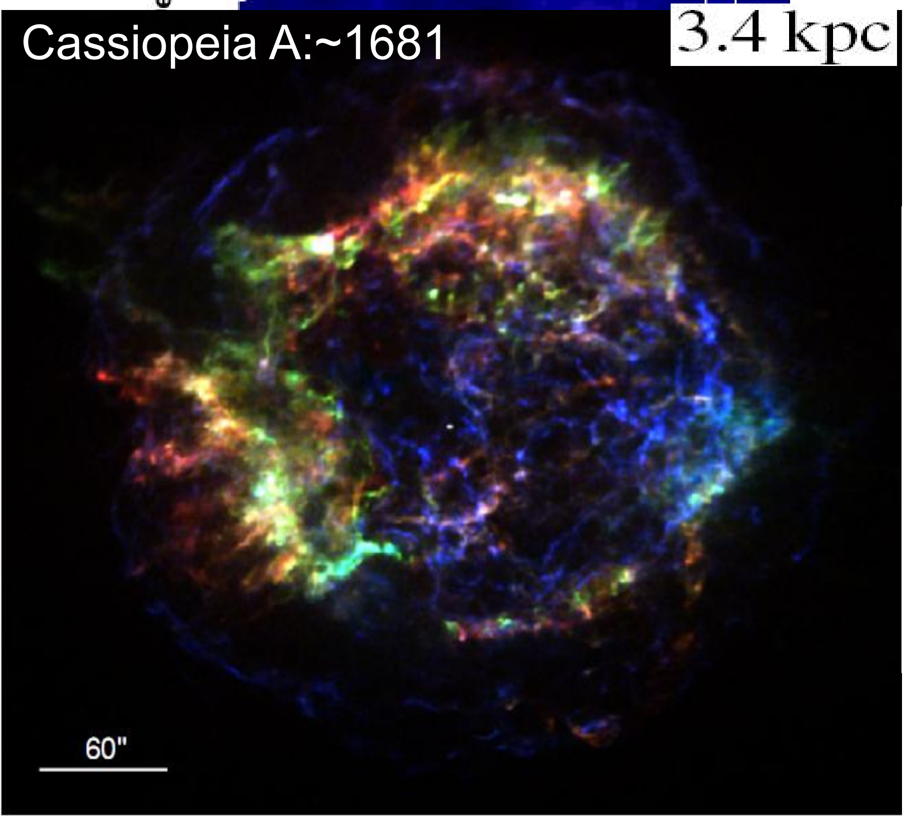

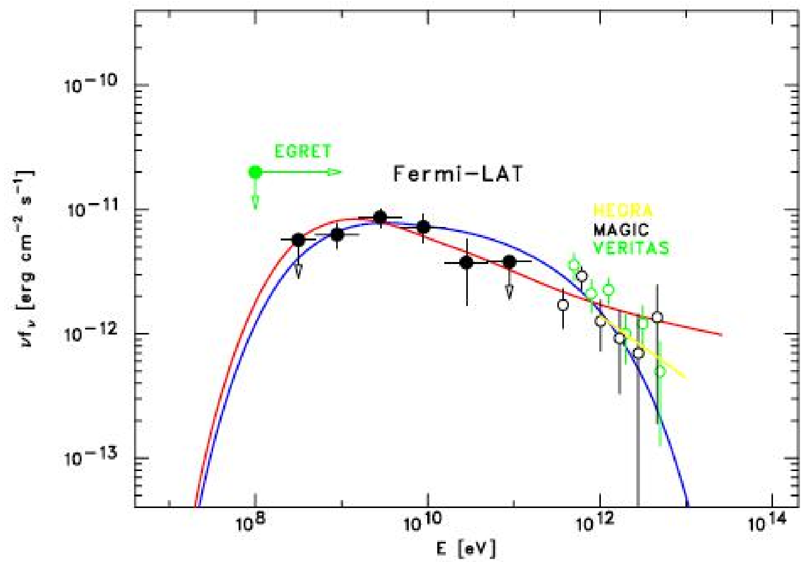

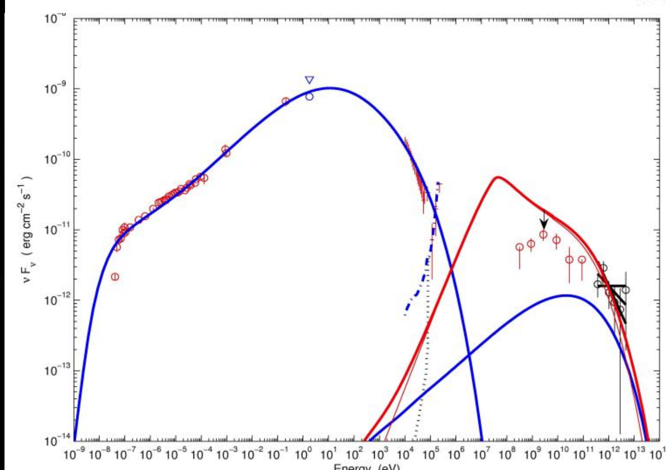

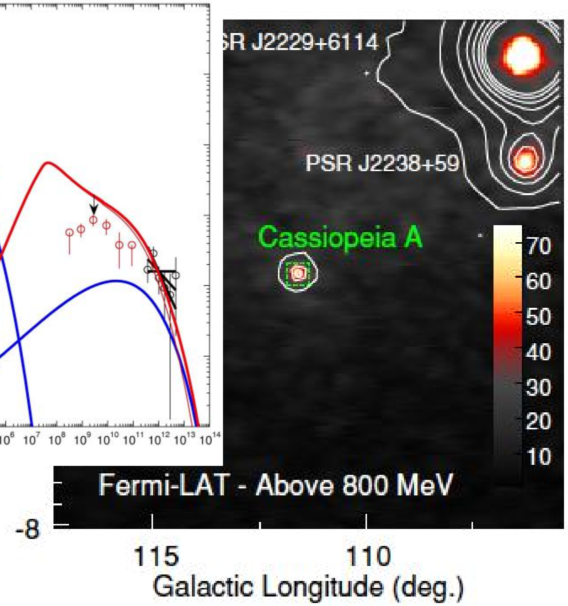

1: Summary

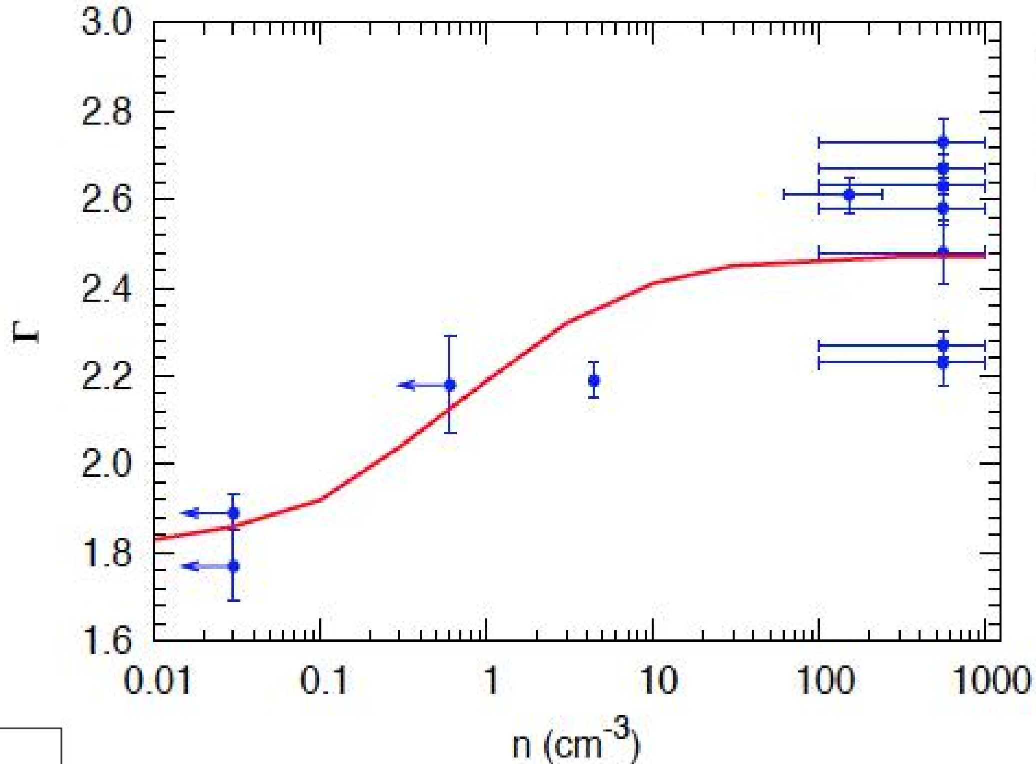

3.0
2.8
2.6
2.4
2.2
2.0
1.8
1.6
Γ
0.01
0.1
1
10
100
1000
n (cm-3)

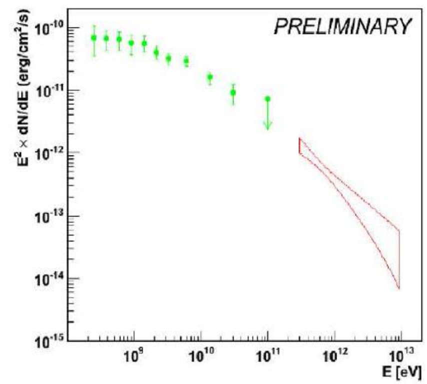

PRELIMINARY
E2 × dN/dE (erg/cm2/s)
E [eV]

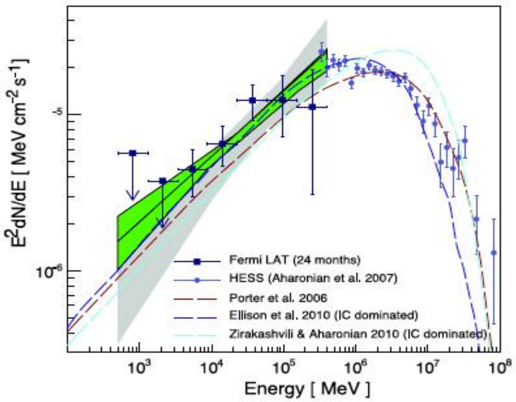

E2dN/dE [MeV cm-2 s-1]
Energy [MeV]
Fermi LAT (24 months)
HESS (Aharonian et al. 2007)
Porter et al. 2006
Ellison et al. 2010 (IC dominated)
Zirakashvili & Aharonian 2010 (IC dominated)

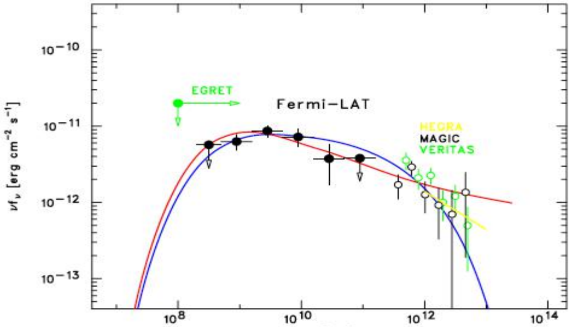

EGRET
Fermi-LAT
HEGRA
MAGIC
VERITAS
νfν [erg cm-2 s-1]
E [eV]

1: Modeling of Gamma-ray Spectra

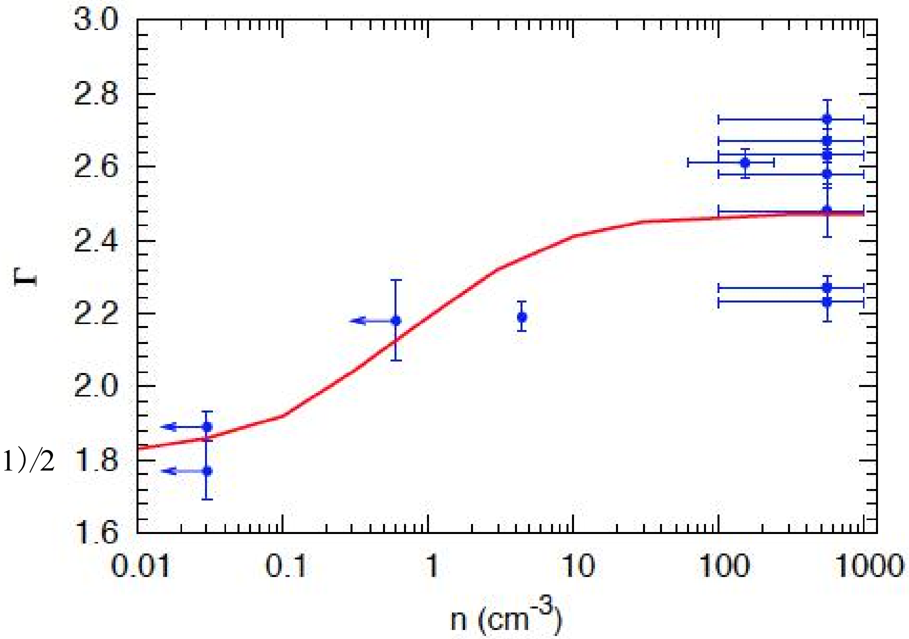

$alpha = 2.52$

$(alpha + 1)/2$

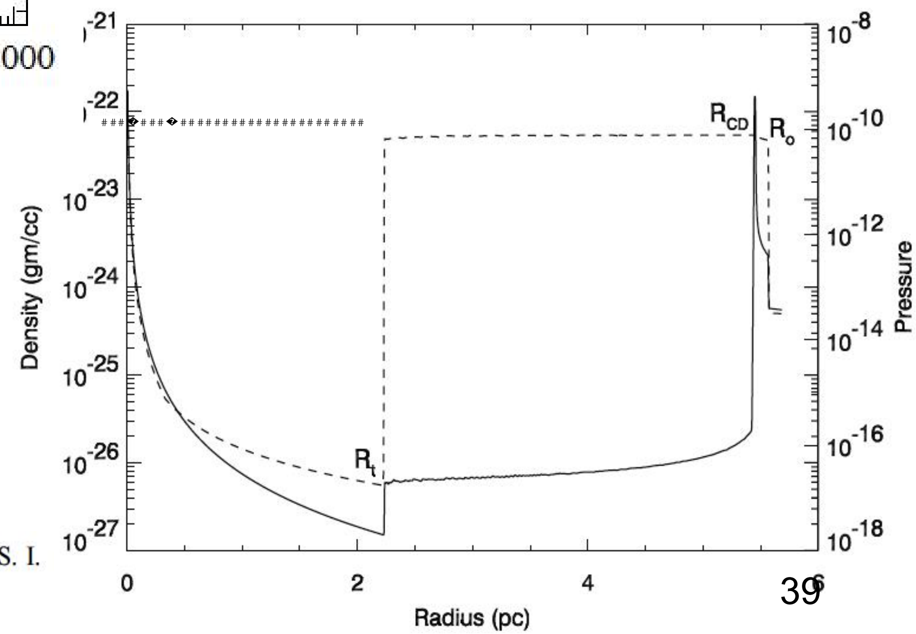

THE EVOLUTION OF SUPERNOVAE IN CIRCUMSTELLAR WIND-BLOWN BUBBLES. I. INTRODUCTION AND ONE-DIMENSIONAL CALCULATIONS

VIKRAM V. DWARKADAS

γ-rays from molecular clouds illuminated by accumulated diffusive protons. II: interacting supernova remnants

Hui Li[1] and Yang Chen[1,2]⋆
[1] Department of Astronomy, Nanjing University, Nanjing 210093, P. R. China
[2] Key Laboratory of Modern Astronomy and Astrophysics, Nanjing University, Ministry of Education, Nanjing 210093, China

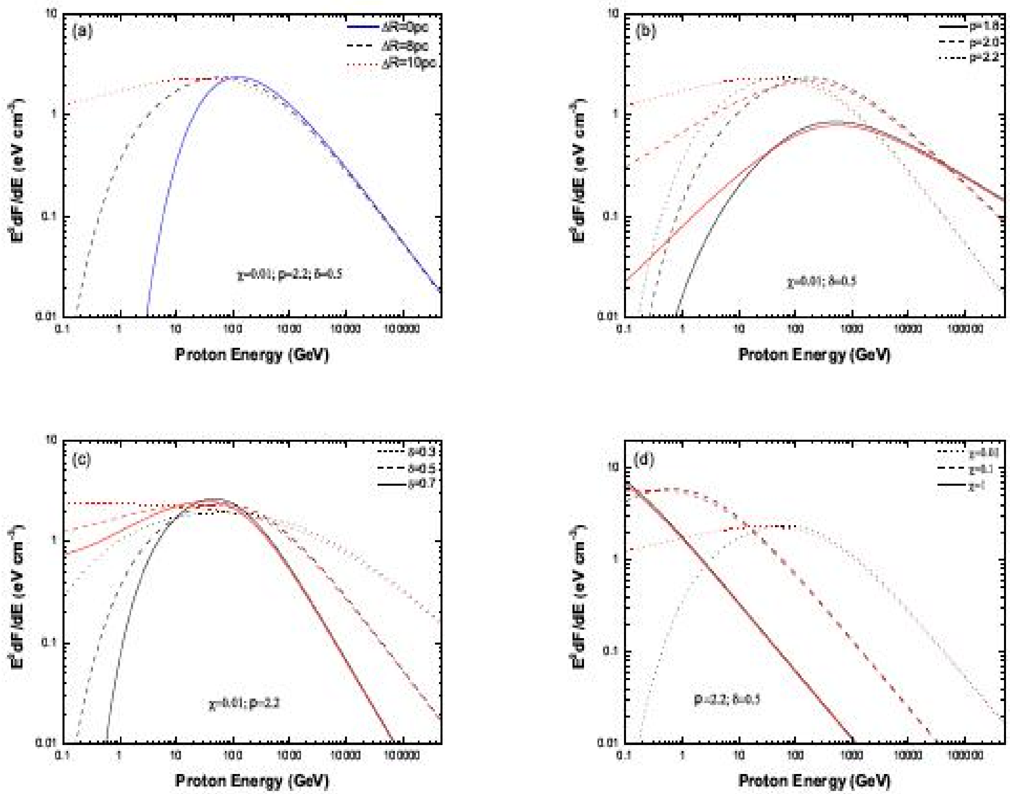

2: Shell Type TeV SNRs

A joint spectro-imaging analysis of the *XMM-Newton* and HESS observations of the supernova remnant RX J1713.7-3946

F. Acero[1], J. Ballet[1], A. Decourchelle[1], M. Lemoine-Goumard[2,3], M. Ortega[4], E. Giacani[4], G. Dubner[4], and G. Cassam-Chenaï[5]

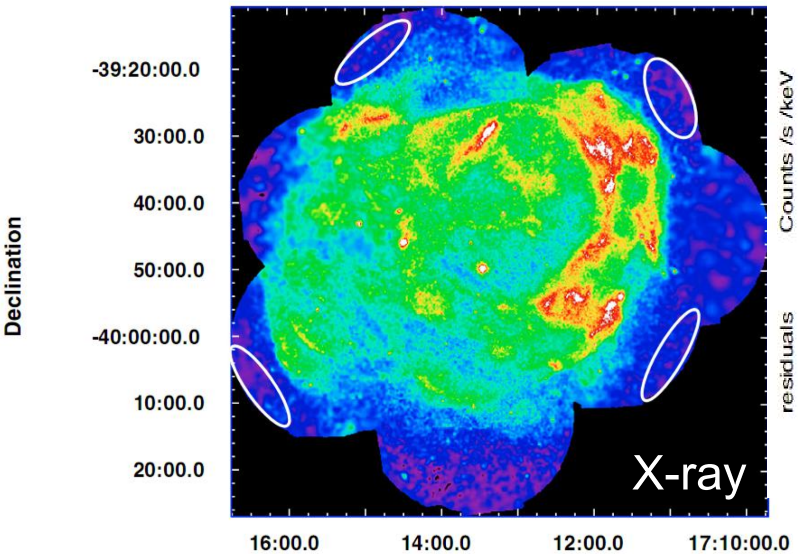

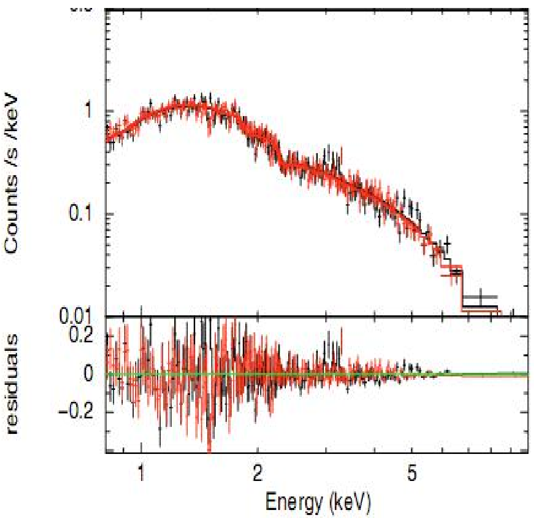

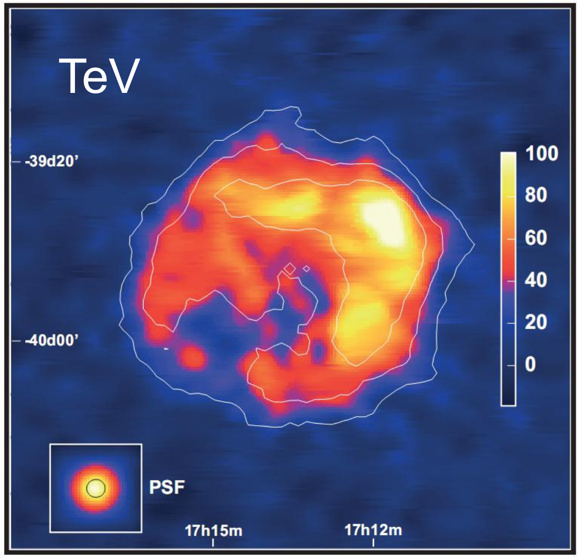

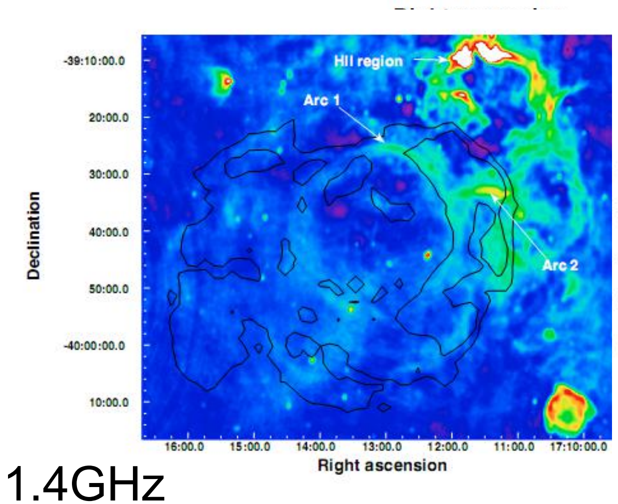

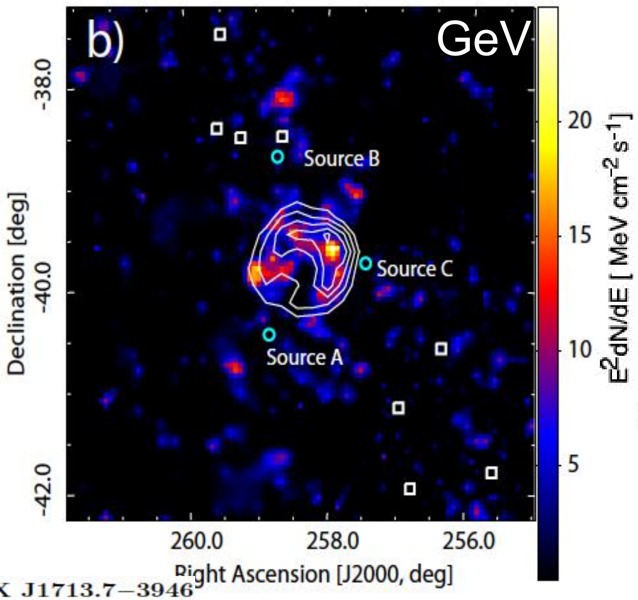

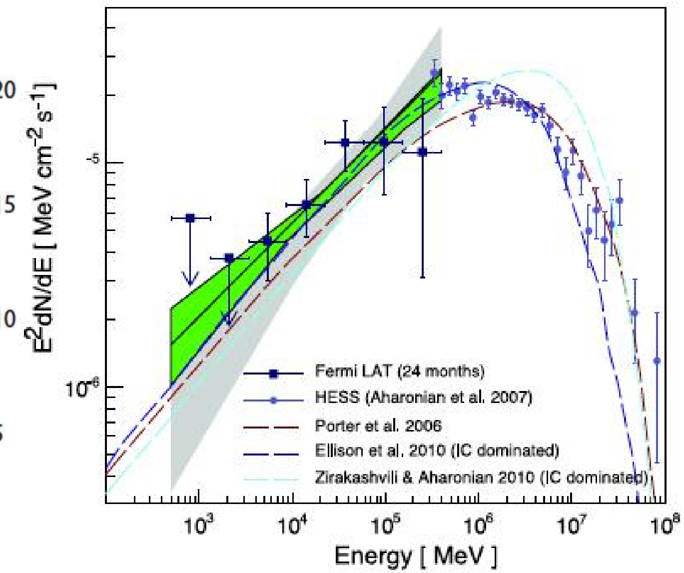

Observations of the young Supernova remnant RX J1713.7−3946 with the *Fermi* Large Area Telescope

A. A. Abdo[2], M. Ackermann[3,1], M. Ajello[3], A. Allafort[3], L. Baldini[4], J. Ballet[5],

DERIVATION OF THE ELECTRON DISTRIBUTION IN SUPERNOVA REMNANT RX J1713.7−3946 VIA A SPECTRAL INVERSION METHOD

Hui Li[1], Siming Liu[2], and Yang Chen[1,3]
[1] Department of Astronomy, Nanjing University, Nanjing 210093, China
[2] Key Laboratory of Dark Matter and Space Astronomy, Purple Mountain Observatory, Chinese Academy of Sciences, Nanjing 210008, China

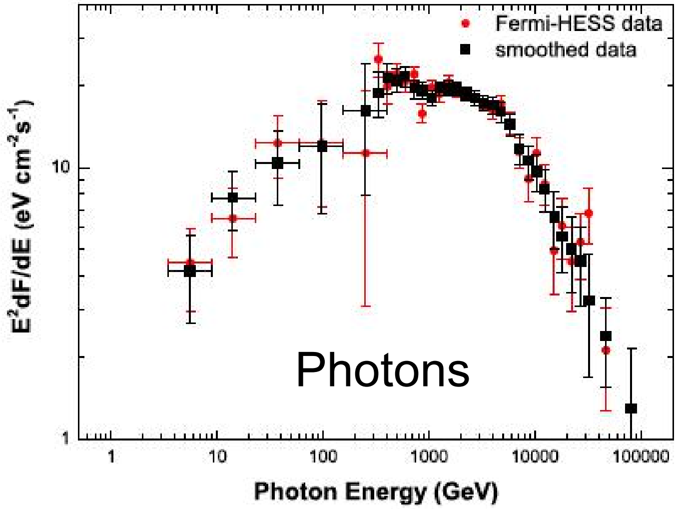

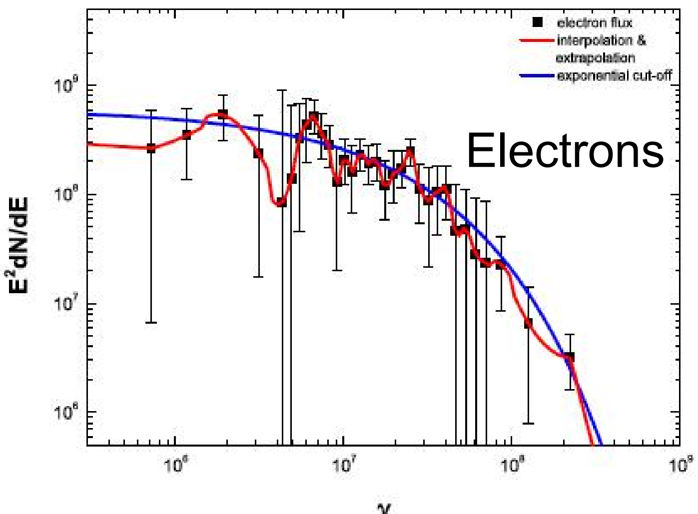

$$\gamma^{-2} \exp\left[-(\gamma/1.3 \times 10^{7})^{0.6}\right]$$

$$P(k) = ck \int d\gamma\, N(\gamma) \int d\epsilon\, n_{\rm ph}(\epsilon)\sigma_{\rm IC}(k, \epsilon; \gamma),$$

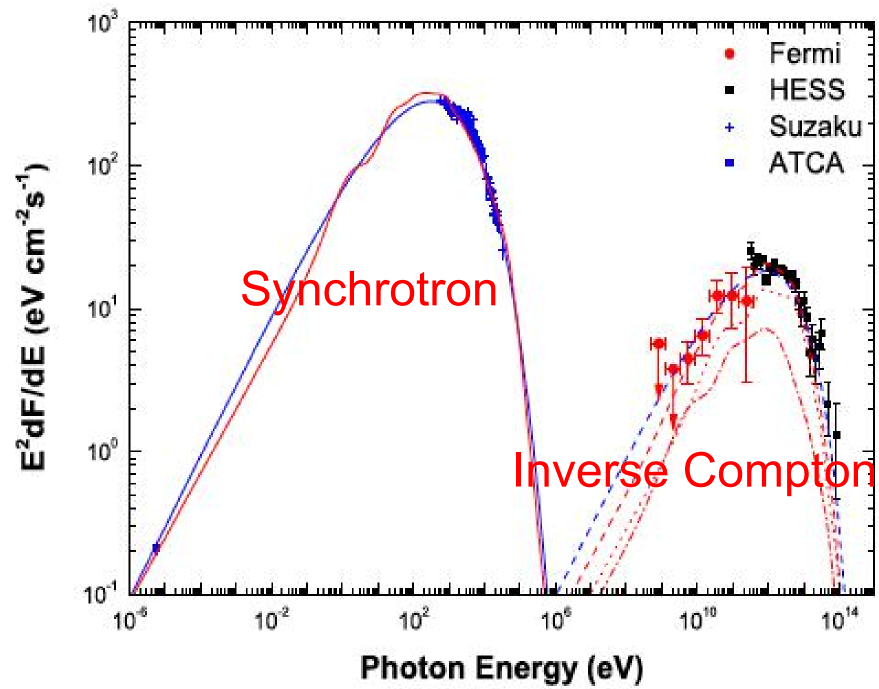

Figure 2. Comparison of the observed radio (Acero et al. 2009), X-ray (Tanaka et al. 2008), and γ-ray fluxes with the synchrotron (solid) and IC (dashed) spectra of the derived electron distributions using our inversion method. The blue lines are for the analytical distribution, whose parameters are described in Section 3. The red lines are the inter- and extrapolated electron distribution, where the dotted and dot-dashed lines are for the IC of IR and CMB photons, respectively.

2: Energy Partition between Magnetic Field and Energetic Electrons

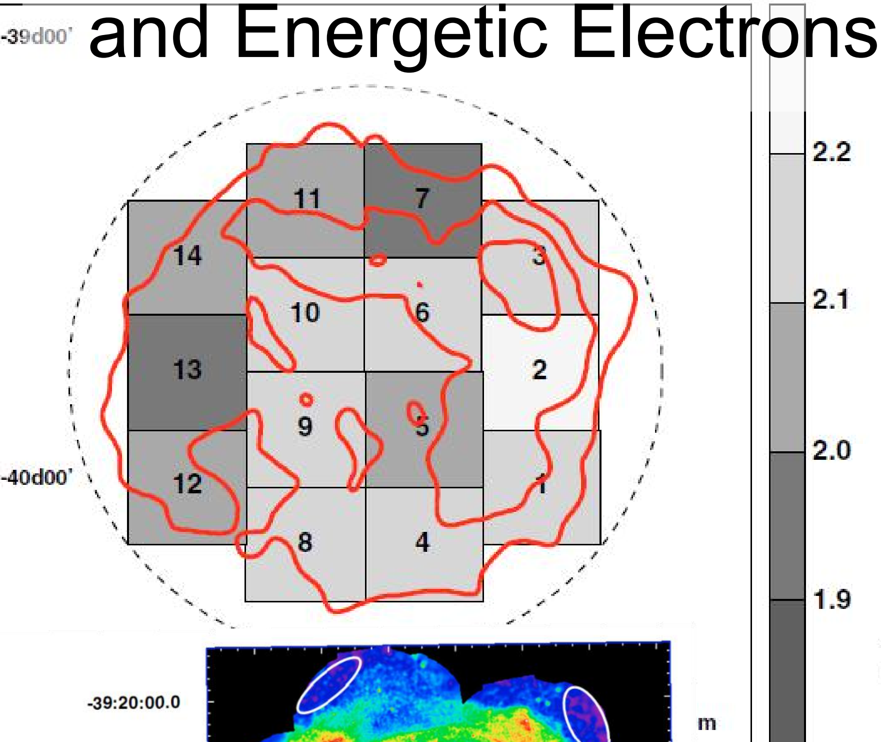

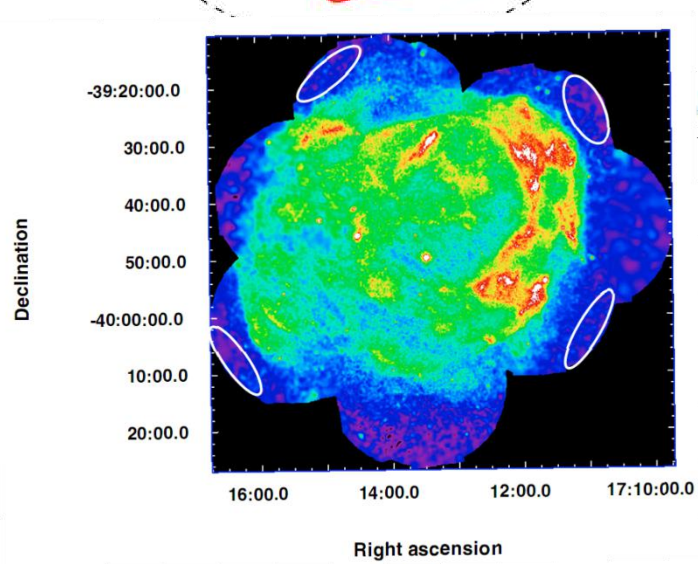

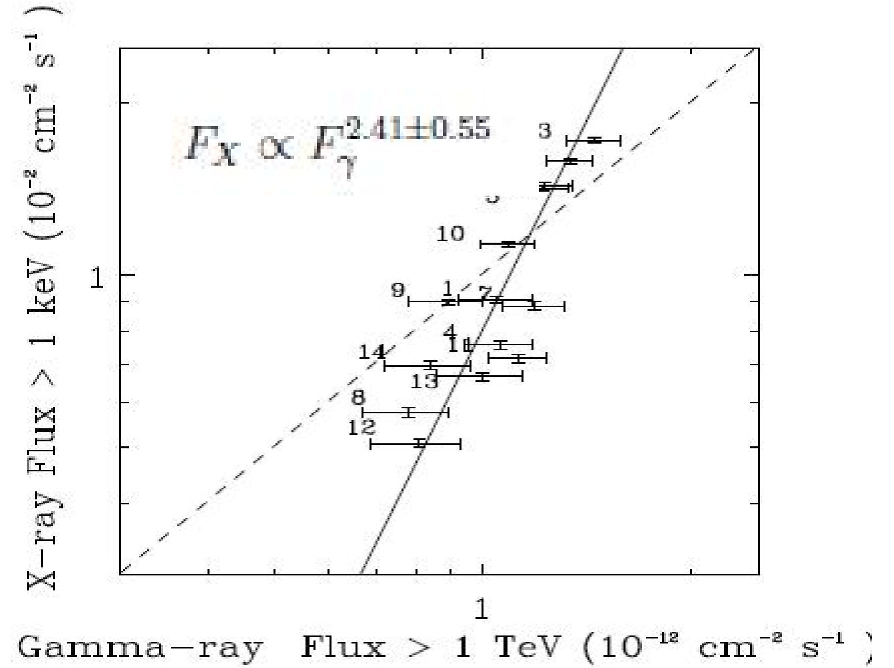

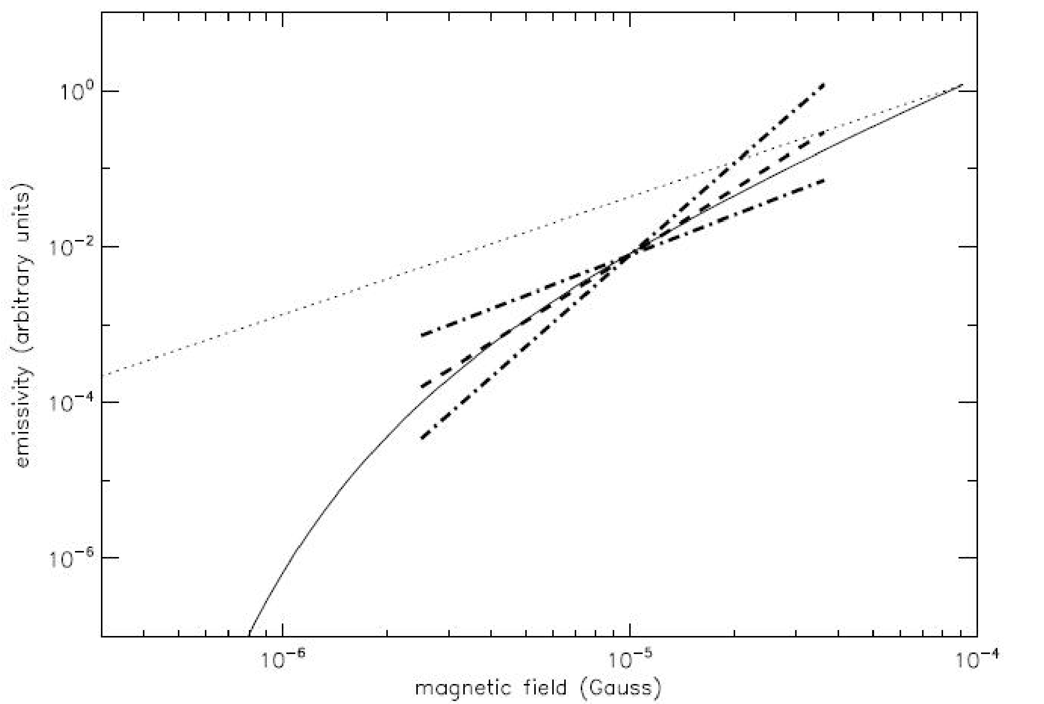

1: Energy Partition between Magnetic Field and Energetic Electrons

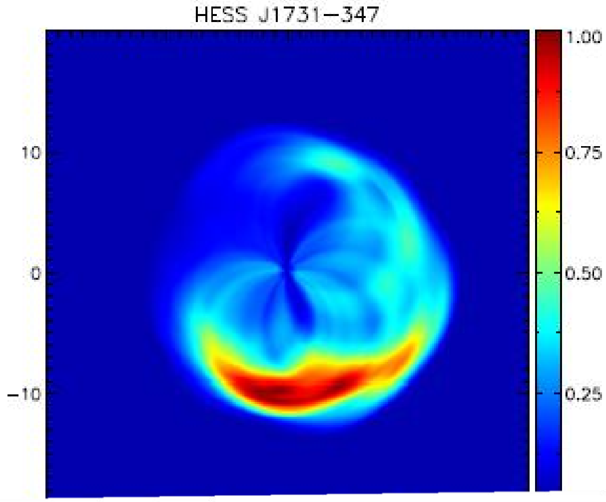

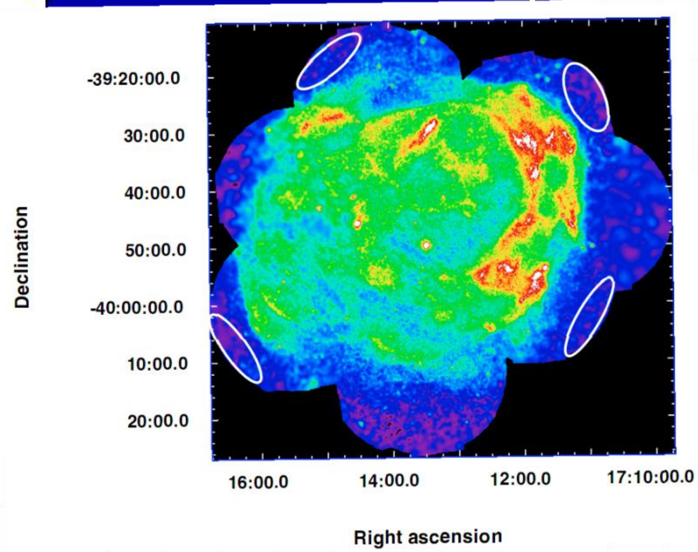

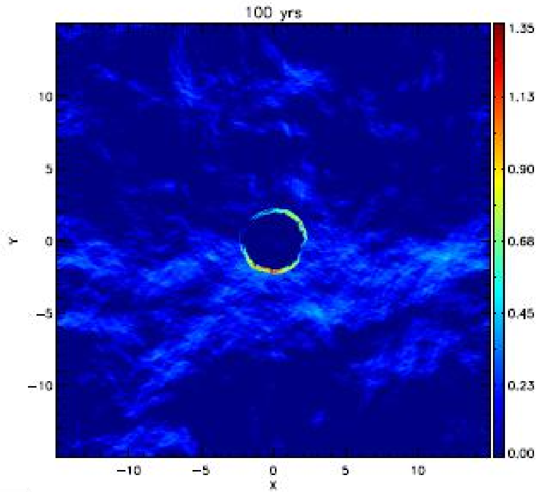

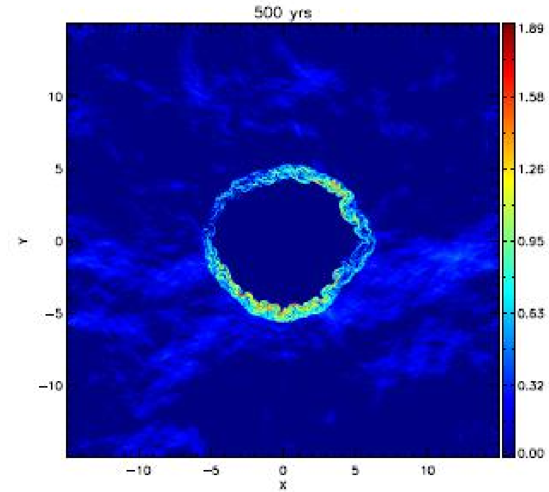

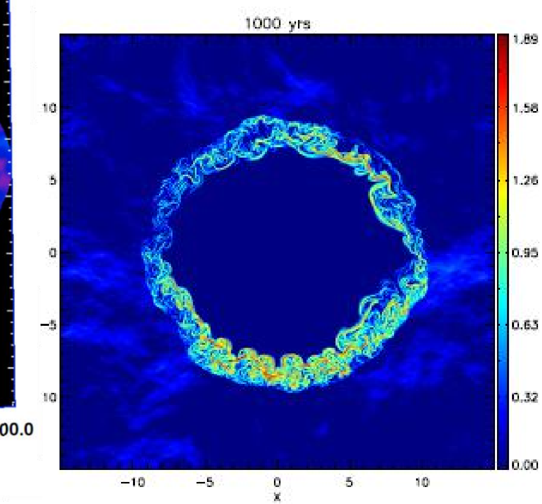

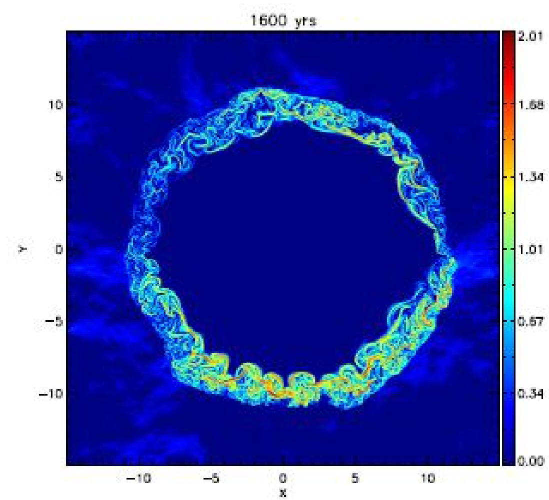

1 Radial Brightness Profiles

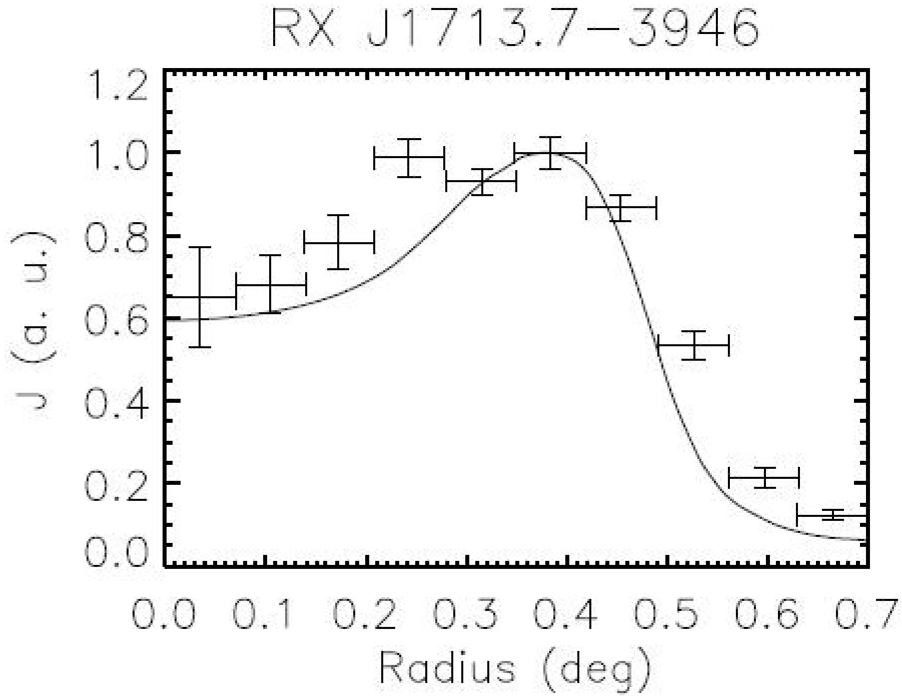

1 Multi-wavelength overall spectral fit

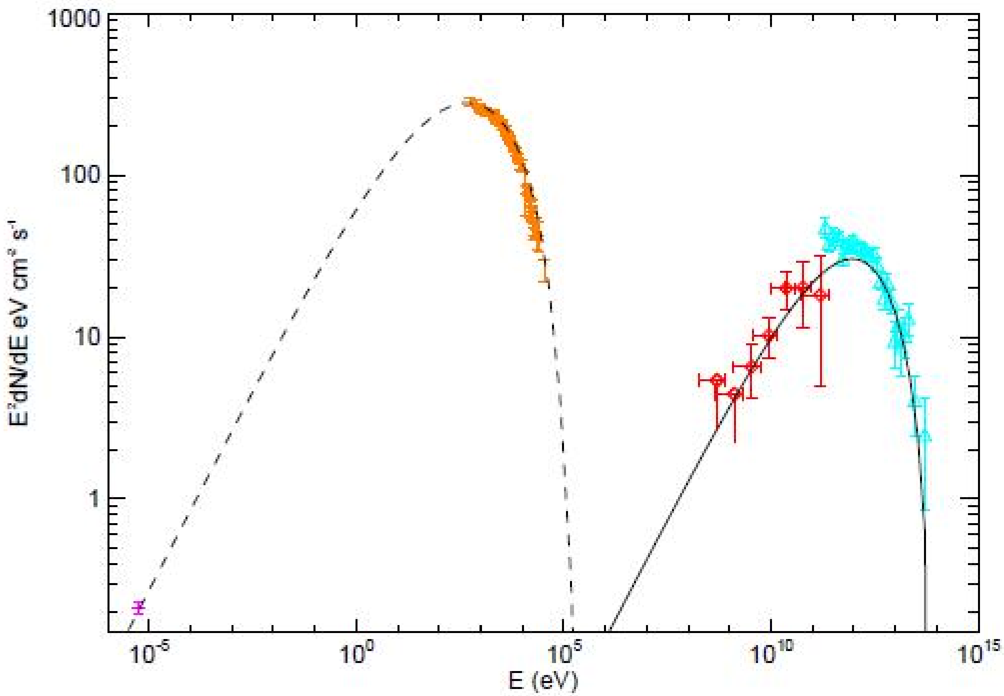

Name	$F_\gamma^{\rm a}/F_X^{\rm b}$	Diameter[c]	$B^{\rm d}$	$W_e^{\rm d}$	W_B
	10^{-10}erg s^{-1}cm^{-2}	pc	μG	10^{47} erg	10^{47} erg
RX J1713.7-3946	0.68/5.4	$17.4(D/1)$	12	$3.9(D/1)^2$	$4.0(D/1)^3(f/0.87)^{\rm e}$
RX J0852-4622	$0.66^{\rm e,f}/0.83$	$34(D/1)$	9.4	$10(D/1)^2$	$10(D/1)^3(f/0.49)^{\rm f}$
J1731-347	$0.09/1.0^{\rm a}$	27(D/3.2)	28	$2.3(D/3.2)^2$	$85(D/3.2)^3(f/0.9)^{\rm a}$

1 Energy Partition between Magnetic Field and Energetic Electrons

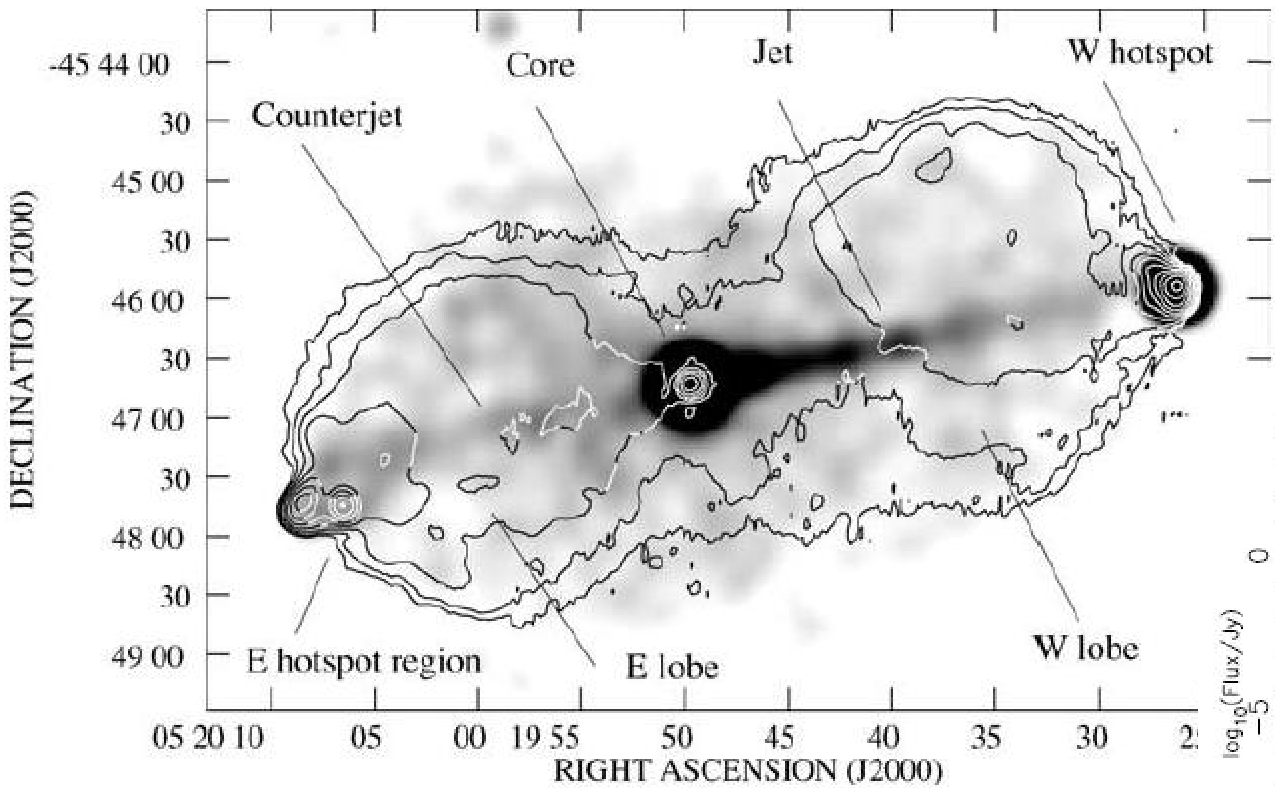

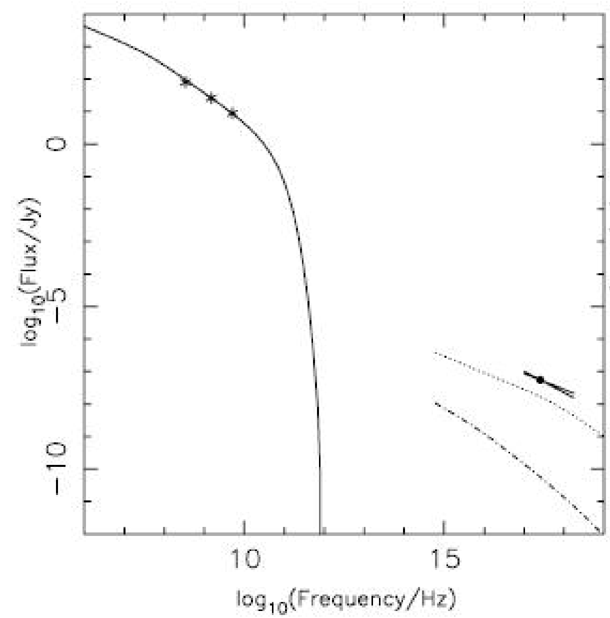

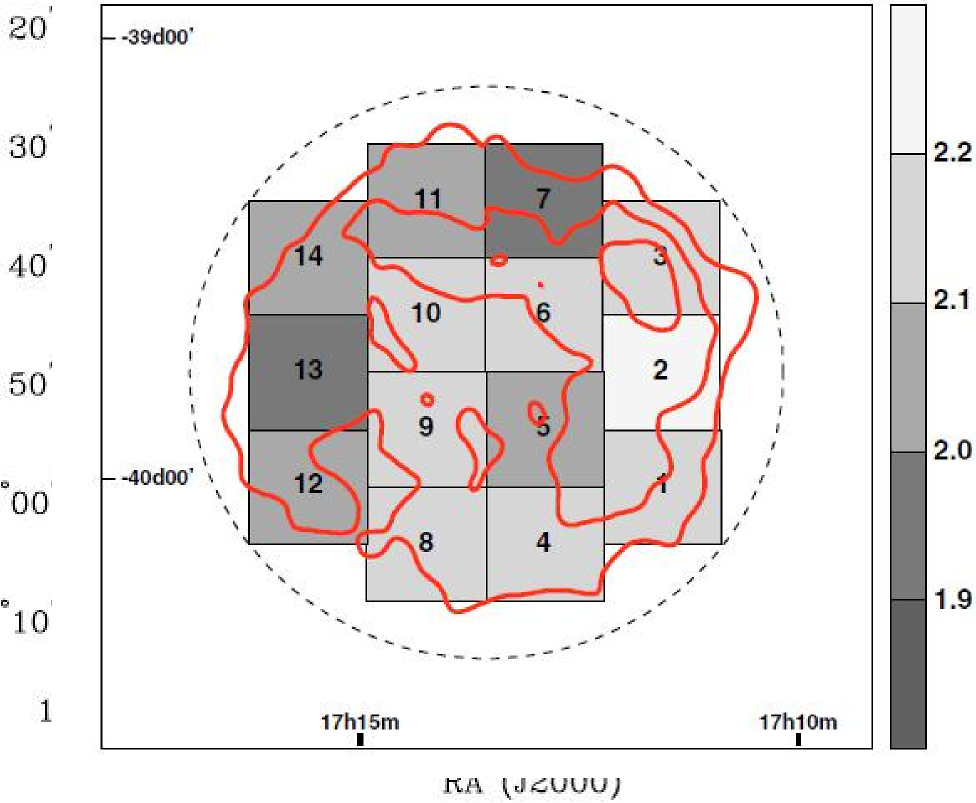

-39d00'
-40d00'
17h15m
17h10m
2.2
2.1
2.0
1.9
11
7
14
3
10
6
13
2
9
5
12
1
8
4

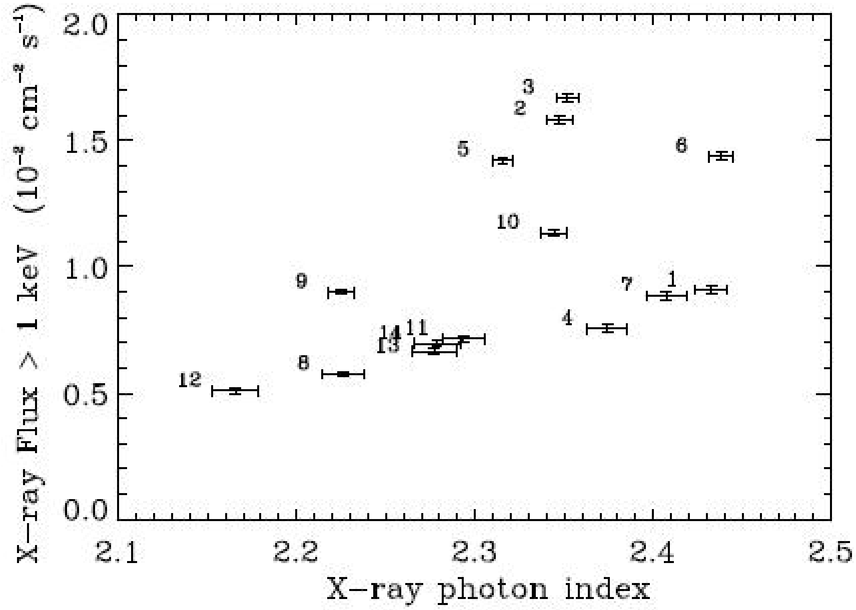

X-ray Flux > 1 keV (10^{-2} cm^{-2} s^{-1})
X-ray photon index
2.0
1.5
1.0
0.5
0.0
2.1
2.2
2.3
2.4
2.5

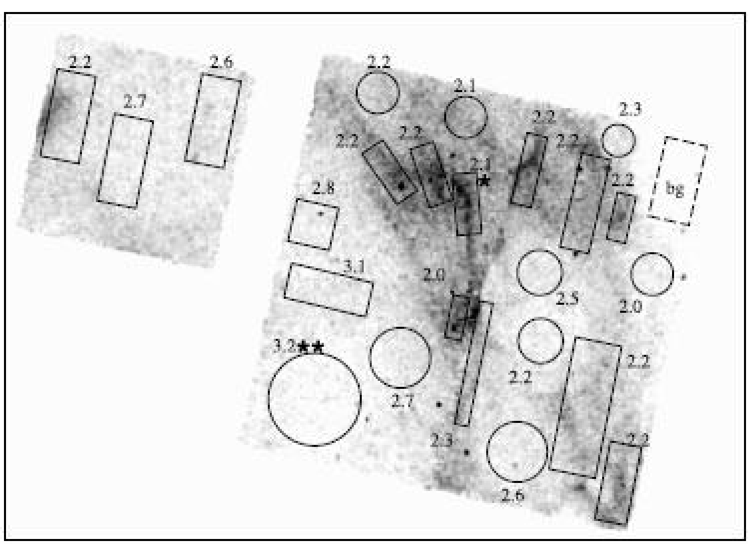

bg

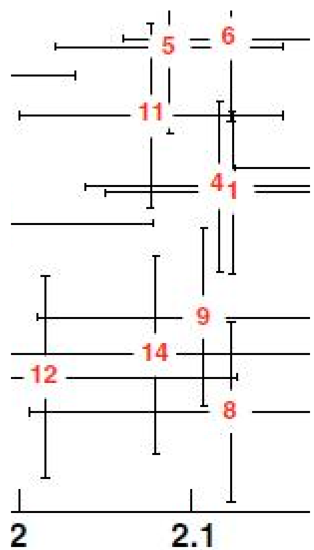

2
2.1

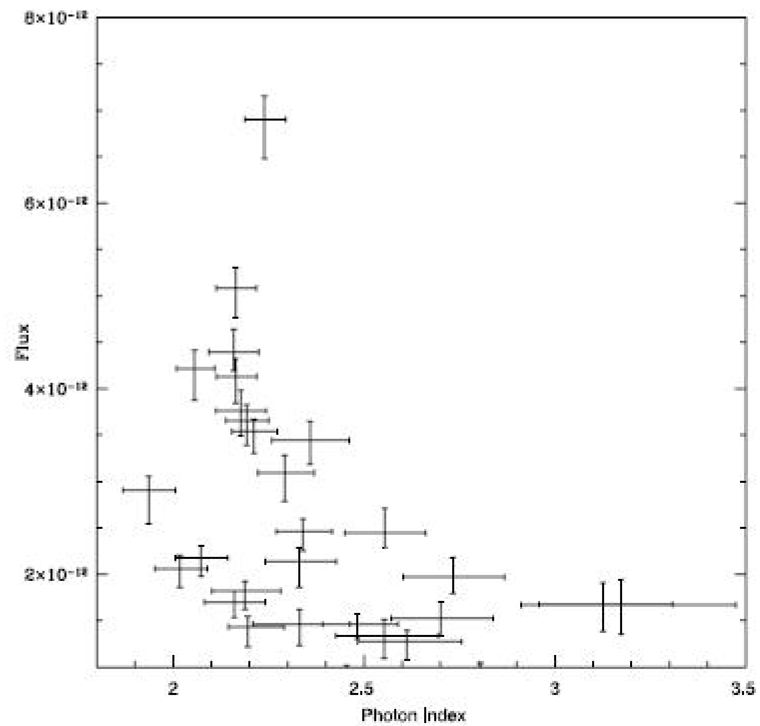

Flux
Photon Index

3: Future Studies

1: 3D MHD Simulations to Study Source structure

2: Multi-wavelength spectral fit

3: Evolution of SNRs

4: Incorporating the thermal component

2: Cosmic Rays

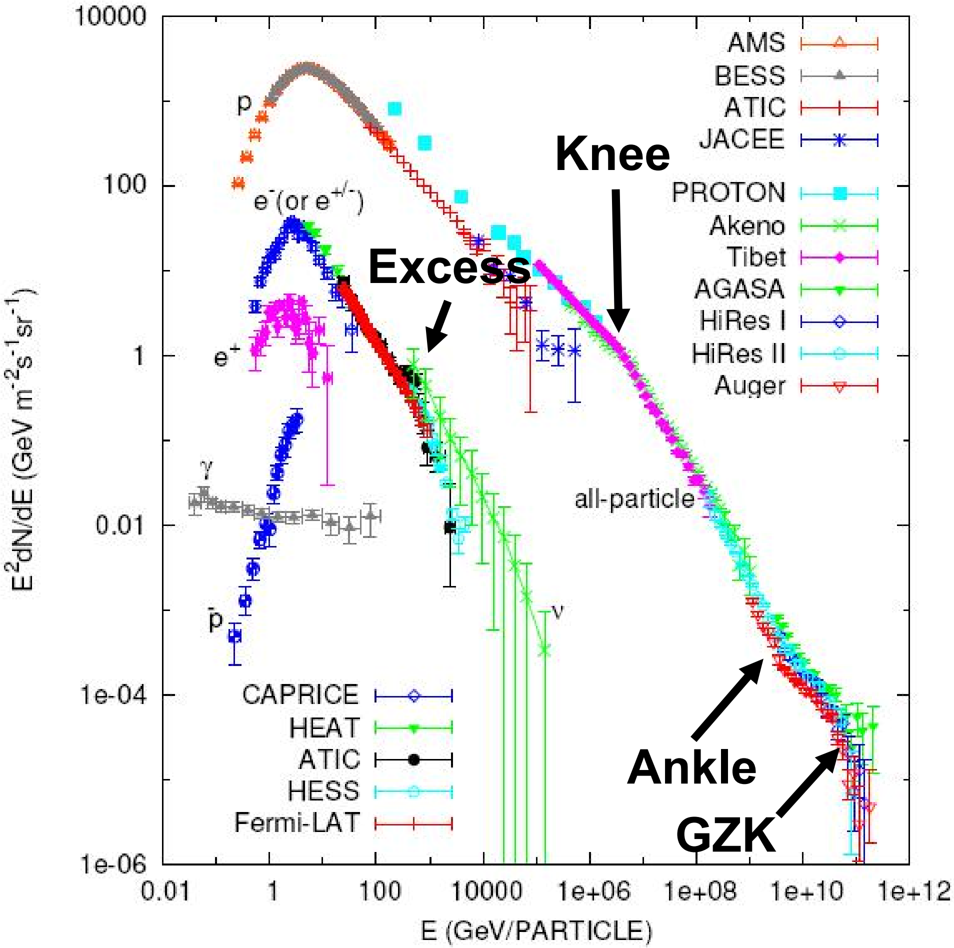

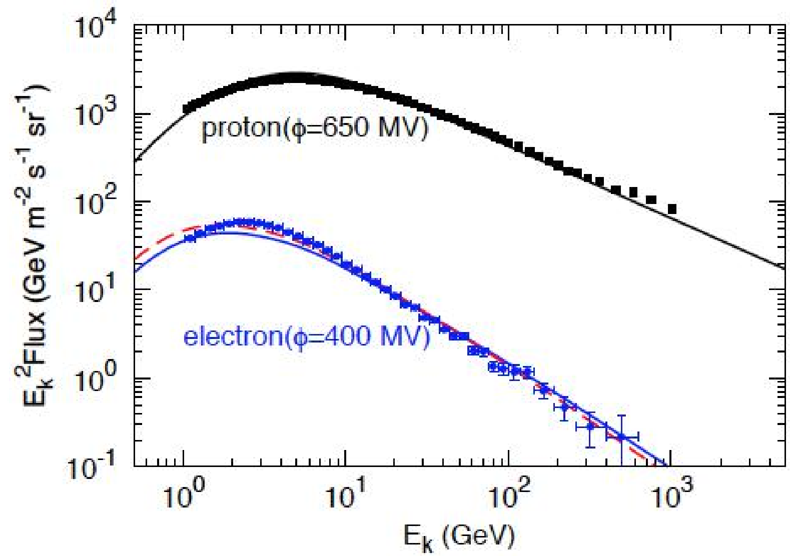

G. 1.— The expected fluxes of CR protons and electrons at Earth, for the same spectral shape of the injected particles, pared with the PAMELA observational data (Adriani et al. .a,b). We adopt two parameter settings to calculate the elec- spectrum: for solid line the magnetic field is the canonical adopted in GALPROP and $K_{ep} \approx 1.3\%$; for dashed line the netic field is two times larger and $K_{ep} \approx 1.9\%$.

4.1 Source Structure: Magnetic Field Amplification

MAGNETIC FIELD AMPLIFICATION BY SHOCKS IN TURBULENT FLUIDS

J. Giacalone and J. R. Jokipii

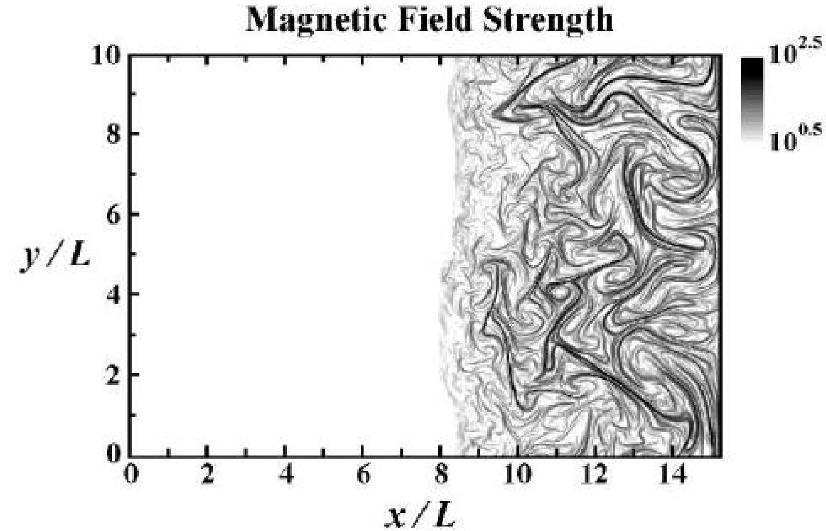

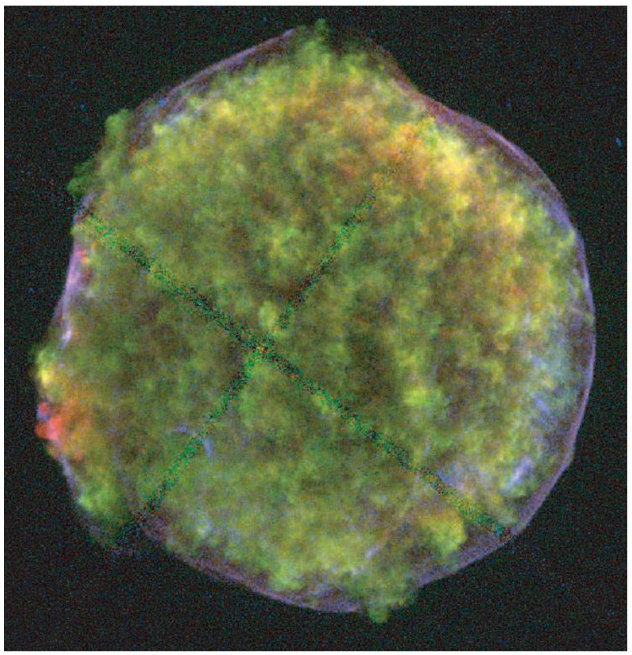

Turbulent amplification of magı acceleration of cosmic rays

A. R. Bell*

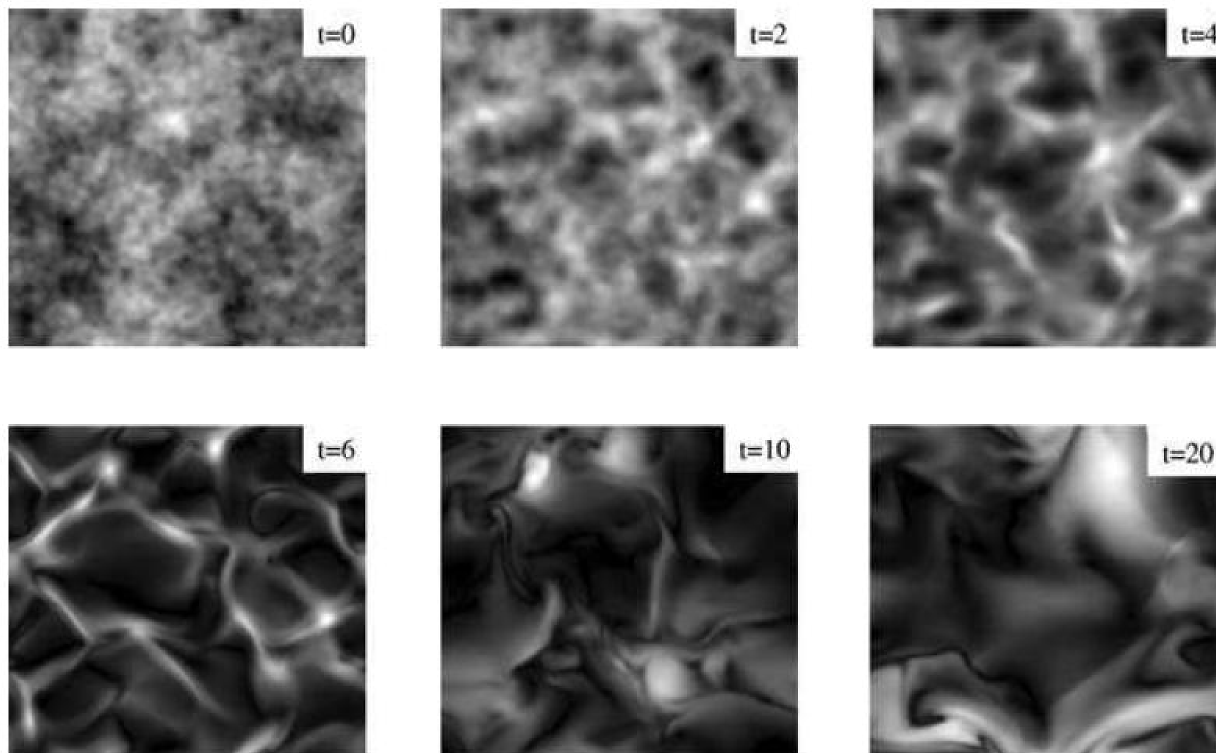

4.2 Multi-wavelength spectral fit

GAMMA RAYS FROM THE TYCHO SUPERNOVA REMNANT: MULTI-ZONE VERSUS SINGLE-ZONE MODELING

ARMEN ATOYAN[1] AND CHARLES D. DERMER[2]

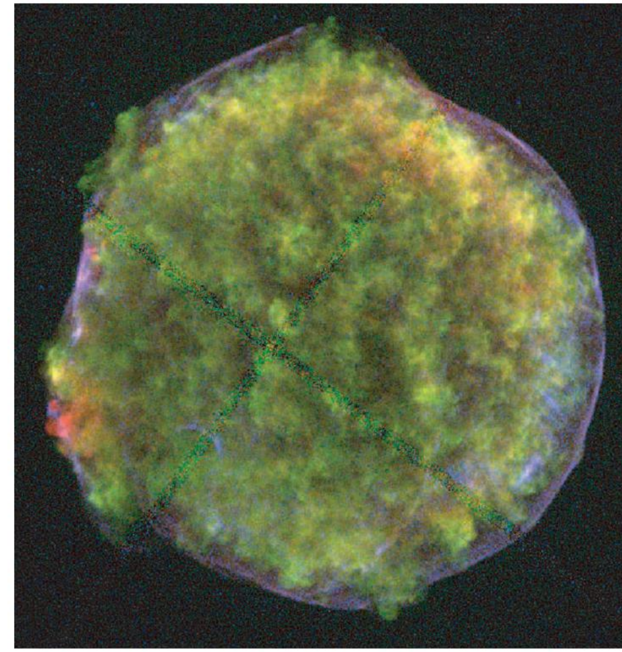

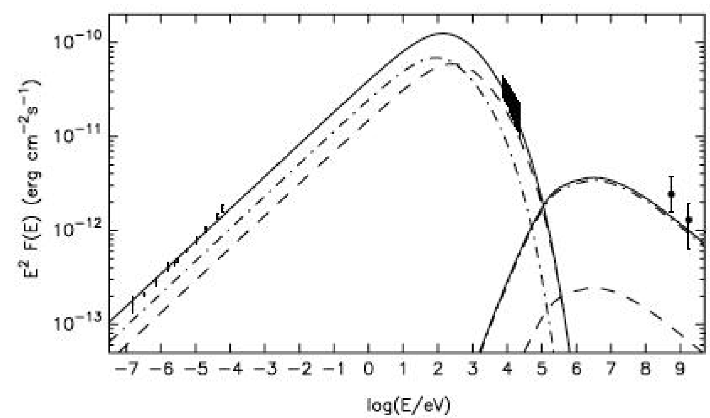

Figure 1. Synchrotron fluxes from radio through X-rays in the two-zone model. Dashed and dot-dashed lines show the fluxes from zone 1 and zone 2, respectively, and the total flux is shown by the solid line. Calculations assume density $n_2 \approx 3\,\mathrm{cm}^{-3}$ at $d_{\mathrm{kpc}} = 2.8$, $n_1 \approx n_2$, $B_1 = 100\,\mu$G and $B_2 = 34\,\mu$G, $\eta = 0.2$, $\alpha = 2.31$, and $E_{\mathrm{cut}} = 40$ TeV. Also shown are the lower-energy ($\lesssim$GeV) bremsstrahlung fluxes produced by relativistic electrons in zones 1 and 2.

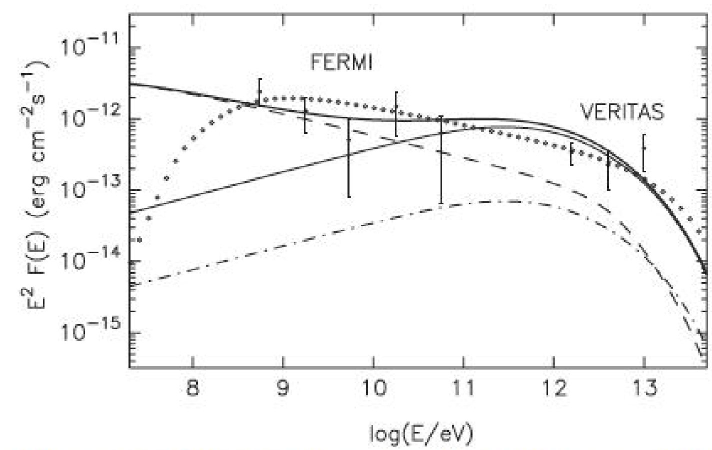

Figure 2. γ-ray fluxes in the two-zone model with parameters described in Figure 1. The heavy solid line shows the total flux of leptonic origin. The total bremsstrahlung and Compton radiation fluxes are shown by dashed and solid (thin) lines, respectively. For comparison, the Compton flux contribution from zone 1 is also shown (dot-dashed line). The open dotted curve shows the flux of hadronic origin calculated for protons with total energy $E_p = 3 \times 10^{49}$ erg.

4.2 Multi-wavelength spectral fit

PRIMARY VERSUS SECONDARY LEPTONS IN THE EGRET SUPERNOVA REMNANTS

Marco Fatuzzo[1] and Fulvio Melia[2]

Received 2004 December 17; accepted 2005 May 6

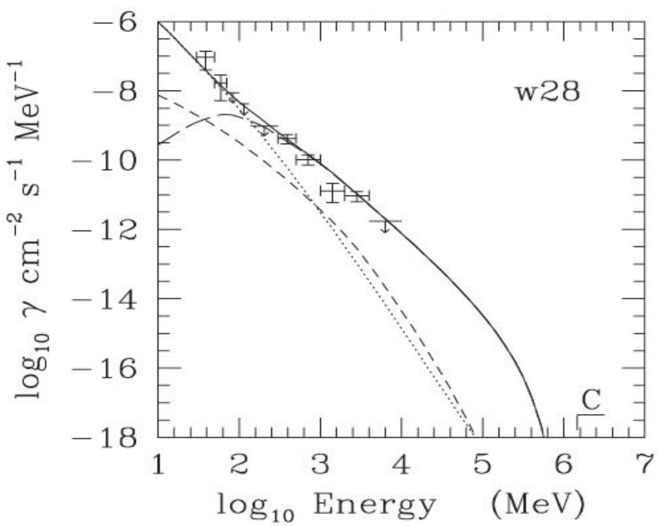

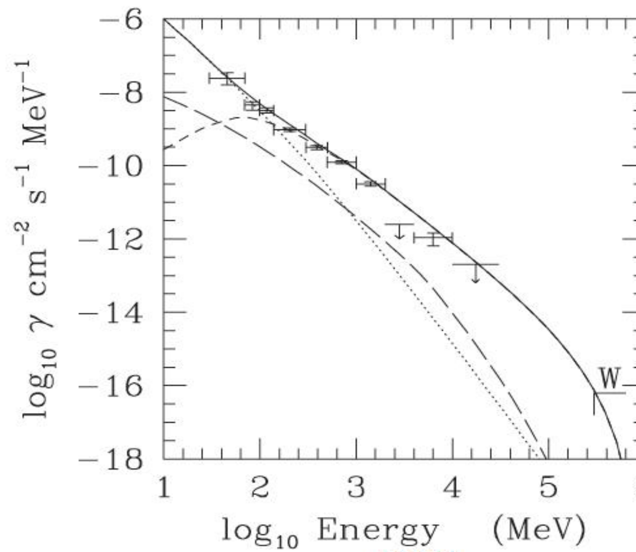

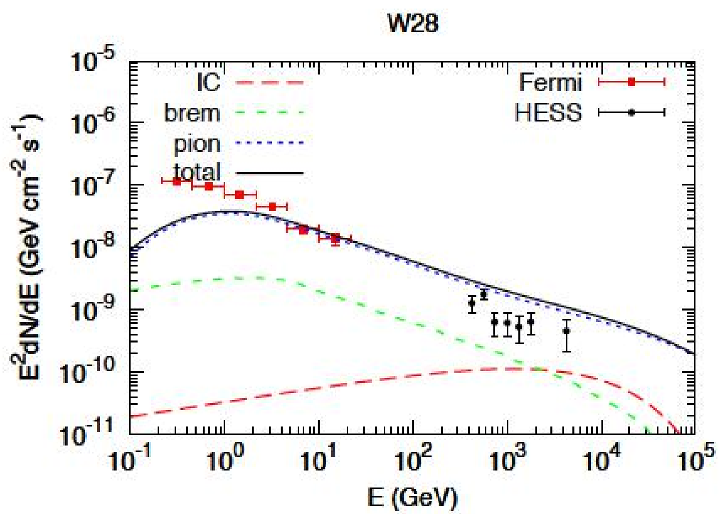

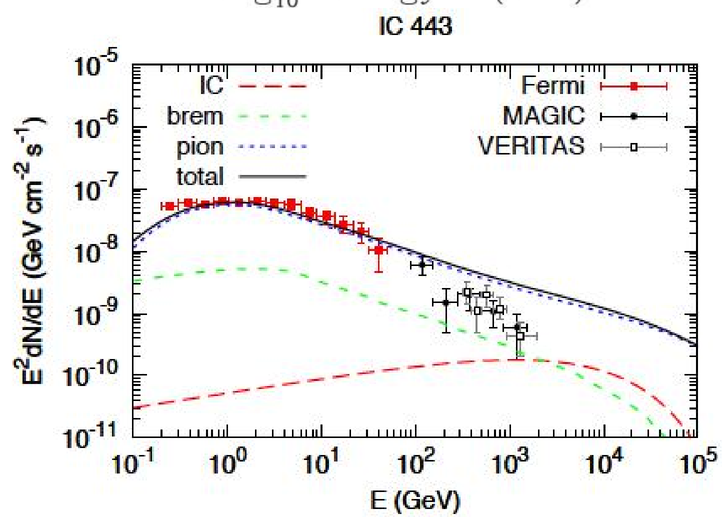

RADIO TO GAMMA-RAY EMISSION FROM SHELL-TYPE SUPERNOVA REMNANTS: PREDICTIONS FROM NONLINEAR SHOCK ACCELERATION MODELS

MATTHEW G. BARING[1]

Laboratory for High-Energy Astrophysics, Code 661, NASA Goddard Space Flight Center, Greenbelt, MD 20771; baring@lheavx.gsfc.nasa.gov

DONALD C. ELLISON AND STEPHEN P. REYNOLDS

Department of Physics, North Carolina State University, Box 8202, Raleigh NC 27695; don_ellison@ncsu.edu, steve_reynolds@ncsu.edu

AND

ISABELLE A. GRENIER AND PHILIPPE GORET

Service d'Astrophysique, CEA, DSM, DAPNIA, Centre d'Etudes de Saclay, 91191 Gif-sur-Yvette, France; isabelle.grenier@cea.fr, goret@sapvxg.saclay.cea.fr

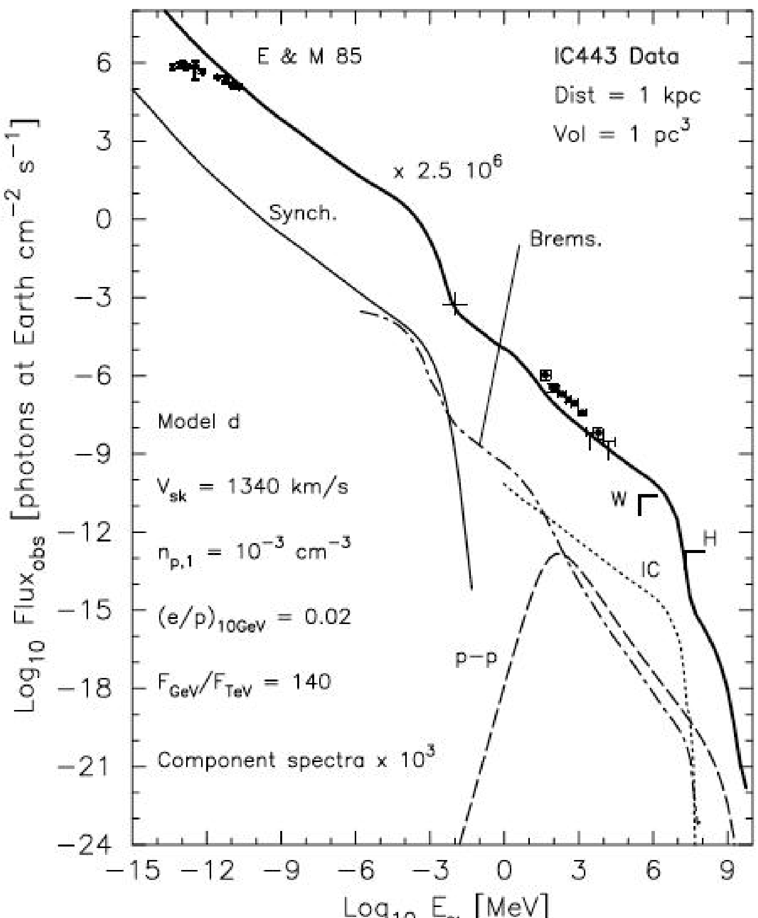

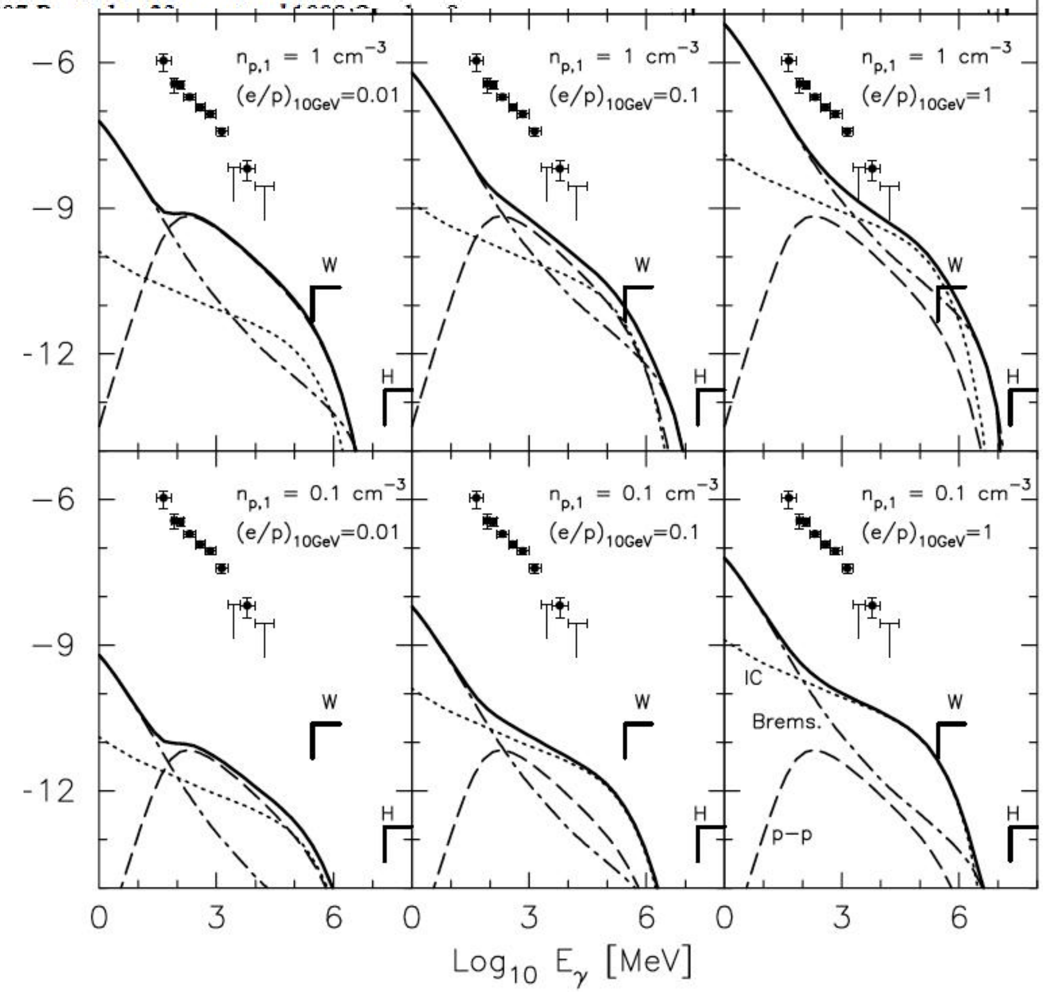

4.4 Thermal Emission

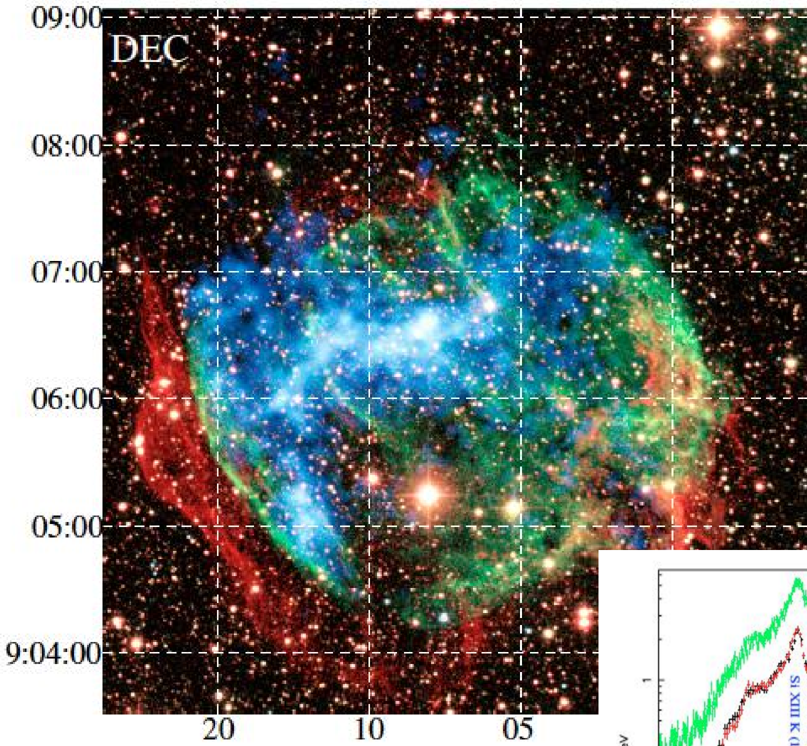

Fig. 2. Color composite *Chandra* X-ray image (in
2.12 μm molecular hydrogen (in red), and 1.64
green) images of W49B (from http://chandra
press/04_releases/press_060204.html).

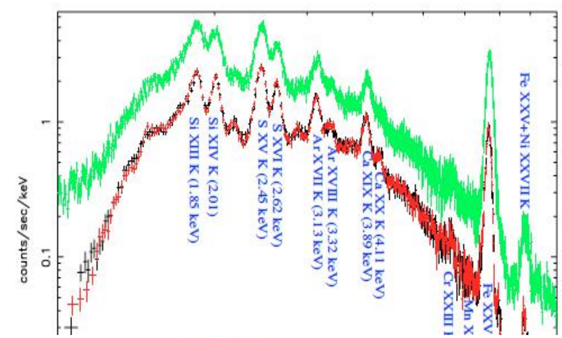

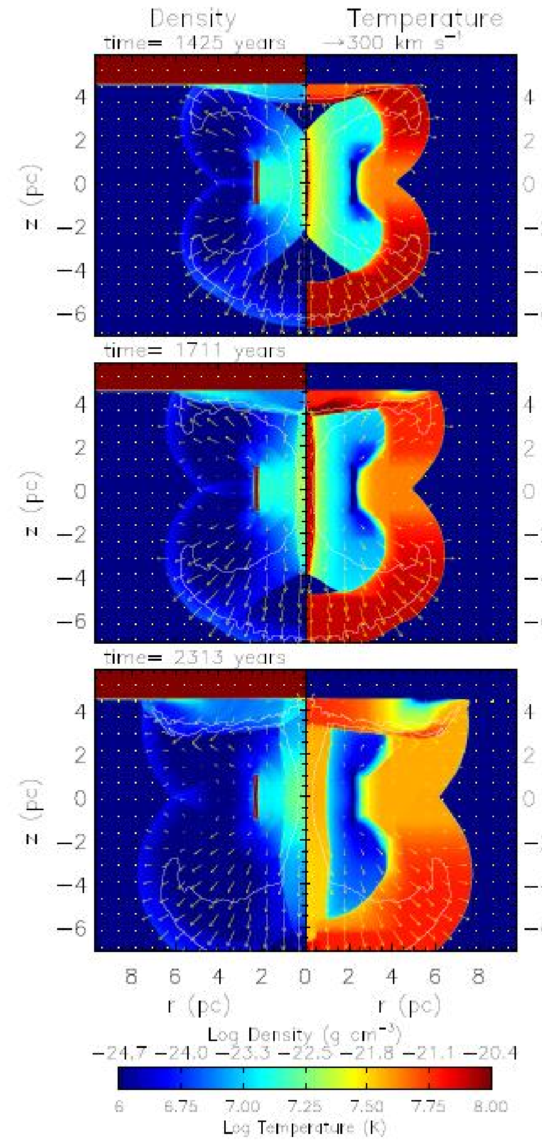

Unveiling the spatial structure of the overionized plasma in the supernova remnant W49B

Xin Zhou[1,2], Marco Miceli[3,2], Fabrizio Bocchino[2], Salvatore Orlando[2], and Yang Chen[1,4]

1: Two emission models for SNR RX J1713.7-3946

Leptonic $F_e(E) \propto E^{-\alpha_e} \exp\left[-(E/E_c^e)^{\delta_e}\right]$ Hadronic

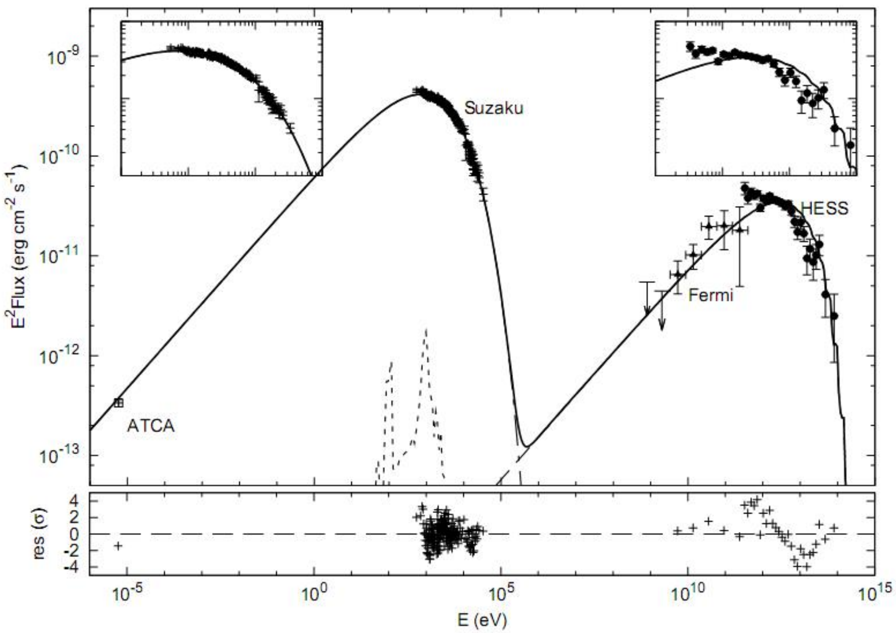

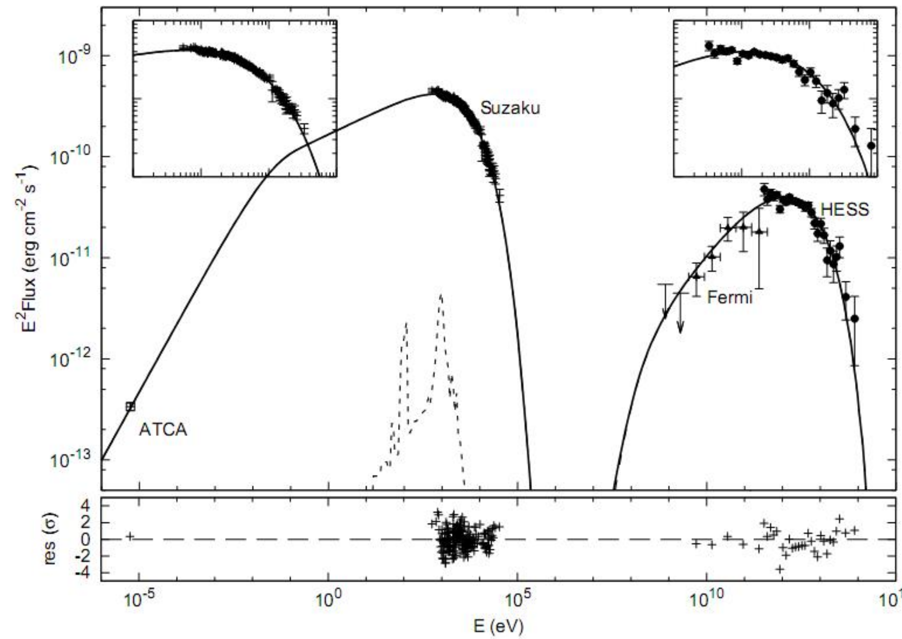

	α_e	E_c^e (TeV)	W_e (10^{47}erg)	δ_e	B (μG)	$n_{\rm ISM}$ (10^{-2}cm^{-3})	α_p	E_c^p (TeV)	W_p (10^{52}erg)
leptonic	$2.15^{+0.01}_{-0.01}$	$51.3^{+2.3}_{-2.2}$	$5.5^{+0.3}_{-0.3}$	$1.21^{+0.04}_{-0.04}$	$11.6^{+0.1}_{-0.1}$	< 0.7	—	—	—
hadronic	$1.64^{+0.09}_{-0.08}$	$14.5^{+4.8}_{-3.9}$	$0.05^{+0.05}_{-0.02}$	$2.1^{+0.2}_{-0.2}$	$428.2^{+233.9}_{-159.6}$	< 1.1	$1.58^{+0.06}_{-0.06}$	$53.7^{+7.1}_{-6.2}$	> 1.6
hadronic*	$1.58^{+0.05}_{-0.05}$	$12.3^{+2.1}_{-1.8}$	$0.03^{+0.01}_{-0.01}$	$1.9^{+0.1}_{-0.1}$	$596.8^{+173.0}_{-129.0}$	< 1.2	—	$54.7^{+6.0}_{-5.7}$	> 1.4

The Astrophysical Journal, 735:120 (9pp), 2011 July 10
doi:10.1088/0004-637X/

MODELING THE MULTI-WAVELENGTH EMISSION OF THE SHELL-TYPE SUPERNOVA REMNANT RX J1713.7−3946

Qiang Yuan[1], Siming Liu[2,3], Zhonghui Fan[4], Xiaojun Bi[1,5], and Christopher L. Fryer[6,7]
[1] Key Laboratory of Particle Astrophysics, Institute of High Energy Physics, Chinese Academy of Sciences, Beijing 100049, China
[2] Department of Physics and Astronomy, University of Glasgow, Glasgow G12 8QQ, UK
[3] Key Laboratory of Dark Matter and Space Astronomy, Purple Mountain Observatory, Chinese Academy of Sciences, Nanjing 210008, China

3: Future Studies

1: 3D MHD Simulations to Study Source structure

2: Multi-wavelength spectral fit

3: Evolution of SNRs

4: Incorporating the thermal component

4.3 Time Evolution